Rosa Maria Magalhães Rego

Development of gas sensors for binary mixtures and solvent-free sample preparation techniques based on polymeric membranes

Dissertation presented for the degree of
Doctor in Chemical Engineering
by
University of Oporto

Supervisor
Adélio Miguel Magalhães Mendes

LEPAE - Chemical Engineering Department

Oporto, October 2005

Melhor é conhecer,
saber
como quem vê uma paisagem inteira
e entende
- folha a folha -
o antes e depois:
a intenção e a aventura

Fernando Lanhas

Acknowledgements

This work would not have been completed without the help and support of many people. To them I would like to express my sincere gratitude.

First of all, I would like to thank Prof. Seita for providing me with the opportunity to work in the Chemistry Department of the University of Trás-os-Montes e Alto Douro (DQ-UTAD). He stimulated a professional, ambitious and positive atmosphere within the group and will be remembered for his good judgment.

I wish to thank my supervisor, Prof. Adélio Mendes for the research theme, for giving me the opportunity to carry out this work at the Laboratory of Process, Environment and Energy Engineering (LEPAE), for advice and support throughout the work and for careful revision of this thesis.

I am also grateful to Prof. Rui Vale and Prof. Nídia Caetano for co-supervision.

This thesis is based on the work carried out at DQ-UTAD and at the Chemical Engineering Department of the Engineering Faculty of the University of Oporto (DEQ-FEUP). I wish to express my gratitude to the members of the staff, my friends and colleagues of both the above mentioned institutions for helping me in my work and for providing a thoroughly enjoyable atmosphere. In particular I record my thanks to:

Prof. Verónica Bermudez, for encouragement, valuable comments and careful revision of parts of the introduction and paper 6, Prof. Paulo Herbert, for valuable comments and helpful discussions, Prof. Pedro Tavares and Prof. Luís Carvalho, for helpful discussions, Prof. Fernão Magalhães, for careful revision of paper 1, and Mr. Sousa Vale, for assistance.

GKSS Forschungszentrum Geesthacht GmbH, Germany, for supplying the membranes (Mr. Kneifel, Dr. Fritsch and Dr. Peinemann).

Prof. Manuela Silva (University of Minho) for TGA measurements.

Eng. Nuno Martins for SEM and EDS analyses.

Many thanks to my friends…

To my family, for never-ending encouragement and support.

To Manuela, my sister, thanks for everything.

To André, my god-son, for all the hours I could not be with him.

This work was supported by Agência de Inovação, s.a., (project P0046/ICPME/S - Gassense).

Preface

This thesis is in four parts. Part I provides a brief description of the previous work done to date in the areas of membrane-based sample preparation techniques, with an emphasis on principles and examples of recent applications in the biological, food and environmental areas and the developing role of membranes as gas concentration sensors, pH sensors, ion-selective sensors, bio-sensors, etc, as well as describing how research has advanced in these fields.

Part II deals with the development of a new and very low cost concentration gas sensor for binary mixtures based on the permselectivity of polymeric membranes. The technology developed has been characterized and optimized for selected applications. In order to evaluate the overall performance of the sensor data on response curves, repeatability, sensitivity, response time, reversibility, long-term stability and the influence of temperature were obtained. Mono- and bi-component permeation (k) and ideal selectivities (α) were obtained for the membranes used in the developed gas concentration sensors. The selected gas mixtures were oxygen/nitrogen (paper 1), carbon dioxide/methane or helium (papers 2 and 3) and hydrogen/methane or nitrogen (paper 4), targeting medical oxygen concentrators, biogas controlling units and hydrogen manufacturing plants applications, respectively. A very simple mathematical model describing the relationship between the gas feed molar fraction and permeate pressure is proposed and used to describe the sensors response curves with two gas mixtures. Part II ends with paper 5, where a simple method to compensate most of the temperature effect on the developed sensor's response is described.

Part III focuses on the development of a new solvent-free membrane-based extraction technique, the membrane extraction thermal desorption (METD). Paper 6 opens with a description of the experimental set-up developed to test this new technique. The membranes used were

characterized to assess their performance as matrices for extraction by several techniques. The investigated properties are morphology, thermal stability and sorption/desorption of selected analytes (molinate and cycloate). This paper concludes with a study of the applicability of the METD technique to determine the selected herbicides concentration in aqueous solutions.

General conclusions are presented in Part IV, together with a brief summary of the main results obtained and a description of other promising aspects, which were referred to but not fully investigated in the course of the present research.

The author performed all the experimental work reported in this thesis, except the thermal gravimetric analysis (Prof. Manuela Pinto, University of Minho), and the scanning electron microscope and the electron-dispersive spectroscopy analyses in which she was helped by Eng. Nuno Martins from *Unidade de Microscopia Electrónica* (UME), UTAD.

Contents

PART III - Membrane-based extraction tecniques

PART IV - General conclusions and future work

Figure captions

Table captions

Abstract

Hollow fiber polymeric membranes have been applied in the development of new concentration gas sensors for binary or pseudo-binary mixtures and for solvent-free sample preparation techniques.

The asymmetric membranes used were poly(dimethylsiloxane) (PDMS), poly(etherimide) (PEI) and Teflon-AF hollow fibers. To achieve optimal performance in the applications considered the hollow fiber membranes were characterized by scanning electron microscopy (SEM, morphology), gas permeation (mono- and bicomponent mass transfer and ideal selectivities, α), thermal analysis (thermal stability and sorption/desorption) and electron-dispersive spectroscopy (EDS, concentration profile of sorbed herbicides across the membrane thickness).

The gas concentration sensor consists of a permselective membrane module whose permeate stream is linked to a needle valve. For a stabilized feed pressure its composition is related to the permeate build up pressure, measured using a pressure transducer. The present work describes the sensor and its use with oxygen/nitrogen, carbon dioxide/methane, carbon dioxide/helium, hydrogen/methane and hydrogen/nitrogen gas mixtures. It has been subjected to a series of experiments to assess its response in terms of sensitivity, stability, response time, working range, precision and accuracy of the measurements, as well as the effect of temperature. A simple mathematical model has been developed and applied to oxygen/nitrogen and hydrogen/methane mixtures. Good agreement with the experimental results was obtained for both mixtures. A simple method to compensate most of the temperature effect on the sensor's response is also described. This strategy proved to be particularly effective when dealing with oxygen/nitrogen and carbon dioxide/helium gas mixtures. These sensors are low cost and aimed at a low/medium precision market, such as medical oxygen concentration units, biogas controlling units (wastewater treatment

plants and landfills), as well as manufacturing plants that use or produce hydrogen. Other applications are possible.

The concentration gas sensor showed a fast, continuous, reversible, reproducible and long-term stable response in the range 0-100%. The oxygen/nitrogen as well as the carbon dioxide/methane sensors are the most attractive applications of the devised technology.

Membrane extraction thermal desorption (METD) is a new technique for the analysis of semi-volatile organic compounds proposed in the framework of the present research. The technique uses a hollow fiber membrane to selectively pre-concentrate the analytes and exclude water from the GC system. The membrane is put in direct contact with the sample or its headspace. Next, the fiber is heated in an oven to desorb the analytes. The stripping gas (GC carrier gas) that flows inside the membrane transfers the desorbed analytes to the GC-FID for quantitative analysis. Two herbicides belonging to the class of thiocarbamates (molinate and cycloate) were chosen as model compounds. METD proved to be a robust and low cost technique using a single hollow fiber of variable length that can pre-concentrate the solutes orders of magnitude in a selective way.

Sumário

No âmbito do presente trabalho, foram usadas membranas poliméricas de fibra oca no desenvolvimento de sensores de concentração de misturas gasosas binárias ou pseudo-binárias e técnicas de preparação de amostras sem solvente.

As membranas assimétricas de fibras ocas usadas foram poli(dimetilsiloxano) (PDMS), poli(éterimida) (PEI) e Teflon-AF. Foi necessária a caracterização das membranas de forma a possibilitar a optimização da sua utilização. As técnicas utilizadas na caracterização foram microscopia de varrimento electrónico (SEM, obtenção da morfologia), permeação gasosa (coeficientes de transferência de massa mono- e bicomponentes, *k*, e selectividades ideais, α), análise térmica (estabilidade térmica e sorção/desorção) e espectroscopia de dispersão de energia (EDS, perfil de concentração dos herbicidas sorvidos ao longo da espessura da membrana).

O sensor de concentração de misturas gasosas binárias é constituído por um módulo de membranas *permselectivas* cujo caudal de permeado passa através de uma válvula de agulha. Para uma alimentação ao módulo de membranas a pressão constante, a composição da alimentação relaciona-se com o aumento da pressão do permeado. O aumento da pressão é medido com um transdutor de pressão. O presente trabalho descreve o sensor e a sua aplicação às seguintes misturas gasosas: oxigénio/azoto, dióxido de carbono/metano, dióxido de carbono/hélio, hidrogénio/metano e hidrogénio/azoto. Foram realizadas uma série de experiências com este sensor de forma a conhecer a sua resposta em termos de sensibilidade, estabilidade, tempo de resposta, intervalo de concentração, precisão e exactidão dos resultados, assim como os efeitos da temperatura.

Um modelo matemático simples foi desenvolvido e aplicado na representação das respostas às misturas oxigénio/azoto e

hidrogénio/metano. Foi ainda descrito um método para compensar o efeito da temperatura na resposta do sensor. Este método mostrou ser particularmente útil para as misturas de oxigénio/azoto e dióxido de carbono/hélio. Os sensores têm um custo baixo e estão vocacionados para aplicações de média/baixa precisão, como, por exemplo, nos concentradores de oxigénio para utilização médica, nas unidades de controlo de biogás (estações de tratamento de águas residuais e aterros sanitários), como também nas indústrias que usem ou produzam hidrogénio.

O sensor de concentração para misturas gasosas tem uma resposta rápida, contínua, reversível e estável no intervalo de concentrações de 0 a 100%. Os sensores de oxigénio/azoto e dióxido de carbono/metano foram identificados como sendo as aplicações mais interessantes da tecnologia desenvolvida.

A técnica de *membrane extraction thermal desorption* (METD) é uma nova técnica vocacionada para a análise de compostos semi-voláteis, proposta no presente trabalho de investigação. A técnica utiliza uma membrana de fibra oca para pré-concentrar selectivamente os analitos e elimina a água do sistema (METD-GC-FID). O gás de arrasto que circula no interior da membrana transfere os analitos desorvidos para o GC-FID para análise quantitativa. Foram escolhidos como analitos modelo dois herbicidas pertencentes à classe dos tiocarbamatos (molinato e cicloato). A técnica de METD mostrou ser robusta e de baixo custo, usa uma única fibra oca com comprimento variável e pode pré-concentrar os analitos em várias ordens de grandeza de uma forma selectiva.

Résumé

Dans le domaine du présent travail, on a utilisé des membranes polymériques de fibre creuse dans le développement de senseurs de concentration de mélanges gazeux binaires ou pseudo binaires et des techniques de préparation d'échantillons sans solvant.

Les membranes asymétriques de fibres creuses utilisées ont été celles de polidiméthylsiloxane (PDMS), de polyéthylènimine (PEI) et de Teflon-AF. La caractérisation des membranes s'est révélée essentielle afin de rendre possible l'optimisation de leur utilisation. Les techniques utilisées pour la caractérisation ont été celles de la microscopie de balayage électronique (SEM, pour l'obtention de la morphologie), de la perméabilité gazeuse (coefficients de transfert de masse mono et bicomposantes, *k*, et sélectivités idéales, α), l'analyse thermique (stabilité thermique et *sorption*/désorption) et la spectroscopie de dispersion d'énergie (EDS, profil de concentration des herbicides absorbés le long de l'épaisseur de la membrane).

Le senseur de concentration de mélanges gazeux binaires est constitué d'un module de membranes permsélectives dont le débit de perméat passe au travers d'une valve à régulation fine. Pour une alimentation au module de membranes à pression constante, la composition de l'alimentation à un rapport direct avec l'augmentation de la pression du perméat. L'augmentation de la pression est mesurée à l'aide d'un transducteur de pression. Cette étude décrit le senseur et son application dans les mélanges gazeux suivants: oxygène/azote, dioxyde de carbone/méthane, dioxyde de carbone/hélium, hydrogène/méthane et hydrogène/azote. Une série d'expérience avec ce senseur ont été réalisées afin de connaître sa réaction en matière de sensibilité, stabilité, temps de réaction, intervalle de concentration, précision et exactitude des résultats ainsi que les effets de la température. Un modèle mathématique simple a été développé et appliqué dans la représentation des réponses aux

mélanges oxygène/azote et hydrogène/méthane. Une méthode de compensation à l'effet de la température dans la réaction du senseur a été également décrite. Cette méthode se révèle particulièrement utile dans les mélanges oxygène/azote et dioxyde de carbone/hélium. Les senseurs ont un bas coût et sont destinés aux applications de moyenne/basse précision comme, par exemple, dans les concentrateurs d'oxygène utilisés aux applications médicales, dans les unités de contrôle de biogaz (centres de traitement des eaux résiduelles et des remblais sanitaires) ainsi que dans les industries qui utilisent ou produisent de l'hydrogène.

Le senseur de concentration pour les mélanges gazeux a une réponse rapide, continue, réversible et stable dans l'intervalle de concentrations de 0 à 100%. Les senseurs d'oxygène/azote et de dioxyde de carbone/méthane ont été identifiés comme étant ceux dont les applications sont les plus intéressantes dans la technologie étudiée.

La technique de *membrane extraction thermal desorption* (METD) est une technique nouvelle destinée à l'analyse des composants semi volatiles et qui est proposée dans ce travail d'investigation. La technique utilise une membrane de fibre creuse pour préconcentrer sélectivement les analytes et élimine l'eau du système (METD-GC-FID). Le gaz porteur qui circule à l'intérieur de la membrane transfert les analytes désorbés pour une analyse quantitative. Comme analytes modèle, on a choisi deux herbicides qui appartiennent à la classe des *thiocarbamates* (*molinate* et *cycloate*). La technique de METD c'est montrée robuste et de bas coût, elle utilise une seule fibre creuse à longueur variable et peut pré-concentrer les analytes dans plusieurs ordres de grandeur d'une manière sélective.

PART I

Introduction

1. Trends in membrane-based research used in sample preparation techniques and sensors

1.1. Introduction

The original Greek meaning of membrane is "thin skin", but this description does not reflect the common use of the term in analytical chemistry, nor the many types of membranes available and the various processes in which membranes are involved [1].

According to the IUPAC recommendation, a membrane is a "structure, having lateral dimensions much greater than its thickness, through which mass transfer may occur under a variety of driving forces" [2]. Following this definition, the classification of membranes can be made by taking into account their nature - biological or synthetic; their structure or morphology - porous, nonporous, asymmetric (composite or integral) or symmetric; their chemical composition - organic or not organic (metallic, glass or ceramic); and their role on the mass transport, which can be active or passive [3]. Generally, "a membrane can be considered as a selective barrier or interface between two phases". The phase from which the transfer of mass occurs is called the donor or feed phase and the phase that receives the flow is called the acceptor or permeate phase [3] (Fig.1.1).

Currently, major fields of membrane application are in the desalination of natural waters by reverse osmosis and electrodialysis, the purification and concentration of impurities from wastewaters or industrial sewage by electrodialysis, the treatment of patients with chronic and acute uremia by hemodialysis, the splitting of gas streams or removal of specific gases (gas separation), the degasification of water using membrane contactors and the purification of enzymes by ultra-filtration [4, 5, 1].

More recently, membranes have gained widespread use in sample preparation in analytical chemistry, mainly in micro- or ultra-filtration.

Moreover, they have been consolidated as indispensable barriers in ion-chromatography (IC), being commonly used for eluent generation and conductivity suppression via electrodialysis and Donnan dialysis [1]. Protective membranes and reagents-impregnated films have also played an outstanding role in the design of electrochemical sensors [6] and optodes [7], as well as gas-sensing, ion-selective electrodes [8].

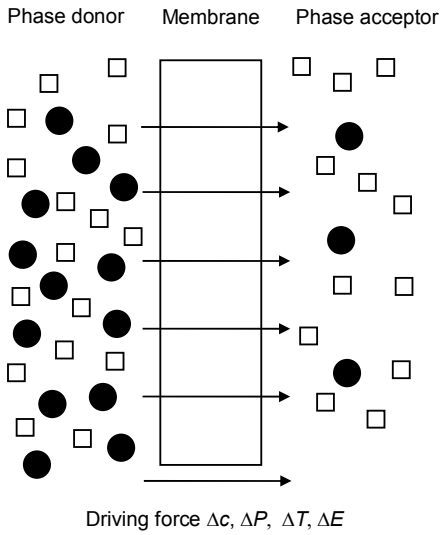

Fig. 1.1. Schematic representation of the transport through membranes (based on [3]).

New areas of applications of membrane related technologies are also being explored in promising fields [9], such as nano- and microcapsules delivery systems, intelligent membranes, low cost membrane-based sensors, allowing for the improvement of performance and safety of small to medium size gas separation units, proton exchange membranes for fuel cells [10], catalytic membrane reactors [11], yielding more environmentally safe and economically efficient processes and ultra-nano-porous membranes [12] (zeolite and carbon molecular sieve membranes) for highly efficient gas separation.

The main objective of this thesis is to describe two promising developments of membrane science: the use of polymeric membranes in sensors and solvent-free membrane-based sample preparation techniques. The present introduction gives an overview of the current status of the membrane-based sample preparation techniques, with emphasis on principles and a description of examples of recent applications of these techniques in analysis of biological, food and environmental samples. The developing role of membranes as gas sensors, pH sensors, ion-selective sensors, humidity sensors, bio-sensors devices, sensor arrays, etc, is also reviewed and discussed in this work.

1.2. Membrane-based sample preparation techniques

Sample preparation is currently regarded as one of the fundamental steps in the analytical process, as well as the bottleneck in several analytical methodologies. The main objectives of sample preparation are: clean-up of the sample, which involves the removal of the matrix compounds disturbing the subsequent chemical derivatization reaction and/or the detection principle; and dilution or pre-concentration of the sample to bring the analyte concentration within the linear dynamic working range of the established procedure [1]. New approaches for sample preparation are thus being sought.

One of the most versatile techniques for the extraction and enrichment of analytes from liquid samples is liquid-liquid extraction (LLE) [13]. However, LLE has some well-known drawbacks, such as labor, time and solvent consumption, waste production, difficulty of automation and on-line connection to analytical instruments, and an often tiresome formation of emulsions. LLE has been largely replaced in the past few years by solid-phase extraction (SPE) using a variety of adsorbents to increase selectivity and reduce bleeding phenomena [14-18]. Indeed, SPE overcomes several disadvantages of LLE, such as the high volume of organic solvent that is required, often chlorinated and sometimes carcinogenic, and the complexity

of coupling it on-line with gas or liquid chromatography. However, SPE is a multi-step process (involving washing, conditioning and elution steps) that is prone to lose analytes if not fully automated and still involves the use of toxic solvents. Furthermore, SPE is limited to semi-volatile compounds, as the boiling points of the analytes must be substantially above those of the solvents. Polar compounds are also difficult to extract using SPE due to their great affinity to water whenever present in the matrix. Finally, breakthrough volumes of cartridges or disk adsorbents normally used in SPE are often too small to achieve sufficient detection limits [19]. Matrix solid-phase dispersion (MSPD) is a more recent technique, based on SPE, and addresses some of the drawbacks of this technique. MSPD is an easier application and reduces the need for organic solvents and consequently is a faster technique [20].

Recently, several new techniques have been developed to overcome the limitations of previous sampling techniques, in particular, the solvent-less procedure, that is more environmentally friendly and less laborious. Among these new techniques are supercritical fluid extraction (SFE) [21, 22], the automated purge and trap system [23], solid-phase microextraction (SPME) [24, 19, 25, 26], pressurized hot water extraction (PHWE) [27, 28], stir bar sorptive extraction (SBSE) [29, 30], solvent-free microwave extraction (SFME) [31], and membrane-based sample preparation techniques [32].

Membrane-based extraction techniques have been used in a variety of analytical applications in recent years [33-35, 5, 32, 1]. Typical membrane extraction involves the flow of sample on one side (referred to as the donor or retentate) of the membrane, while an extractant (gas or liquid) flows on the other side (referred to as the acceptor or sweep stream), and the analytes selectively permeate across the membrane. Since the donor and the acceptor can flow continuously, this approach offers the unique advantage of selective extraction on a continuous basis. Membranes have been interfaced with gas chromatography (GC) [27, 36-38], high performance liquid chromatography (HPLC) [39-41], mass spectrometry (MS) [42-45], capillary electrophoresis [46], flow injection spectrophotometry [47], and CO_2 and solid state SnO_2 gas sensors [48-51], for continuous on-line monitoring. Membrane extraction has also been used in connection with

atomic absorption spectrophotometry (AAS) in off-line mode [52]. There has been much interest in the miniaturization of membrane-based extraction techniques, as well as of analytical instrumentation because it offers several advantages, such as inexpensive mass production and low reagent consumption [53-56, 37, 41].

The main membrane-based techniques (Table 1.1) that have been used for analytical applications can be classified depending on whether the membrane is porous or nonporous (dense) during the extraction of the sample solution [33, 32, 28]. A clear difference is that selectivity for porous membranes is mainly based on size exclusion and selective ion transport (electrodialysis) [33]. A nonporous membrane can be either a porous membrane impregnated with a liquid or entirely a solid, such as silicone rubber. On the other hand, the permeability of a nonporous membrane towards a compound can be determined from the product of the sorption and diffusion coefficients [3]. The emphasis of the present chapter is on the nonporous membrane-based extraction techniques. Examples of such techniques are membrane extraction with sorbent interface (MESI) [57] and membrane inlet mass spectrometry (MIMS) [58], which are three-phase systems (donor, receiver and membrane phase). The membrane extraction techniques are summarized in Table 1.1.

Membranes have also been used in micro-, ultra-, nano- and hyper filtration (reverse osmosis) [59, 4, 5]. However, membrane filtration techniques are strictly no extraction techniques [33, 32, 28] and will not be considered within the framework of this thesis.

Table 1.1

Different major membrane-based sample preparation techniques used in analytical chemistry.

Name	Abbreviation	Membrane type	Phase combination used Donor/membrane/acceptor	Ref.
Filtration	-	porous	aq/membrane/aq	[28]
Dialysis	-	porous	aq/membrane/aq	[28]
Supported liquid membrane extraction	SLM	nonporous	aq/org/aq	[32]
Microporous membrane liquid-liquid extraction	MMLLE	nonporous	aq/org/org org/org/aq	[32]
Polymer membrane extraction	PME	nonporous	aq/polymer/aq org/polymer/aq aq/polymer/org	[32]
Membrane inlet mass spectrometry	MIMS	nonporous	gas/polymer/vacuum aq/polymer/vacuum	[28]
Membrane extraction with sorbent interface	MESI	nonporous	gas/polymer/gas liq/polymer/gas	[28]

1.2.1. Extraction with porous membranes

Dialysis is a general term that encompasses passive dialysis, electrodialysis and Donnan dialysis, where the driving forces behind the separation are the concentration gradient alone, driven by an electric field, or an ionic strength gradient driven across an ion-exchange membrane, respectively [33]. Dialysis through porous films is the oldest process that makes use of separation through membranes [5]. Passive dialysis is commonly employed in analytical applications to separate low-molecular mass compounds from interfering macromolecules, humic substances, colloidal matter and suspended particles [60, 61]. Donnan or active dialysis is an ion exchange membrane process that can be used for the purification and concentration of diluted solutions. It is based on a chemical potential difference between two compartments separated by an ion exchange membrane polymer. Typical applications are trace-metal enrichment, recovery and speciation followed by atomic absorption spectrophotometric detection [62, 63]. Like Donnan dialysis, electrodialysis can be used to enrich ionic compounds, such as chloride in industrial effluents [64] and to remove salt from produced water (water co-produced with gas and oil) [65]. Applications can also be found in ion-chromatography (IC) systems for generating the eluent in-line, neutralizing alkaline samples prior to analysis and suppressing conductivity with self-regenerating of solutions [1]. Traditionally, microdialysis sampling has extensively been used in the areas of neurochemistry and pharmacokinetic studies. Recently, the applicability of microdialysis sampling has been reported for wastewater quality monitoring, such as metals ions and saccharides in wastewater effluent from a beverage industry, and monitoring of the uptake of metal ions by plants, such as tomatoes grown on sewage sludge manure [66, 67].

1.2.2. Extraction with nonporous membranes

Supported liquid membrane (SLM) extraction was first suggested by Audunsson [68]. It is a versatile, flow-through membrane extraction (ME) technique suitable for selective removal of polar compounds, such as organic acids or bases, charged compounds and metal ions from aqueous samples [69, 34, 35]. It is a three-phase system, where the analytes are extracted from a water sample into an aqueous acceptor through an organic extractant held in the pores of the membrane by capillary action. The organic phase (e.g., n-undecane or kerosene, di-n-hexyl ether and tri-n-octylphosphate or solvent-mixture) is held typically in a microporous hydrophobic membrane (e.g., poly(tetrafluoroethylene) (PTFE) or polypropylene (PP)). The membrane liquid should also be insoluble in water to assure the desired stability. SLM can be seen as a combination of dialysis with two-step liquid-liquid extraction with the use of a low amount of organic solvents, resulting in lower chemical costs. The analytes on one side of the membrane are maintained at a determined pH, where they are uncharged and can be extracted into the organic phase in the membrane pores. On the other side of the membrane, there is a solution at a different pH, into which the analytes are back-extracted in their ionic forms [34, 32]. The driving force is the difference in concentration of the uncharged analyte across the membrane (Fig. 1.2). The main limitation of SLM is that its applicability is restricted to ionisable organic analytes with hydrophobicity values, i.e. logarithm of octanol-water partition coefficient values in the range 2-4 [70]. However, its extension to compounds outside this range, including various permanently charged compounds and metal ions, is feasible via carrier mediated-SLM based on the solubilisation of crown ethers or ion-pairing, hydrogen bonding or chelating reagents (e.g., methyltrioctyl-ammonium chloride, tri-n-octylphosphine oxide (TOPO) and di-2-ethylhexylphosphoric acid, respectively) into the membrane phase. As a result, neutral, extractable species are formed at the donor-membrane interface and are swept irreversibly into the receiver solution after partitioning in the liquid membrane [35]. Typical SLM extraction modules have been made using flat sheet

membranes in a flow cell [39, 40, 52, 41] or using multiple parallel hollow fibers in a shell-and-tube format [54, 52]. With SLM, various analytes in complex matrices have been efficiently enriched and quantified, such as bambuterol (aromatic amine) in blood plasma [54], methoxy-*s*-triazine herbicides in river water [39], phenolic acids in the nutrient solution of greenhouse crops of tomato [40], Ni(II) in effluents in the metal finishing industry [52], and haloacetics acids (HAAs) in drinking water [41], among others.

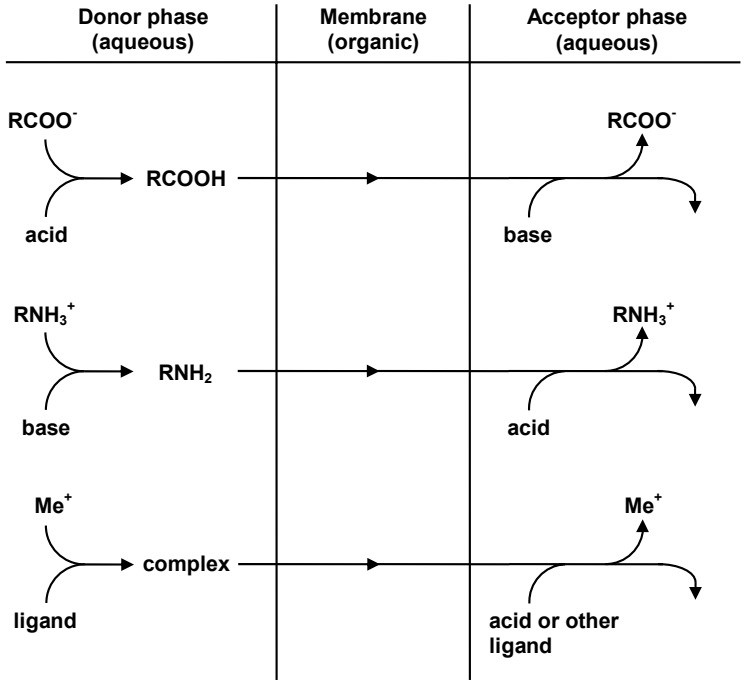

Fig. 1.2. Schematic representation of the principle of the extraction of carboxylic acids, amines and metal ions using the supported liquid membrane (SLM) extraction technique (based on [69]).

Microporous membrane liquid-liquid extraction technique (MMLLE) [71, 34, 35] is a two-phase system that uses a porous membrane with an

organic solvent both in the membrane pores and in the acceptor phase. MMLLE differs from SLM in that it involves only one liquid-liquid extraction step (aq-org or org-aq) and is more suited for non-polar organic compounds. In Fig. 1.3, the principle of MMLLE is sketched. Both flat sheet and hollow fiber membrane units can be applied in MMLLE. The membrane normally used is PTFE or PP. The acceptor solvents were hexane, isooctane, chlorobutane, cyclopentane, n-octanol, methyl tert-butyl ether (MTBE)-hexane, cyclohexane, toluene and chloroform. Environmental applications include the determination of anionic surfactants in detergents [47], aromatic amines in tap, river and waste waters [46], polycyclic aromatic hydrocarbons (PAHs) in soil and sediment [27, 28], and pesticides in green grapes and red wines [38, 36].

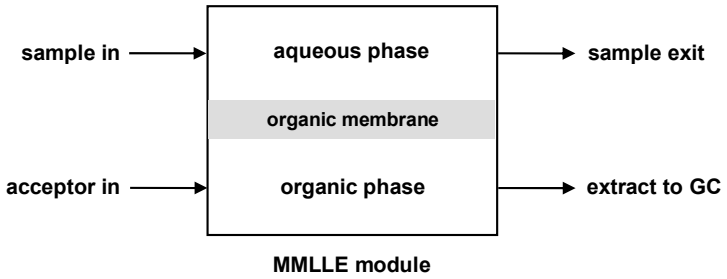

Fig. 1.3. Schematic representation of the principle of the microporous membrane liquid-liquid extraction technique (MMLLE) (based on [32]).

Liquid-phase microextraction (LPME) is a three phase liquid membrane extraction in a porous hollow fiber. The fiber is impregnated with an organic phase (μl) to create both SLM and MMLLE techniques, depending on the nature of the acceptor phase, inside the fibers. Hou and Lee [72] used the LPME technique for the analysis of trace amounts of pesticides in soil.

Melcher and co-workerthiocarbamates (molinate and cycloate)s [73, 74] developed a similar approach, which uses nonporous hollow fiber

membranes (silicone rubber), to interface aqueous samples to flow injection analysis (FIA), gas chromatography and liquid chromatography. In polymeric membrane extraction (PME) applications, the compounds which permeate the membrane from the sample are removed at the other side of the membrane with an extractant liquid. The driving force for the extraction is related to the diffusion coefficient and the ratio of partition coefficient of the analyte between the sample matrix and the membrane on one side of the membrane and between the membrane and the extractant on the other side of the membrane. This system yields a more stable membrane, but provides less versatility and slower mass transfer rates than SLM. There are possibilities for both aqueous-polymer-aqueous extraction including trapping in the acceptor in a way similar to SML extraction and also, for example, aqueous-polymer-organic extraction similar to MMLLE [32]. The technique was applied to the determination of chlorinated aromatic compounds and pesticides, as well as pentachlorophenol and other chlorinated phenols in wastewater effluent [73, 74].

Membrane introduction mass spectroscopy (MIMS) is an analytical technique able to detect trace organics in aqueous solutions. Analytes of interest are introduced into a mass spectrometer through a membrane by pervaporation [58, 75, 76]. Pervaporation is a membrane-based process in which the retentate stream is liquid while the permeate stream emerges at the downstream face of the membrane as a vapor [2]. Hoch and Kok [77] pioneered the development of MIMS to follow the kinetics of photosynthesis, *in situ*, by measuring oxygen and carbon dioxide. A few years later, Westover et al. [78] used MIMS for the quantification of chloroform and methanol. In this application, silicone hollow fiber membranes were used for the first time to interface nitrogen and aqueous solutions directly to a mass spectrometer. A number of studies have since followed. MIMS has been applied for environmental and blood analysis [78, 79], as well as for fermentation monitoring [80]. In the environmental field, MIMS has been used in the determination of volatile organic compounds (VOCs) (mainly BTEX: benzene, toluene, ethylbenzene, xylenes, and chlorinated compounds) in synthetic air and water [81, 44], drinking water [82],

groundwater [83], seawater [42], aroma/flavor constituents in synthetic air [84], semi-volatile organic compounds (SVOCs) and organometallic compounds in synthetic air and water [44], cyanogenic glycosides in cassava (*Manihot esculenta* Crantz) roots extracts [43], cyanogen chloride and cyanogen bromide in synthetic water, saline water, natural surface water and wastewater [45], among others.

Blanchard and Hardy [85, 86] were among the first authors to couple membrane extraction with gas chromatography. They used a flat sheet silicone polycarbonate membrane to separate volatile organic pollutants from an aqueous sample and nitrogen to strip the analytes (sweep gas) from the membrane surface to a bed of activated charcoal. The analytes were then desorbed from the charcoal with carbon disulfide for GC analysis. A solvent-free membrane extraction-GC system for analyzing water samples was developed using microporous PP and nonporous silicone rubber hollow fiber membranes [87]. The conditions under which quantitative extraction occurred were studied through mathematical modeling of the system [88].

The membrane extraction with a sorbent interface (MESI) technique is based on membrane extraction into a gas followed by trapping of the analytes on a solid sorbent (cryofocusing) and subsequent thermal desorption into a GC system [89-91, 57, 92, 93]. The receiving phase is always a carrier gas that continuously strips off and transports the analytes on the sorbent (Fig. 1.4). The basis of selectivity of the method is the difference in solubility and diffusion of various analytes into the nonporous polymer. The application of a hydrophobic silicone membrane prevents excessive amounts of moisture from entering the analytical system. The detailed theory of this technique, applied either for headspace analysis, air or direct aqueous sample extractions, has been described by Pawlizyn et al. [94-96]. The main drawback of MESI is that it has a narrow application window for environmental analysis; only VOCs can be extracted. Typical environmental applications for MESI are analysis of VOCs in tap water [55], surface water and underwater [97], contaminated groundwater and raw sewage [98], clean water and wastewater [99], rain [99, 100], air [99-101, 56], sand [100], soil [101], breath [102, 51], plant emissions [103, 37] and

thermal degradation products of polymers [104, 105]. For the analysis of SVOCs, such as phenols from an aqueous matrix, a high-pressure membrane extraction module has been built and high-density CO_2 used as a stripping phase [106, 107]. The MESI technique has also been improved by introducing catalytic reactions together with the membrane extraction - catalytic membrane [108].

Other membrane-based MESI-like techniques that differ in the type of heating, physical arrangement of the membrane and detector used have been described [109, 110, 49, 111, 50]. In thermal membrane desorption application (TMDA), the analytes are set free by thermal desorption of the membrane module [112]. TMDA has been mainly applied to monitoring fermentation processes [112, 113]. Compared to MESI, TMDA allows more efficient sampling of less volatile organic and polar analytes [114].

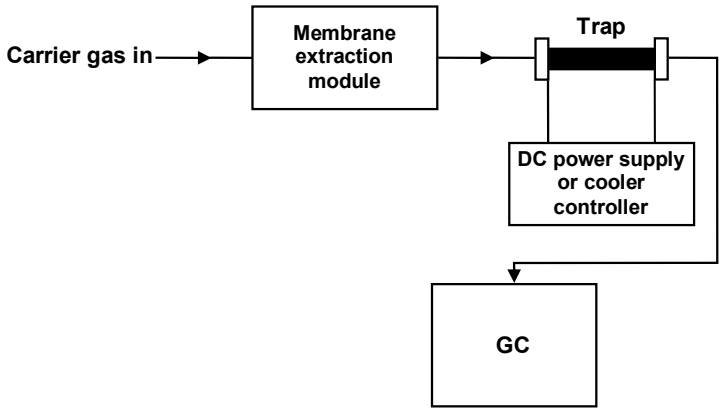

Fig. 1.4. Sketch of the MESI-GC system (based on [51]).

MESI, MIMS and PME with an aqueous acceptor do not require any solvent and SLM extraction requires only negligible amounts of high-boiling organic liquid in the membrane. For MMLLE and PME with an organic acceptor, small amounts of organic solvents are needed, but in most applications the volumes used are less than 1 ml [32].

1.3. Membrane-based sensors

According to the IUPAC definition, a chemical sensor is a device that transforms chemical information, ranging from the concentration of a specific sample component to total composition analysis, into an analytically useful signal. The chemical information, mentioned above, may originate from a chemical reaction of the analyte or from a physical property of the system investigated [115]. Chemical sensors contain two basic functional units: a receptor part and a transducer part (Fig. 1.5). Some sensors may include a separator, which is, for example, a membrane. Chemical sensors may be classified according to the operating principle of the transducer - optical, electrochemical, electrical, mass sensitive, paramagnetic, magnetic, thermometric and other devices (other physical properties); to the method used for measuring the effect - MESI, catalytic devices, etc.; to the analyte/property to be determined - sensors for pH, metal ions, carbon dioxide, etc; and to the mode of application - for use in vivo, in analytical laboratories or for process monitoring. It is possible to use various classifications as long as they are based on clearly defined and logically arranged principles [116, 115]. A biosensor may be considered as a combination of a bio-receptor, as the biological component and a transducer, as the detection method [117]. Sensor technology is a rapidly growing area with new applications being reported every year in the several journals covering this topic. Increasingly, advances in technology bring new features, such as low cost and disposability that are valuable in medical, environmental and industrial applications. Another feature is the incorporation of biological components forming a key part of the sensor in areas where the devices are used for techniques such as screening of bio-molecules or on-line monitoring of patients parameters [118].

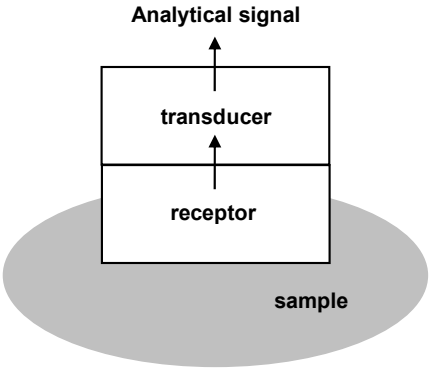

Fig. 1.5. Schematic representation of a chemical sensor (IUPAC definition) (based on [119]).

Semi conducting metal oxides (e.g. SnO_2, ZnO, TiO_2, LaOCl) [120-127] and more generally semiconductors (SiC, InP, CuBr) [128-130], solid electrolytes (e.g. Nasicon: sodium super ionic conductor and hydronium Nasicon) [131-139], ionic membranes, and organic semiconductors (polypyrrole) have been the classical materials used in sensor devices [117].

The role of membranes in chemical- and bio-sensors is now presented. Membranes used in sensor devices either participate in sensing mechanisms or immobilize the component responsible for sensing the analyte [140, 117]. Special emphasis is given to the gas sensors.

1.3.1. Membrane-based sensors for gases analysis

The emission of gaseous pollutants such as sulfur oxide, nitrogen oxide and other toxic gases from related industries has become a serious environmental concern. Sensors are needed to detect and monitor the concentration of such gaseous pollutants. Analytical gas sensors therefore offer a promising and inexpensive solution to problems related to hazardous gases in the environment. Measurement and control of gases are also important in other areas, including industry, the domestic environment, and medicine (respiratory equipment), etc. Table 1.2 shows examples of membrane-based sensors for analyzing specific gases (identification and/or quantification). One of the examples shown is a quartz crystal microbalance (QCM) sensor which is very sensitive to mass changes (ng) because the resonance frequency changes when a given mass of analyte is deposited on the electrode of the quartz crystal [141] (Fig. 1.6).

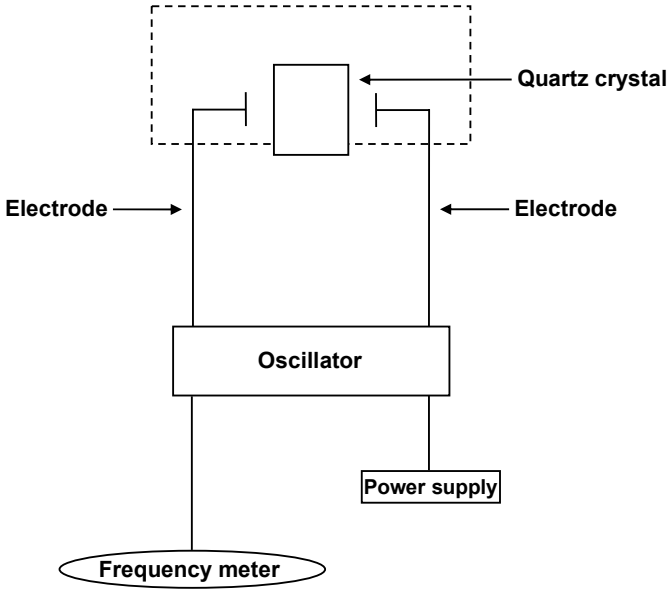

Fig. 1.6. Schematic representation of a quartz crystal microbalance (QCM) sensor (based on [117]).

Table 1.2. Polymers used in various membrane specific gas sensors.

Gas	Device/techniques/principles	Polymer	Fields of application	Ref.
SO_2	Electrochemical/Conductometric sensor	Poly(tetrafluoroethylene) (PTFE) (Teflon®)	Atmospheric air	[142]
NH_3	Optical sensor/absorbance	Poly(vinylchloride) (PVC) with ionophores and Teflon	-	[7]
	Optical sensor/absorbance	Teflon	-	[143]
	Quartz crystal microbalance (QCM)	Poly(acrylic acid) (PAA)	-	[144]
NO_2	Electrochemical/Amperometric sensor based on Pt/Nafion electrode	Nafion® (copolymer of tetrafluoroethylene and sulfonyl fluoride vinyl ether)	-	[145]
NO	Electrochemical/Amperometric sensor	Poly(dimethylsiloxane) (PDMS)	-	[146]
HCl	Optochemical detection	5,10,15,20-tetra(4'-alkoxyphenyl)porphyrin ($TP(OR)PH_2$) embedded in poly(hexylacrylate) (HA), poly(hexylmethacrylate) (HMA), poly(butylmethacrylate) (BuMA)	-	[147]
H_2S	Electrochemical sensor	Nafion	-	[148]
O_2	Optical sensor/luminescence	Tris(2-phenylpyridine anion) iridium(III) complex ($[Ir(ppy)_3]$) immobilized in fluoropolymer, poly(styrene-*co*-2,2,2-trifluoroethylmethacrylate) - (poly(styrene-*co*-TFEM)	-	[149]

Table 1.2. (continued)

Gas	Device/techniques/principles	Polymer	Fields of application	Ref.
O_2	Optical sensor/fluorescence	Aluminum 2,9,16,23-tetraphenoxy-29*H*, 31*H*-phthalocyanine hydroxide (AlPc(OH)-polystyrene (PS)	-	[150]
	Semiconductor sensor (SnO_2)	Teflon	-	[151]
	Electrochemical/Amperometric transducer	Poly(dimethylsiloxane) (PDMS)	-	[146]
	Optical sensor/colorimetric sensor/absorbance	2,6-dichloroindophenol (2,6-DCIP) (indicador dye) with fructose and base in ethylcellulose (EC)	-	[152]
	Electrochemical/amperometric sensor	Poly(ethylene) (PE)	-	[153]
O_2, CO_2	Electrochemical sensor	Poly(ethylene) (PE) Teflon	Photosynthesis process	[154]
CO_2	Electrochemical/Potentiometric sensor	Tefzel (Teflon-like material)	-	[155]
	Electrochemical/Coulometric sensor	Teflon	Air	[156]

Table 1.2. (continued)

Gas	Device/techniques/principles	Polymer	Fields of application	Ref.
CO_2 (dissolved)	Electrochemical/Coulometric sensor	Silicone	Water and synthetic seawater	[157]
	Electrochemical/Amperometric sensor	Silicone	Blood serum	[158]
CH_4	Electrochemical/Stripping voltammetry (Pt/Nafion electrode)	Nafion	-	[159]
Toluene, p-xylene diethylether chloroform acetone	Quartz crystal resonator microbalance	Propylene-butyl copolymer	-	[141]
H_2	Electrochemical/Potentiometric measurement	Ion-selective poly(vinylchloride) (PVC) and Polypyrrole (PPy)	-	[160]
Ethane, propane butane	Electrochemical/Stripping voltammetry (Pt/Nafion electrode)	Nafion	-	[159]
Polar and non-polar gases (ethanol, propan-1-ol, trichloromethane, etc)	Capacitive sensor (CMOS technology)	Poly(etherurethane) (PUT) poly(cyanopropylmethylsiloxane) (PCM) poly(epichlorohydrine) (PECH) ethylcellulose (EC)	-	[161]

1.3.2. Membrane-based sensors for non-gas species analysis

Membrane-based sensors have found extensive applications in clinical, food and chemical analysis, as well as environmental monitoring. Devices have been applied, for example, to the determination of transaminases and pH in blood serum [162, 163], urea [164], ethanol in alcoholic beverages [165], hydrogen sulfite (HSO_3^-) in foods [166], fructose in fruit juices [167], humidity [168], flavonol in olive oil [169] and ascorbic acid in pharmaceutical tablets [6]. Sensors have also been developed for environmental control, for instance, for the determination of organic solvents in wastewater [143], chlorinated hydrocarbons in water [48], the hardness of tap water [8], biological oxygen demand (BOD) in various substrates and domestic wastewater [170, 171], hydrazines in both ambient and vacuum environments [172], triazine herbicides (simazine, atrazine, and propazine) [173], nitrate in fertilizers, as well as in drinking and natural water (well and ditch) [174, 175], and chemical oxygen demand (COD) in water from lakes [176], sulfite ion (SO_3^{2-}) [177], among others.

Among the most important applications of enzyme sensors, considered as the combination of a transducer and a thin enzymatic layer, is the determination of reducing sugars, such as glucose [178-180] and fructose [181, 167]. A schematic representation of an enzyme sensor is given in Fig. 1.7. The sensitive surface of the transducer remains in contact with an enzymatic layer, and it is assumed that there is no mass transfer across this interface. The external surface of the enzymatic layer is kept immersed in a solution containing the analyte under study. The analyte migrates towards the interior of the layer and is converted into reaction products when it reacts with the immobilized enzyme [117].

Sensor arrays for multi-component analysis coupled with pattern recognition are useful in the discrimination of the aroma and taste of certain foods and beverages. Examples using electrical conducting polymers include the detection of component parts of taste and aroma in coffee, tea, red wine and extra-virgin olive oil [182-184]. Zeolite and carbon membranes have also been used in different types of chemical sensors in order to

increase their selectivity [134, 185-189].

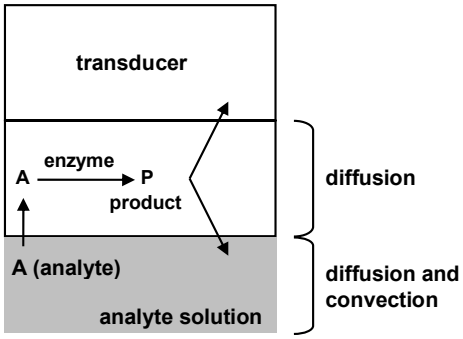

Fig. 1.7. Schematic representation of an enzyme sensor. Diffusion of the analyte A from solution to enzyme layer and the product P via enzymatic reaction to the transducer (based on [117]).

Research is now focused on the development of more robust and reliable sensors, aiming to achieve the highest possible specificity, minimizing interferences, as well as ensuring a long useful life. Attention is also being paid to the development of new types of sensors by taking advantage of the growing availability of new materials [190]. Also, the automation of the sensors is rapidly being improved. The main goal is to be able to monitor the results, obtained at different points, from a remote location using a communication network, where, unlike the usual classical procedure in which the samples were taken into a laboratory for analysis, or in a more modern version samples are analyzed *in situ* and the results stored in a laptop [191]. Finally, the miniaturization of sensors, minimizing the reagents consumption, waste and cost, is being reinforced. These sensors also need a small sample volume, a short period of analysis and are compatible with miniaturized data acquisition [119].

Membranes have long been used in a broad range of applications. Within this thesis, hollow fiber membranes have been applied in the

development of new concentration gas sensors for binary or pseudo-binary mixtures and solvent-free sample preparation techniques.

The asymmetric hollow fibers membranes used were poly(dimethylsiloxane) (PDMS) and Teflon-AF composite membranes and a poly(etherimide) (PEI) integral membrane. PEI is the porous support (shell side) for both composite membranes. Fig. 1.8 shows the repeat units of PDMS and PEI polymers, as well as the copolymer of poly(2,2-bistrifluoromethyl-4,5-difluoro-1,3-dioxole) and poly(tetrafluoroethylene) (PDD/PTFE) (Teflon-AF) [192]. All membranes are very stable even at temperatures close to 500ºC.

(a)

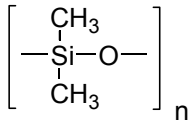

(b)

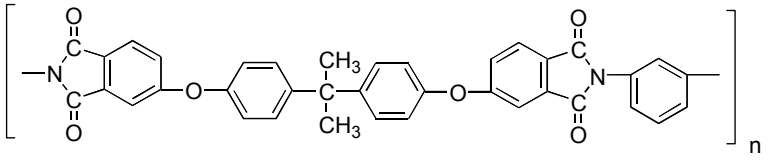

(c)

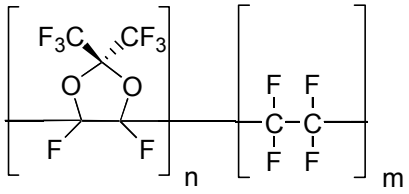

Fig. 1.8. Repeat units of the polymers (a): PDMS; (b): PEI; and (c): PDD/PTFE (copolymer).

The new concentration gas sensor was applied to binary mixtures of oxygen/nitrogen, carbon dioxide/methane, carbon dioxide/helium, hydrogen/methane and hydrogen/nitrogen.

A new solvent-free extraction technique, the membrane extraction thermal desorption technique is described and tested. This technique was applied to the quantification of two commonly used herbicides, molinate and cycloate, whose chemical structures are shown in Fig. 1.9.

(a)

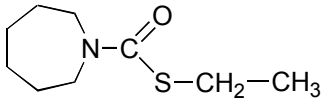

(b)

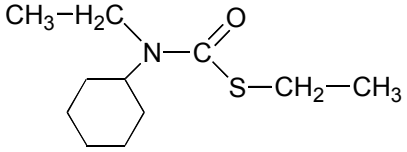

Fig. 1.9. Chemical structures of molinate (a) and cycloate (b).

References

[1] M. Miró, W. Frenzel, Automated membrane-based sampling and sample preparation exploiting flow-injection analysis, Trends Anal. Chem. 23 (2004) 624-636.

[2] W.J. Koros, Y.H. Ma, T. Shimidzu, Terminology for membranes and membrane processes, Pure & Appl. Chem. 68 (1996) 1479-1489.

[3] M. Mulder, Basic Principles of Membrane Technology, second ed., Kluwer Academic Publishers, Dordrecht, 2000 (Chapter 1).

[4] R. Singh, Industrial membrane separation processes, Chemtech (*now* Chem. Innov.) 28 (1998) 33-44.

[5] C.G. Pinto, M.E.F. Laespada, J.L.P. Pavón, B.M. Cordero, Analytical applications of separations techniques through membranes, Lab. Autom. Inform. Manage. 34 (1999) 115-130.

[6] P.G. Veltsistas, M.I. Prodromidis, C.E. Efstathiou, All-solid-state potentiometric sensors for ascorbic acid by using a screen-printed compatible solid contact, Anal. Chim. Acta 502 (2004) 15-22.

[7] S. Ozawa, P.C. Hauser, K. Seiler, S.S.S. Tan, W.E. Morf, W. Simon, Ammonia-gas-selective optical sensors based on neutral ionophores, Anal Chem. 63 (1991) 640.

[8] Z. Hu, D. Qi, Water hardness ion-selective electrode based on a neutral carrier, Anal. Chim. Acta 248 (1991) 177-181.

[9] A. Mendes, F. Magalhães, C. Costa, New Trends on Membrane Science in: J. Fraissard, C.W. Conner (Eds.), Fluid Transport in Nanoporous Materials, Kluwer Academic Publishers, in press.

[10] V. Silva, Direct methanol fuel cell: Analysis based on experimentation and modelling. Ph.D. Thesis, Universidade do Porto, Portugal (2005) 1-225.

[11] L. Brandão, D. Fritsch, L.M. Madeira, A.M. Mendes, Kinetics of propylene hydrogenation on nanostructured palladium clusters, Chemical Engineering Journal 103 (2004) 89-97.

[12] S. Lagorsse, A. Leite, F.D. Magalhães, N. Bischofberger, J. Rathenow, A. Mendes, Novel carbon molecular sieve honeycomb membrane module: configuration and membrane characterization, Carbon 43 (2005) 809-819.

[13] C.J. Soderquist, J.B. Bowers, D.G. Crosby, Dissipation of molinate in a rice field, J. Agric. Food Chem. 25 (1977) 940-945.
[14] J.M. Soriano, B. Jiménez, M.J. Redondo, J.C. Moltó, Comparison of different sorbents for on-line liquid-solid extraction followed by high-performance liquid chromatographic determination of nitrogen-containing pesticides, J. Chromatogr. A 822 (1998) 67-73.
[15] T.A. Albanis, D.G. Hela, T.M. Sakellarides, I.K. Konstantinou, Monitoring of pesticide residues and their metabolites in surface and underground waters of Imathia (N. Greece) by means of solid-phase extraction disks and gas chromatography, J. Chromatogr. A 823 (1998) 59-71.
[16] C. Aguilar, I. Ferrer, F. Borrull, R.M. Marcé, D. Barceló, Monitoring of pesticides in river water based on samples previously stored in polymeric cartridges followed by on-line solid-phase extraction-liquid chromatography-diode array detection and confirmation by atmospheric pressure chemical ionization mass spectrometry, Anal. Chim. Acta 386 (1999) 237-248.
[17] A. Di Corcia, M. Nazzari, R. Rao, R. Samperi, E. Sebastiani, Simultaneous determination of acidic and non-acidic pesticides in natural waters by liquid chromatography-mass spectrometry, J. Chromatogr. A 878 (2000) 87-98.
[18] P.C. Nascimento, A.L.B. Rohlfes, D. Bohrer, L.M. Carvalho, E.J. Pilau, HPLC based method using sample precolumn cleanup for the determination of triazines and thiolcarbamates in hemodialysis saline solutions, Talanta 65 (2005) 211-216.
[19] J. Pawliszyn, Solid Phase Microextraction, Theory and Practice; Wiley-VCH, Inc.: New York, 1997.
[20] X.-G. Chu, X.-Z. Hu, H.-Y. Yao, Determination of 266 pesticide residues in apple juice by matrix solid-phase dispersion and gas chromatography-mass selective detection, J. Chromatogr. A 1063 (2005) 201-210.
[21] J.J. Langenfeld, S.B. Hawthorne, D.J. Miller, J. Pawliszyn, Effects of temperature and pressure on supercritical fluid extraction efficiencies of polycyclic aromatic hydrocarbons and polychlorinated biphenyls, Anal. Chem. 65 (1993) 338-344.

[22] S. Bøwadt, L. Mazeas, D. J. Mi ller, S. H. Hawthorne, Field-portable determination of polychlorinated biphenyls and polynuclear aromatic hydrocarbons in soil using supercritical fluid extraction, J. Chromatogr. A 785 (1997) 205-217.

[23] A. Ekdahl, K. Abrahamsson, A simple and sensitive method for the determination of volatile halogenated organic compounds in sea water in the amol l^{-1} to pmol l^{-1} range, Anal. Chim. Acta 357 (1997) 197-209.

[24] Z. Zhang, M.J. Yang, J. Pawliszyn, Solid-phase microextraction, Anal. Chem. 66 (1994) 844A-853A.

[25] M. Sakamoto, T. Tsutsumi, Applicability of headspace solid-phase microextraction to the determination of multi-class pesticides in waters, J. Chromatogr. A 1028 (2004) 63-74.

[26] C. Deng, J. Zhang, X. Yu, W. Zhang, X. Zhang, Determination of acetone in human breath by gas chromatography-mass spectrometry and solid-phase microextraction with on-fiber derivatization, J. Chromatogr. B 810 (2004) 269-275.

[27] K. Kuosmanen, T. Hyötyläinen, K. Hartonen, M.-L. Riekkola, Analysis of polycyclic aromatic hydrocarbons in soil and sediment with on-line coupled pressurized hot water extraction, hollow fiber microporous membrane liquid-liquid extraction and gas chromatography, Analyst 128 (2003) 434-439.

[28] K. Lüthje, On-line coupling of pressurized hot water extraction and microporous membrane liquid-liquid extraction with chromatography in analysis of environmental samples, Ph.D. Thesis, University of Helsinki, Finland (2004) 1-77.

[29] P. Sandra, B. Tienpont, F. David, Multi-residue screening of pesticides in vegetables, fruits and baby food by stir bar sorptive extraction-thermal desorption-capillary gas chromatography-mass spectrometry, J. Chromatogr. A 1000 (2003) 299-309.

[30] G. Roy, R. Vuillemin, J. Guyomarch, On-site determination of polynuclear aromatic hydrocarbons in seawater by stir bar sorptive extraction (SBSE) and thermal desorption GC-MS, Talanta 66 (2005) 540-546.

[31] M.E. Lucchesi, F. Chemat, J. Smadja, Solvent-free microwave extraction of essential oil from aromatic herbs: comparison with conventional hydro-distillation, J. Chromatogr. A 1043 (2004) 323-327.
[32] J.-Å. Jönsson, L. Mathiasson, Membrane-based techniques for sample enrichment, J. Chromatogr. A 902 (2000) 205-225.
[33] N.C. van de Merbel, Membrane-based sample preparation coupled on-line to chromatography or electrophoresis, J. Chromatogr. A 856 (1999) 55-82.
[34] J.-Å. Jönsson, L. Mathiasson, Liquid membrane extraction in analytical sample preparation. I. Principles, Trends Anal. Chem. 18 (1999) 318-325.
[35] J.-Å. Jönsson, L. Mathiasson, Liquid membrane extraction in analytical sample preparation. II. Applications, Trends Anal. Chem. 18 (1999) 325-334.
[36] T. Hyötyläinem, K. Lüthje, M. Rautiainen-Rämä, M.-L. Riekkola, Determination of pesticides in red wines with on-line coupled microporous membrane liquid-liquid extraction-gas chromatography, J. Chromatogr. A 1056 (2004) 267-271.
[37] X. Liu, R. Pawliszyn, L. Wang, J. Pawliszyn, On-site monitoring of biogenic emissions from Eucalyptus dunnii leaves using membrane extraction with sorbent interface combined with a portable gas chromatograph system, Analyst 129 (2004) 55-62.
[38] K. Lüthje, T. Hyötyläinen, M. Rautiainen-Rämä, M.-L. Riekkola, Pressurized hot water extraction-microporous membrane liquid-liquid extraction coupled on-line with gas chromatography-mass spectrometry in the analysis of pesticides in grapes, Analyst 130 (2005) 52-58.
[39] N. Megersa, T. Solomon, J.-Å. Jönsson, Supported liquid membrane extraction for sample work-up and preconcentration of methoxy-*s*-triazine herbicides in a flow system, J. Chromatogr. A 830 (1999) 203-210.
[40] V. Jung, L. Chimuca, J.-Å. Jönsson, N. Niedack, P. Bowens, B. Alsanius, Supported liquid membrane for identification of phenolic compounds in the nutrient solution of closed hydroponic growing systems for tomato, Anal. Chim. Acta 474 (2002) 49-57.
[41] X. Wang, C. Saridara, S. Mitra, Microfluidic supported liquid membrane extraction, Anal. Chim. Acta 543 (2005) 92-98.

[42] N. Kasthurikrishnan, R.G. Cooks, On-line flow injection analysis of volatile organic compounds in seawater by membrane introduction mass spectrometry, Talanta 42 (1995) 1325-1334.

[43] L.A.B. Moraes, M.N. Eberlin, J.R. Cagnon, L.H. Urbano, A new method for the selective quantification of cyanogenic glycosides by membrane introduction mass spectrometry, Analyst 125 (2000) 1529-1531.

[44] T.M. Allen, M.E. Cisper, P.H. Hemberger, C.W. Wilkerson Jr., Simultaneous detection of volatile, semivolatile organic compounds, and organometallic compounds in both air and water matrices by using membrane introduction mass spectrometry, Int. J. Mass Spectrom. 212 (2001) 197-204.

[45] X. Yang, C. Shang, Quantification of aqueous cyanogen chloride and cyanogen bromide in environmental samples by MIMS, Water Res. 39 (2005) 1709-1718.

[46] Q. Zhou, G. Jiang, J. Liu, Y. Cai, Combination of microporous membrane liquid-liquid extraction and capillary electrophoresis for the analysis of aromatic amines in water samples, Anal. Chim. Acta 509 (2004) 55-62.

[47] L. Jing-fu, J. Gui-bin, Determination of anionic surfactants in detergents by microporous membrane liquid-liquid extraction and flow injection spectrophotometry, Microchemical Journal, 68 (2001) 29-33.

[48] J.R Stetter, Z. Cao, Gas sensor and permeation apparatus for the determination of chlorinated hydrocarbons in water, Anal. Chem. 62 (1990) 182-185.

[49] M. Straková, E. Matisová, P. Šimon, J. Annus, J.M. Lisý, Silicone membrane measuring system with SnO_2 gas sensor for on-line monitoring of volatile organic compounds in water, Sens. Actuators B 52 (1998) 274-282.

[50] M. Straková, E. Matisová, P. Šimon, On-line combination of a silicone-tubing-probe measuring system with HRGC for the analysis of VOCs from water samples, Intern. J. Environ. Anal. Chem. 73 (1999) 59-69.

[51] Y. Yu, J. Pawliszyn, On-line monitoring of breath by membrane extraction with a sorbent interface coupled with CO_2 sensor, J. Chromatogr. A 1056 (2004) 35-41.

[52] I. van de Voorde, L. Pinoy, R.F. De Ketelaere, Recovery of nickel ions by supported liquid membrane (SLM) extraction, J. Membr. Sci. 234 (2004) 11-21.

[53] E. Thordarson, S. Pálmarsdóttir, L. Mathiasson, J.-Å. Jönsson, Sample preparation using a miniaturized supported liquid membrane device connected on-line to packed capillary liquid chromatography, Anal. Chem. 68 (1996) 2559-2563.

[54] T. Górecki, J. Pawliszyn, Modern sample-preparation technologies for fast GC analysis with field-portable instrumentation, LC·GC Int. 12 (1999) 123-127.

[55] A. Segal, T. Górecki, P. Mussche, J. Lips, J. Pawliszyn, Development of membrane extraction with a sorbent interface-micro gas chromatography system for field analysis, J. Chromatogr. A 873 (2000) 13-27.

[56] I. Ciucanu, J. Pawliszyn, Design of continuous-monitoring device based on membrane extraction with sorbent interface and micro-gas chromatograph, Field Analyt. Chem. Technol. 5 (2001) 69-74.

[57] M.J. Yang, J. Pawliszyn, Membrane extraction with a sorbent interface, LC·GC Int. 9 (1996) 283-296.

[58] T. Kotiaho, F.R. Lauritsen, T.K. Choudhury, R.G. Cooks, G.T. Tsao, Membrane introduction mass spectrometry, Anal. Chem. 63 (1991) 875A-883A.

[59] D.C. Warren, New frontiers in membrane technology and chromatography: applications for biotechnology, Anal. Chem. 56 (1984) 1529A-1544A.

[60] K.K. Stewart, L.C. Craig, Thin film dialysis studies with highly acetylated cellophane membranes, Anal. Chem. 42 (1970) 1257-1260.

[61] B. Strandberg, P.-A. Bergqvist, C. Rappe, Dialysis with semipermeable membranes as an efficient lipid removal method in the analysis of bioaccumulative chemicals, Anal. Chem. 70 (1998) 526-533.

[62] D.-E. Akretche, H. Kerdjoudj, Donnan dialysis of copper, gold and silver cyanides with various anion exchange membranes, Talanta 51 (2000) 281-289.

[63] A.L. Nolan, M.J. Mclaughlin, S.D. Mason, Chemical speciation of Zn, Cd, Cu, and Pb in pore waters of agricultural and contaminated soils using Donnan dialysis, Environ. Sci. Technol. 37 (2003) 90-98.

[64] J.F. van Staden, C.J. Hattingh, Incorporation o electrodialysers into the conduits of FIA systems: enhancement of the mass transfer of chloride anions through passive neutral membranes, Talanta, 45 (1998) 485-492.

[65] T. Sirivedhin, J. McCue, L. Dallbauman, Reclaiming produced water for beneficial use: salt removal by electrodialysis, J. Membr. Sci. 243 (2004) 335-343.

[66] N. Torto, B. Lobelo, L. Gorton, Determination of saccharides in wastewaster from the beverage industry by microdialysis sampling, microbore high performance anion exchange chromatography and integrated pulsed electrochemical detection, Analyst 125 (2000) 1379-1381.

[67] N. Torto, J. Mwatseteza, G. Sawula, A study of microdialysis sampling of metal ions, Anal. Chim. Acta 456 (2002) 253-261.

[68] G. Audunsson, Aqueous/aqueous extraction by means of a liquid membrane for sample cleanup and preconcentration of amines in a flow system, Anal. Chem. 58 (1986) 2714-2723.

[69] J.-Å. Jönsson, L.Mathiasson, Supported liquid membrane techniques for sample preparation and enrichment in environmental and biological analysis, Trends Anal. Chem. 11 (1992) 106-114.

[70] L. Chimuca, L. Mathiasson, J.-Å. Jönsson, Role of octanol-water partition coefficients in extraction of ionisable organic compounds in a supported liquid membrane with a stagnant acceptor, Anal. Chim. Acta 416 (2000) 77-86.

[71] Y. Sahleström, B. Karlberg, An unsegmented extraction system for flow injection analysis, Anal. Chim. Acta 179 (1986) 315-325.

[72] L. Hou, H.K. Lee, Determination of pesticides in soil by liquid-phase microextraction and gas chromatography-mass spectrometry, J. Chromatogr. A 1038 (2004) 37-48.

[73] R.G. Melcher, P.L. Morabito, Membrane/gas chromatographic system for automated extraction and determination of trace organics in aqueous samples, Anal. Chem. 62 (1990) 2183-2188.

[74] R.G. Melcher, D.W. Bakke, G.H. Hughes, On-line membrane/liquid chromatographic analyzer for pentachlorophenol and other trace phenols in wastewater, Anal. Chem. 64 (1992) 2258-2262.
[75] S. Bauer, Membrane introduction mass spectrometry; an old method that is gaining new interest through recent technological advances, Trends Anal. Chem. 14 (1995) 202-213.
[76] N. Srinivasan, R.C. Johnson, N. Kasthurikrishnan, P. Wong, R.G. Cooks, Membrane introduction mass spectrometry, Anal. Chim. Acta 350 (1997) 257-271.
[77] G. Hoch, B. Kok, A mass spectrometer inlet system for sampling gases dissolved in liquid phases, Arch. Biochem. Biophys. 101 (1963) 160-170.
[78] L.B. Westover, J.C. Tou, J.H. Mark, Novel mass spectrometric sampling device-hollow fiber probe, Anal. Chem. 46 (1974) 568-571.
[79] J.S. Brodbelt, R.G. Cooks, J.C. Tou, G.J. Kallos, M.D. Dryzga, In vivo mass spectrometric determination of organic compounds in blood with a membrane probe, Anal. Chem. 59 (1987) 454-458.
[80] M.E. Bier, R.G. Cooks, Membrane interface for selective introduction of volatile compounds directly into the ionization chamber of a mass spectrometer, Anal. Chem. 59 (1987) 597-601.
[81] M.A. LaPack, J.C. Tou, C.G. Enke, Membrane mass spectrometry for the direct trace analysis of volatile organic compounds in air and water, Anal. Chem. 62 (1990) 1265-1271.
[82] L.E. Slivon, M.R. Bauer, J.S. Ho, W.L. Budde, Helium-purged hollow fiber membrane mass spectrometer interface for continuous measurement of organic compounds in water, Anal. Chem. 63 (1991) 1335-1340.
[83] V.T. Virkki, R.A. Ketola, M. Ojala, T. Kotiaho, V. Komppa, A. Grove, S. Facchetti, On-site environmental analysis by membrane inlet mass spectrometry, Anal. Chem. 67 (1995) 1421-1425.
[84] J.C. Tou, D.C. Rulf, P.T. DeLassus, Mass spectrometric system for the measurement of aroma/flavor permeation rates across polymer films, Anal. Chem. 62 (1990) 592-597.

[85] R.D. Blanchard, J.K. Hardy, Use of a permeation sampler for determination of volatile priority pollutants, Anal. Chem. 56 (1984) 1621-1624.

[86] R.D. Blanchard, J.K. Hardy, Continuous monitoring device for the collection of 23 volatile organic priority pollutants, Anal. Chem. 58 (1986) 1529-1532.

[87] K.F. Pratt, J. Pawliszyn, Water monitoring system based on gas extraction with a single hollow fiber membrane and gas chromatographic cryotrapping, Anal. Chem. 64 (1992) 2107-2110.

[88] K.F. Pratt, J. Pawliszyn, Gas extraction kinetics of volatile organic species from water with a hollow fiber membrane, Anal. Chem. 64 (1992) 2101-2106.

[89] A.A. Boyd-Boland, M. Chai, Y.Z. Luo, Z. Zhang, M.J. Yang, J.B. Pawliszyn, T. Górecki, New solvent-free sample preparation techniques based on fiber and polymer technologies, Environ. Sci. Technol. 28 (1994) 569A-574A.

[90] M.J. Yang, Y.Z. Luo, J. Pawliszyn, A two-step sample prep for GC, Chemtech 24 (1994) 31-37.

[91] J. Pawliszyn, Process and device for continuous extraction and analysis of fluid using membrane, U. S. Patent 5,492,838 (1996).

[92] M.J. Yang, J. Pawliszyn, Multiplex gas chromatography: a practical approach for environmental monitoring, Trends Anal. Chem. 15 (1996) 273-278.

[93] Y. Luo, Membrane extraction with a sorbent interface, Ph.D. Thesis, University of Waterloo, Ontario, Canada (1999) 1-173.

[94] M.J. Yang,; M. Adams, J. Pawliszyn, Kinetic model of membrane extraction with a sorbent interface, Anal. Chem. 68 (1996) 2782-2789.

[95] Y.Z. Luo, M. Adams, J. Pawliszyn, Aqueous sample direct extraction and analysis by membrane extraction with a sorbent interface, Analyst 122 (1997) 1461-1469.

[96] Y.Z. Luo, M. Adams, J. Pawliszyn, Kinetic study of membrane extraction with a sorbent interface for air analysis, Anal. Chem. 70 (1998) 248-254.

[97] Y.Z. Luo, J. Pawliszyn, Membrane extraction with a sorbent interface for headspace monitoring of aqueous samples using a cap sampling device, Anal. Chem. 72 (2000) 1058-1063.

[98] M. J. Yang, J. Pawliszyn, Multiplex gas chromatography with a hollow fiber membrane interface for determination of trace volatile organic compounds in aqueous samples, Anal. Chem. 65 (1993) 1758-1763.

[99] M.J. Yang, S. Harms, Y.Z. Luo, J. Pawliszyn, Membrane extraction with a sorbent interface for capillary gas chromatography, Anal. Chem. 66 (1994) 1339-1346.

[100] Y.Z. Luo, M.J. Yang, J. Pawliszyn, Membrane extraction combined with a sorbent coated fiber interface for capillary gas chromatography, J. High Resol. Chromatogr. 18 (1995) 727-732.

[101] M.J. Yang, J. Pawliszyn, Headspace membrane extraction combined with multiplex gas chromatography and mass selective detector for monitoring of volatile organic compounds, J. Microcolumn Separations, 8 (1996) 89-98.

[102] H. Lord, Y. Yu, A. Segal, J. Pawliszyn, Breath analysis and monitoring by membrane extraction with a sorbent interface, Anal. Chem. 74 (2002) 5650-5657.

[103] L. Wang, H. Lord, R. Morehead, F. Dorman, J. Pawliszyn, Sampling and monitoring of biogenic emissions by eucalyptus leaves using membrane extraction with sorbent interface (MESI), J. Agric. Food Chem. 50 (2002) 6281-6286.

[104] M. Kaykhaii, A. Sarafraz-Yazdi, M. Chamsaz, J. Pawliszyn, Membrane extraction with a sorbent interface-gas chromatography as an effective and fast means for continuous monitoring of thermal degradation products of polyacrylonitrile, Analyst 127 (2002) 912-916.

[105] I. Ciucanu, M. Kaykhaii, L. Montero, J. Pawliszyn, J. Szubra, Continuous monitoring of thermooxidative degradation products of polystyrene by membrane extraction with sorbent interface-gas chromatography, J. Chromatogr. Sci. 40 (2002) 350-354.

[106] M.J. Yang, J. Pawliszyn, Extraction of semivolatile organic compounds from aqueous samples using high-density carbon dioxide and hollow fiber membrane module, Anal. Chem. 65 (1993) 2538-2541.
[107] M.J. Yang, Membrane extraction techniques for sample preparation, Ph.D. Thesis, University of Waterloo, Ontario, Canada (1995) 1-245.
[108] Y. Shen, J. Pawliszyn, Catalytic reductions in membrane extraction as sample preparation for gas chromatographic analysis, J. Sep. Sci. 24 (2001) 623-626.
[109] B.V. Burger, W.J.G. Burger, I. Burger, Trace determination of volatile organic compounds in water using permeation through a hollow fiber membrane and carrier gas stripping, J. High Resol. Chromatogr. 19 (1996) 571-576.
[110] S. Mitra, N. Zhu, X. Zhang, B. Kebbekus, Continuous monitoring of volatile organic compounds in air emissions using an on-line membrane extraction-microtrap-gas chromatographic system, J. Chromatogr. A 736 (1996) 165-173.
[111] X. Guo, S. Mitra, Theoretical analysis of non-steady-state, pulse introduction membrane extraction with a sorbent trap interface for gas chromatographic detection, Anal. Chem. 71 (1999) 4587-4593.
[112] G. Matz, F. Lennemann, On-line monitoring of biotechnological processes by gas chromatographic-mass spectrometric analysis of fermentation suspensions, J. Chromatogr. A 750 (1996) 141-149.
[113] G. Matz, M. Loogk, F. Lennemann, On-line gas chromatography-mass spectrometry for process monitoring using solvent-free sample preparation, J. Chromatogr. A 819 (1998) 51-60.
[114] G. Matz, G. Kibelka, J. Dahl, F. Lennemann, Experimental study on solvent-less sample preparation methods: membrane extraction with a sorbent interface, thermal membrane desorption application and purge-and-trap, J. Chromatogr. A 830 (1999) 365-376.
[115] A. Hulanicki, S. Glab, F. Ingman, Chemical sensors definitions and classification, Pure & Appl. Chem. 63 (1991) 1247-1250.
[116] P. Vadgama, Membrane based sensors: a review, J. Membr. Sci. 50 (1990) 141-152.

[117] B. Adhikari, S. Majumdar, Polymers in sensor applications, Prog. Polym. Sci., 29 (2004) 699-766.

[118] P. Ball, Applications of microporous membranes in sensor technology, Sensor Review 19 (1999) 46-51.

[119] Fifth eurosensors school on “Fundamentals of sensor science and technology”, Rome, Italy, September 11-12 (2004).

[120] C. Pijolat, R. Lalauze, P. Tatry, Hydrogen detection by SnO_2 gas sensors, Proceedings of the European Workshop on Chemical Sensors for Metallurgical Processes 8-9 December (1994) Mol, Belgium.

[121] C. Pijolat, G. Tournier, R. Lalauze, C. Testud, P. Tatry, Hydrogen detection by SnO_2 gas sensors, Proceedings of the Eurosensors XI September (1997) Warsaw, Poland.

[122] J.C. Kim, H.K. Jun, J.-S. Huh, D.D. Lee, Tin oxide-based methane gas sensor promoted by alumina-supported Pd catalyst, Sens. Actuators B 45 (1997) 271-277.

[123] G. Tournier, C. Pijolat, Influence of oxygen concentration in the carrier gas on the response of tin dioxide sensor under hydrogen and methane, Sens. Actuators B 61 (1999) 43-50.

[124] B.W. Licznerski, K. Nitsch, H. Teterycz, P.M. Szecówka, K. Wiśniewski, Humidity insensitive thick film methane sensor based on SnO_2/Pt, Sens. Actuators B 57 (1999) 192-196.

[125] S.-D. Choi, D.-D. Lee, CH_4 sensing characteristics of K-, Ca-, Mg impregnated SnO_2 sensors, Sens. Actuators B 77 (2001) 335-338.

[126] A. Marsal, A. Cornet, J.R. Morante, Study of the CO and humidity interference in La doped thin oxide CO_2 gas sensor, Sens. Actuators B 94 (2003) 324-329.

[127] A. Marsal, G. Dezanneau, A. Cornet, J.R. Morante, A new CO_2 gas sensing material, Sens. Actuators B 95 (2003) 266-270.

[128] C.K. Kim, J.H. Lee, S.M. Choi, I.H. Noh; H.R. Kim, N.I. Cho, C. Hong, G.E. Jang, Pd- and Pt-SiC schottky diodes for detection of H_2 and CH_4 at high temperature, Sens. Actuators B 77 (2001) 455-462.

[129] H.-I. Chen, Y.I. Chou, C.-Y. Chu, A novel high-sensitive Pd/InP hydrogen sensor fabricated by electroless plating, Sens. Actuators B 85 (2002) 10-18.

[130] M. Bendahan, P. Lauque, J.-L. Seguin, K. Aguir, P. Knauth, Development of an ammonia gas sensor, Sens. Actuators B 95 (2003) 170-176.

[131] N. Maffei, A.K. Kuriakose, A hydrogen sensor based on a hydrogen ion conducting solid electrolyte, Sens. Actuators B 56 (1999) 243-246.

[132] N. Imanaka, M. Kamikawa, S. Tamura, G. Adachi, Carbon dioxide gas sensing with the combination of trivalent Sc^{3+} ion conducting $Sc_2(WO_4)_3$ and O^{2-} ion conducting stabilized zirconia solid electrolytes, Solid State Ionics 133 (2000) 279-285.

[133] Y. Yang, C.-C. Liu, Development of a Nasicon-based amperometric carbon dioxide sensor, Sens. Actuators B 62 (2000) 30-34.

[134] K. Kaneyasu, K. Otsuka, Y. Setoguchi, S. Sonoda, T. Nakahara, I. Aso, N. Nakagaichi, A carbon dioxide gas sensor based on solid electrolyte for air quality control, Sens. Actuators B 66 (2000) 56-58.

[135] N. Imanaka, A. Ogura, M. Kamikawa, G.-ya Adachi, CO_2 gas sensor with the combination of tetravalent zirconium cation and divalent oxide anion conducting solids with water-insoluble oxycarbonate electrode, Electrochemistry Communications 3 (2001) 451-454.

[136] L.N. van Rij, R.C. van Landschoot, J. Schoonman, Detection of methane in oxygen-poor atmospheres using a catalytic asymmetric sensor design, Sens. Actuators B 75 (2001) 111-120.

[137] N. Imanaka, M. Kamikawa, S. Tamura, G. Adachi, Carbon dioxide gas sensor with multivalent cation conducting solid electrolytes, Sens. Actuators B 77 (2001) 301-306.

[138] J. Ramírez-Salgado, P. Fabry, Feasibility of potentiometric oxygen gas sensor based on perovskite and sodium titanate measuring electrode, Sens. Actuators B 82 (2002) 34-39.

[139] E. Magori, G. Reinhardt, M. Fleischer, R. Mayer, H. Meixner, Thick film device for the detection of NO and oxygen in exhaust gases, Sens. Actuators B 95 (2003) 162-169.

[140] P. Ball, Use of membranes in sensor technology, Membr. Technol. 101 (1998) 9-11.

[141] H. Nanto, N. Dougami, T. Mukai, M. Habara, E. Kusano, A. Kinbara, A smart gas sensor using polymer-film-coated quartz resonator microbalance, Sens. Actuators B 66 (2000) 16-18.

[142] J.S. Symanski, S. Bruckenstein, Conductometric sensor for parts per billion sulfur dioxide determination, Anal. Chem. 58 (1986) 1771-1777.

[143] F.L. Dickert, S.K. Schreiner, G.R. Mages, H. Kimmel, Fiber-optic dipping sensor for organic solvents in wastewater, Anal. Chem. 61 (1989) 2306-2309.

[144] B. Ding, M. Yamazaki, S. Shiratori, Electrospun fibrous polyacrylic acid membrane-based gas sensors, Sens. Actuators B 106 (2005) 477-483.

[145] K.-C. Ho, W.-T. Hung, An amperometric NO_2 gas sensor based on Pt/Nafion® electrode, Sens. Actuators B 79 (2001) 11-16.

[146] F. Mizutani, S. Yabuki, T. Sawaguchi, Y. Hirata, Y. Sato, S. Iijima, Use of a siloxane polymer for the preparation of amperometric sensors: O_2 and NO sensors and enzyme sensors, Sens. Actuators B 76 (2001) 489-493.

[147] K. Nakagawa, Y. Sadaoka, H. Supriyatno, A. Kubo, C. Tsutsumi, K. Tabuchi, Optochemical HCl gas detection using alkoxy substituted tetraphenylporphyrin-polymer composite films. Effects of alkoxy chain length on sensing characteristics, Sens. Actuators B 76 (2001) 42-46.

[148] G. Schiavon, G. Zotti, R. Toniolo, G. Bontempelli, Electrochemical detection of trace hydrogen sulfide in gaseous samples by porous silver electrodes supported on ion-exchange membranes (solid polymer electrolytes), Anal. Chem. 67 (1995) 318-323.

[149] Y. Amao, Y. Ishikawa, I. Okura, Green luminescent iridium(III) complex immobilized in fluoropolymer film as optical oxygen-sensing material, Anal. Chim. Acta 445 (2001) 177-182.

[150] Y. Amao, K. Asai, I. Okura, Fluorescence quenching oxygen sensor using an aluminum phthalocyanine-polystyrene film, Anal. Chim. Acta 407 (2000) 41-44.

[151] J. Atkinson, A. Cranny, C.S. de Cloke, A low-cost oxygen sensor fabricated as a screen-printed semiconductor device suitable for unheated operation at ambient temperatures, Sens. Actuators B 47 (1998) 171-180.

[152] K. Eaton, A novel colorimetric oxygen sensor: dye redox chemistry in a thin polymer film, Sens. Actuators B 85 (2002) 42-51.

[153] K. Katakura, A. Noma, Z. Ogumi, Z.-i. Takehara, An oxygen sensor composed of tightly stacked membrane/electrode/electrolyte, Chem. Lett. 19 (1990) 1291-1294.

[154] M. Takahashi, T. Ishiji, N. Kawashima, Handmade oxygen and carbon dioxide sensors for monitoring the photosynthesis process as instruction material for science education, Sens. Actuators B 77 (2001) 237-243.

[155] R.K. Kobos, S.J. Parks, M.E. Meyerhoff, Selectivity characteristics of potentiometric carbon dioxide sensors with various gas membrane materials, Anal. Chem. 54 (1982) 1976-1980.

[156] T. Trapp, B. Ross, K. Cammann, E. Schirmer, C. Berthold, Development of a coulometric CO_2 gas sensor, Sens. Actuators B 50 (1998) 97-103.

[157] K. Wiegran, T. Trapp, K. Cammann, Development of a dissolved carbon dioxide sensor based on a coulometric titration, Sens. Actuators B 57 (1999) 120-124.

[158] R. Fasching, F. Keplinger, G. Hanreich, G. Jobst, G. Urban, F. Kohl, R. Chabicovsky, A novel miniaturized sensor for carbon dioxide dissolved in liquids, Sens. Actuators B 78 (2001) 291-297.

[159] P. Jacquinot, B. Müller, B. Wehrli, P.C. Hauser, Determination of methane and other small hydrocarbons with a platinum-Nafion electrode by stripping voltammetry, Anal. Chim. Acta 432 (2001) 1-10.

[160] N. Zine, J. Bausells, A. Ivorra, J. Aguiló, M. Zabala, F. Teixidor, C. Masalles, C. Viñas, A. Errachid, Hydrogen-selective microelectrodes based on silicon needles, Sens. Actuators B 91 (2003) 76-82.

[161] C. Cornila, A. Hierlemann, R. Lenggenhager, P. Malcovati, H. Baltes, G. Noetzel, U. Weimar, W. Göpel, Capacitive sensors in CMOS technology with polymer coating, Sens. Actuators B 24-25 (1995) 357-361.

[162] K. Kihara, E. Yasukawa, S. Hirose, Sequential determination of glutamate-oxalacetate transaminase and glutamate-pyruvate transaminase activities in serum using an immobilized bienzyme-poly(vinyl chloride) membrane electrode, Anal. Chem. 56 (1984) 1876-1880.

[163] N. Oyama, T. Hirokawa, S. Yamaguchi, N. Ushizawa, T. Shimomura, Hydrogen ion selective microelectrode prepared by modifying an electrode with polymers, Anal. Chem. 59 (1987) 258-262.

[164] H. Barhoumi, A. Maaref, M. Rammah, C. Martelet, N. Jaffrezic-Renault, C. Mousty, S. Cosnier, E. Perez, I. Rico-Lattes, Insulator semiconductor structures coated with biodegradable latexes as encapsulation matrix for urease, Biosens. Bioelectron. 20 (2005) 2318-2323.

[165] Y. Kitagawa, K. Kitabatake, M. Suda, H. Muramatsu, T. Ataka, A. Mori, K. Tamiya, I. Karube, Amperometric detection of alcohol in beer using a flow cell and immobilized alcohol dehydrogenase. Anal. Chem. 63 (1991) 2391-2393.

[166] M. Kuratli, M. Badertscher, B. Rusterholz, W. Simon, Bisulfite addition reaction as the basis for a hydrogensulfite bulk optode, Anal. Chem. 65 (1993) 3473-3479.

[167] K.T. Kinnear, H.G. Monbouquette, An amperometric fructose biosensor based on fructose dehydrogenase immobilized in a membrane mimetic layer on gold, Anal. Chem. 69 (1997) 1771-1775.

[168] X.-L. Su, X. Xingguo, T. Dallas, S. Gangopadhyay, H. Temkin, X. Wang, R. Walulu, J. Li, P.K. Dasgupta, A microfabricated amperometric moisture sensor, Talanta 56 (2002) 309-321.

[169] J.L. Suárez-Rodríguez, M.E. Días-García, Flavonol fluorecent flow-through sensing based on a molecular imprinted polymer, Anal. Chim. Acta 405 (2000) 67-76.

[170] A. Ohki, K. Shinohara, O. Ito, K. Naka, S. Maeda, T. Sato, H. Akano, N. Kato, Y. Kawamura, A BOD sensor using *Klebsiella Oxytoca* AS1, Intern. J. Environ. Anal. Chem. 56 (1994) 261.

[171] C. Schan, M. Lehmann, K. Chan, P. Chan, C. Chan, B. Gruendig, G. Kunze, R. Renneberg, Designing an amperometric thick-film microbial BOD sensor, Biosens. Bioelectron. 15 (2000) 343-353.

[172] D.L. Ellis, M.R. Zakin, L.S. Bernstein, M.F. Rubner, Conductive polymer films as ultrasensitive chemical sensors for hydrazine and monomethylhydrazine vapor, Anal Chem. 68 (1996) 817-822.

[173] C.G. Siontorou, D.P. Nikolelis, U.J. Krull, K.-L. Chiang, Triazine herbicide minisensor based on surface-stabilized bilayer lipid membranes, Anal. Chem. 69 (1997) 3109-3114.

[174] S.A. Glazier, E.R. Campbell, W.H. Campbell, Construction and characterization of nitrate reductase-based amperometric electrode and nitrate assay of fertilizers and drinking water, Anal. Chem. 70 (1998) 1511-1515.

[175] L.M. Moretto, P. Ugo, M. Zanata, P. Guerriero, C.R. Martin, Nitrate biosensor based on the ultrathin-film composite membrane concept. Anal Chem. 70 (1998) 2163-2166.

[176] Y.-C. Kim, K.-H. Lee, S. Sasaki, K. Hashimoto, K. Ikebukuro, I. Karube, Photocatalytic sensor for chemical oxygen demand determination based on oxygen electrode, Anal. Chem. 72 (2000) 3379-3382.

[177] S.S.M. Hassan, S.A. Marei, I.H. Badr, H.A. Arida, Flow injection analysis of sulfite ion with a potentiometric titanium phosphate-epoxy based membrane sensor, Talanta 54 (2001) 773-782.

[178] M. Koyama, Y. Sato, M. Aizawa, S. Suzuki, Improved enzyme sensor for glucose with an ultrafiltration membrane and immobilized glucose oxidase, Anal. Chim. Acta 116 (1980) 307-314.

[179] M.J. Muehlbauer, E.J. Guilbeau, B.C. Towe, Model for a thermoelectric enzyme glucose sensor, Anal. Chem. 61 (1989) 77-83.

[180] M. Mascini, D. Moscone, L. Bernardi, In vivo continuous monitoring of glucose by microdialysis and a glucose biosensor, Sens. Actuators B 6 (1992) 143-145.

[181] G.F. Khan, E. Kobatake, H. Shinohara, Y. Ikariyama, M. Aizawa, Molecular interface for an activity controlled enzyme electrode and its application for the determination of fructose, Anal. Chem. 64 (1992) 1254-1258.

[182] R. Stella, J.N. Barisci, G. Serra, G.G. Wallace, D. De Rossi, Characterisation of olive oil by an electronic nose based on conducting polymer sensors, Sens. Actuators B 63 (2000) 1-9.

[183] L. Lvova, A. Legin, Y. Vlasov, G.S. Cha, H. Nam, Multicomponent analysis of Korean green tea by means of disposable all-solid-state potentiometric electronic tongue microsystem, Sens. Actuators B 95 (2003) 391-399.

[184] A. Riul Jr., R.R. Malmegrim, F.J. Fonseca, L.H.C. Mattoso, An artificial taste sensor based on conducting polymers, Biosens. Bioelectron. 18 (2003) 1365-1369.

[185] K. Fukui, S. Nishida, CO gas sensor based on Au-La_2O_3 added SnO_2 ceramics with siliceous zeolite coat, Sens. Actuators B 45 (1997) 101-106.

[186] B.K. Miremadi, K. Colbow, A hydrogen selective gas sensor from highly oriented films of carbon, obtained by fracturing charcoal, Sens. Actuators B 46 (1998) 30-34.

[187] G. Li, S. Kawi, MCM-41 modified SnO_2 gas sensors: sensitivity and selectivity properties, Sens. Actuators B 59 (1999) 1-8.

[188] O. Hugon, M. Sauvan, P. Benech, C. Pijolat, F. Lefebvre, Gas separation with a zeolite filter, application to the enhancement of chemical sensors, Sens. Actuators B 67 (2000) 235-243.

[189] M. Vilaseca, J. Coronas, A. Cirera, A. Cornet, J.R. Morante, J. Santamaría, Use of zeolite films to improve the selectivity of reactive gas sensors, Catal. Today 82 (2003) 179-185.

[190] N. Yamazoe, Toward innovations of gas sensor technology, Sens. Actuators B 108 (2005) 2-14.

[191] A. Bonastre, R. Ors, J.V. Capella, M.J. Fabra, M. Peris, In-line chemical analysis of wastewater: present and future trends, Trends Anal. Chem. 24 (2005) 128-137.

[192] I. Pinnau, L.G. Toy, Gas and vapor transport properties of amorphous perfluorinated copolymer membranes based on 2,2-bistrifluoromethyl-4,5-difluoro-1,3-dioxole/tetarfluoroethylene, J. Membr. Sci. 109 (1996) 125-133.

PART II

Membrane-based sensors

2. Development of a new gas sensor for binary mixtures based on the permselectivity of polymeric membranes. Application to oxygen/nitrogen mixture

Abstract

A new oxygen/nitrogen gas concentration sensor is described in this paper. This new sensor is based on the permselectivity of a membrane element. It is especially suited for the very low price market, to determine the concentration of binary or pseudo-binary gas mixtures in the 0-100% range.

The sensor is made of a permselective membrane module whose permeate stream is linked to a needle valve. The feed composition is related to the permeate build up pressure, measured using a pressure transducer. Poly(dimethylsiloxane) (PDMS) and poly(etherimide) (PEI) hollow fiber membranes were tested. The response curves for both membranes at different temperatures display a quasi-linear behavior. The PDMS membrane based sensor enables continuous and rapid oxygen analysis ($t_{0-95\%}$ = 50 s) with a reproducible and long-term stable signal ($\overline{k}$ (O_2) = 2.474 x 10^{-6} dm^3 (STP) s^{-1} m^{-2} Pa^{-1}, s = 0.045 x 10^{-6}, N = 10; $\overline{k}$ (N_2) = 1.173 x 10^{-6} dm^3 (STP) s^{-1} m^{-2} Pa^{-1}, s = 0.010 x 10^{-6}, N = 11) over 5.4 x 10^6 s. The absolute sensitivity of the PDMS based sensor depends on the oxygen feed concentration ranging from 0.0329 to 0.450 MPa.

A simple analytical model was developed and is presented here. Good agreement was obtained with the experimental results for both membranes.

R. Rego, N. Caetano, R. Vale, A. Mendes, J. Membr. Sci. 244 (2004) 35-44.

2.1. Introduction

Membrane-based processes are currently used in a wide range of different industrial applications, such as desalination of seawater, hemodialysis, the treatment of industrial effluents (sometimes with the recovery of components of economic interest), in food technology, etc [1]. In the field of chemical sensor applications membranes have attracted increasing attention. Polymeric membranes have been widely used in different types of sensors, such as optical [2-7] and electrochemical [8-14], in order to increase their selectivity. Also, zeolite membranes have been proposed to increase the selectivity of semiconductor and optical chemical sensors [15-18]. Kaneyasu et al. reported the use of zeolite as a filter material in order to minimize the effect of interfering gases on the electromotive force of a carbon dioxide gas sensor [19].

This paper describes a new oxygen/nitrogen gas sensor based on the permselectivity of polymeric membranes for binary gas mixtures. The sensor is made of a permselective membrane, a pressure transducer for measuring the permeate pressure and a non-selective barrier (e.g. needle valve) [20]. The non-selective barrier is used to control the permeate outlet to the atmosphere. This new sensor is based on the fact that different gases have different permeabilities on a selective membrane. When the feed pressure is kept constant, the permeate flow is proportional to the gas mixture concentration. However, gas flow meters are expensive and using this principle to determine concentration is not a promising solution. However, if a non-selective barrier, such as a needle valve, is placed on the permeate outlet, the permeate pressure is then proportional to the permeate flow rate and, therefore, to the feed concentration. The permeate pressure can be measured with a cheap pressure transducer. Based on a similar principle, it has been reported that the concentration or partial pressure of gases, especially oxygen, in fluids could be measured with a plastic material that is permeable to only specific gases and is in contact with the fluid [21]. Also, devices to sense dissolved carbon dioxide in beverages using a membrane to interface with the liquid phase have been developed [22]. The molecular

mass distribution of a polymer can be inferred from the observed osmotic pressure across a membrane of a solution of this polymer [23].

In the development of an oxygen/nitrogen sensor it is critical to consider the potential applications, since the design can be adapted/optimized to the purpose. There is a need for a very cheap and reliable oxygen/nitrogen sensor of low/medium precision (±2.5%) for medical oxygen concentrators. These concentrators separate oxygen from air by means of an adsorption process known as pressure swing adsorption (PSA). The sensor described here is especially applicable to these oxygen concentrators where the world market is around 400,000 units/year [24]. The oxygen concentration delivered by these units should never be below 85%, thus a sensor with an incorporated alarm could be provided. It is possible to directly adapt the new sensor to these oxygen concentrators because the product stream pressure is maintained relatively constant at about 0.25 MPa, absolute pressure. To the best of our knowledge the only oxygen sensor that can share the same market as the permselective sensor is one based on the ultrasound speed dependence on a binary gas mixture composition and marketed under the name DigiFLO [25]. The newly proposed oxygen/nitrogen sensor could be further developed into a portable device with a satisfactory sensitivity.

In addition to the application for oxygen monitoring of the outlet stream of medical oxygen concentrators, the new sensor can also be used for determining the composition of other bi-component mixtures in the 0-100% range, such as carbon dioxide/methane, carbon dioxide/helium, hydrogen/nitrogen and hydrogen/methane.

This paper describes the new sensor and reports all tests performed. A simple mathematical model describing its behavior is also reported. Two different polymeric membranes are used: poly(dimethylsiloxane) (PDMS) and poly(etherimide) (PEI) hollow fibers. Results are reported for oxygen/nitrogen gas mixtures. For both membranes, response curves were obtained at three different temperatures. The reproducibility, sensitivity, response time and reversibility, time stability and temperature dependence of the sensor for these two polymers are discussed.

2.2. Mathematical model

The sketch of the binary gas mixture sensor is shown in Fig. 2.1. The gas mixture to be analyzed is supplied at a constant pressure that must be higher than the outlet permeate pressure. In our system the feed pressure (P^F) was set to 0.3 MPa, while the permeate pressure after the needle valve (V) was the ambient pressure (P^{amb}).

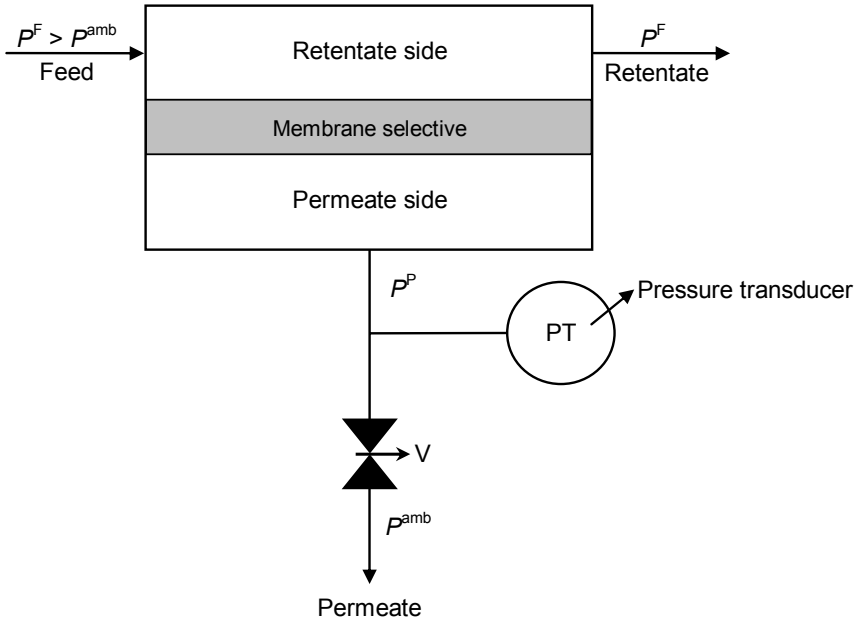

Fig. 2.1. Sketch of the binary gas mixture sensor.

A simple mathematical model of this sensor was developed based on the following main assumptions: isothermal operation, ideal gas behavior, complete mixing flow pattern in both permeate and retentate sides, constant and composition independent permeabilities, constant feed pressure and molar flow rate at the needle valve outlet proportional to the difference

between permeate and ambient pressures. For both membranes considered in this study, nitrogen is the slowest gas while oxygen is the fastest when their permeation characteristics are compared. The model can be written as follows (see mathematical deduction in appendix):

$$x(\mathrm{O}_2) = \frac{P^{\mathrm{P}} - P^{\mathrm{P}}_{\mathrm{min}}}{P^{\mathrm{P}}_{\mathrm{max}} - P^{\mathrm{P}}_{\mathrm{min}}}\left[1 - \frac{P^{\mathrm{amb}}\left(P^{\mathrm{P}} - P^{\mathrm{P}}_{\mathrm{max}}\right)}{P^{\mathrm{F}}\left(P^{\mathrm{P}} - P^{\mathrm{amb}}\right)}\right] \tag{2.1}$$

where $x(\mathrm{O}_2)$ is the oxygen feed molar fraction, P^{P} is the pressure at the permeate side, $P^{\mathrm{P}}_{\mathrm{min}}$ is the minimum pressure at the permeate side, attained when the feed contains only the slowest permeable gas (nitrogen), and $P^{\mathrm{P}}_{\mathrm{max}}$ is the maximum pressure at the permeate side, attained when the feed contains only the fastest gas (oxygen).

When P^{amb} approaches zero Eq. (2.1) becomes linear:

$$x(\mathrm{O}_2) = \frac{P^{\mathrm{P}} - P^{\mathrm{P}}_{\mathrm{min}}}{P^{\mathrm{P}}_{\mathrm{max}} - P^{\mathrm{P}}_{\mathrm{min}}} \tag{2.2}$$

Eq. (2.1) also approaches linearity when the term $\left(P^{\mathrm{P}} - P^{\mathrm{P}}_{\mathrm{max}}\right)$ tends to zero that is for low membrane selectivities.

2.3. Experimental

The sketch of the experimental set-up developed for testing the oxygen/nitrogen sensor is shown in Fig. 2.2.

The oxygen and nitrogen gases used were from Air Liquide, 99.995% purity. Different oxygen/nitrogen compositions in the range of 0-100% (v/v) were produced by controlling the flow rates of oxygen and nitrogen fed to the membrane module using needle valves (V1 and V2). The feed line is made of a 3.9 ID/mm poly(urethane) tube (Festo, PU-4). The feed gas mixture was introduced at the desired flow rate in the bore side of the hollow fiber module

through a three-way valve (V6). The gas flow rate of the feed (MFM1), permeate (MFM2) and retentate (MFM3) were measured using mass flow meters (Bronkhorst Hi-Tec, F-110C-HAD-22-V, F-100D-HAD-11-V, F-111C-HAD-11-V, STP, < ±1% of the full span (FS)). The feed pressure was controlled using two pressure regulators in series (Festo, LRP-1/4-4) and was measured with a pressure transducer (Lucas Schaevitz, P941, range 0-1 MPa, ≤ ±0.1% FS). The permeate pressure was also measured with a pressure transducer (Lucas Schaevitz, PS10061, range 0-0.25 MPa, ≤ ±0.1% FS) and controlled using a needle valve (Swagelok, SS-SS2), V4, which allows a precise flow rate regulation. The retentate flow rate was controlled with a similar needle valve (V5).

The experiments were run until approximately 1000 s after the steady state was attained (stable signal). Data acquisition was done using an acquisition card (Advantech, PCL-818HG). The composition of the feed was measured on-line using a paramagnetic oxygen analyzer (M&C, PMA 22, range 0-100% v/v, ±1% FS). The paramagnetic analyzer was connected to the computer and was used to record the feed oxygen concentration. The analyzer was calibrated every day, following the manufacturer's procedure. After calibration, its accuracy should be ±1% of the full span. The temperature for all the experiments was kept constant with a thermostatic bath (Huber, Polystat K6-1) and was measured with a K type thermocouple (Omega, KMQSS-M150, accuracy ±1.1ºC) connected to a digital thermometer (TES, TES-1300, ± (0.3% + 1.0ºC)). The reproducibility of the oxygen/nitrogen sensor was verified by repeating each experiment two or three times on different days.

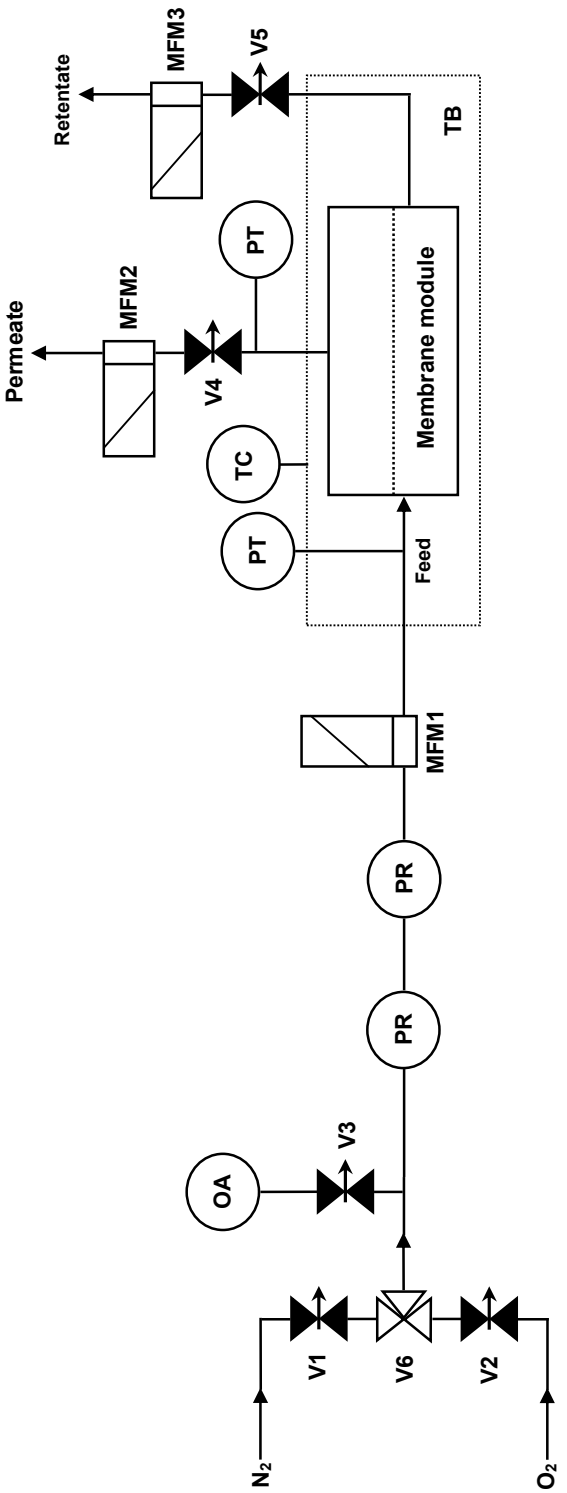

Fig. 2.2. Sketch of the experimental set-up. V1, V2, V3, V4 and V5 are needle valves; V6 is a three-way valve; OA is a paramagnetic oxygen analyzer; PR is a pressure regulator; MFM1, MFM2 and MFM3 are mass flow meters; PT is a pressure transducer; TC is a thermocouple and TB is a thermostatic bath.

Two different hollow fiber membranes were used: a poly(dimethylsiloxane) (PDMS) composite membrane and a poly(etherimide) (PEI) integral asymmetric membrane (GKSS, Germany). Fig. 2.3 shows a scanning electron microscopy of a composite PDMS-PEI hollow fiber with a PDMS selective dense layer (bore side) and a PEI porous support (shell side).

Three membrane modules were prepared in our laboratory by inserting the hollow fibers into a poly(urethane) tube of 5.9 x 10^{-3} m (ID) (Festo, PU-6). Both ends of the modules were sealed with epoxy glue (Degussa AG, Agomet P 76). The modules were tested for leakage with hydrogen before being used. Fig. 2.4 depicts a hollow fiber membrane module.

The characteristics of the hollow fiber membranes and the membrane modules are shown in Table 2.1.

Table 2.1

Characteristics of the hollow fiber membranes and membrane modules.

	Module reference		
	Poly(dimethylsiloxane) (PDMS)		Poly(etherimide) (PEI)
#	PDMS #1	PDMS #2	PEI #1
Number of fibers	15	10	14
Fiber OD/mm	1.04	1.04	1.04
Fiber ID/mm	0.71	0.71	0.72
Work fiber length/mm	133	133	98

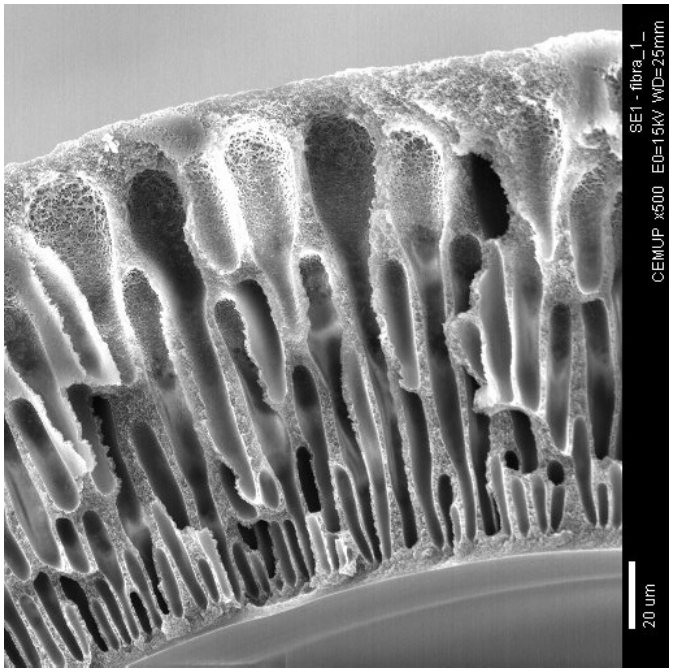

(b)

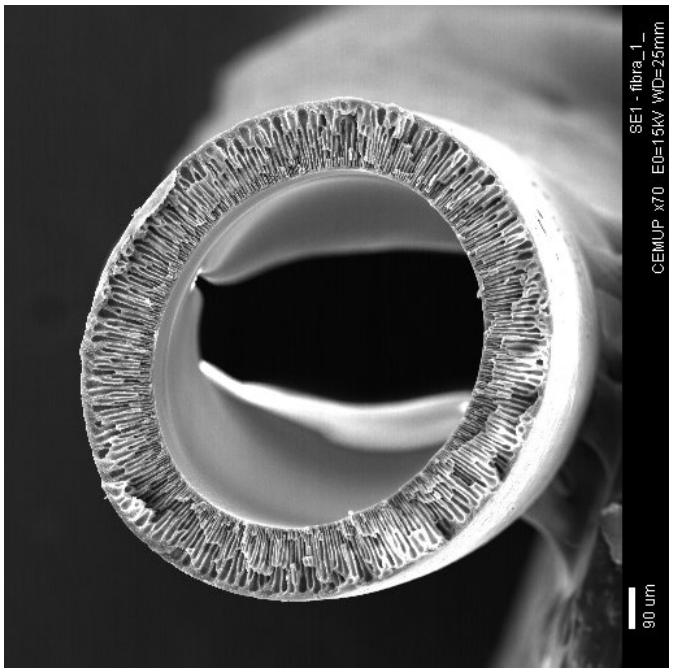

(a)

Fig. 2.3. Scanning electron microscopy image of the PDMS-PEI membrane: (a) overall view of the cross-section (magnification x70); (b) view of the bore and shell sides of the fiber with PDMS film in the bore side and PEI in the shell side (magnification x500).

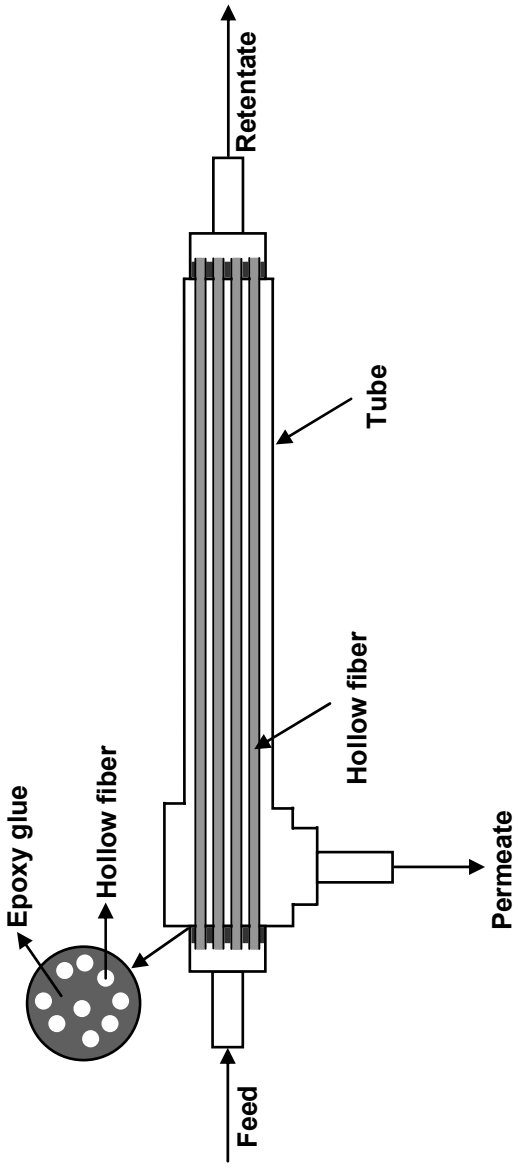

Fig. 2.4. Schematic view of the hollow fiber membrane module.

2.4. Results and discussion

The main objective of this work is to study the performance of the membrane-based sensors. Thus, the following items were evaluated for the oxygen/nitrogen gas sensor: response curves, reproducibility, response time and reversibility and long-term stability. The influence of operating conditions, such as temperature, was also analyzed.

Membranes were also characterized for pure and mixture mass transfer coefficients.

The experimental results presented below were obtained using the PDMS membrane module #1 and PEI membrane module #1. The results obtained with the PDMS membrane module #2 were included whenever available. To study the response time and reversibility of the sensor, only the PDMS membrane module #2 was used.

2.4.1. Pure and mixture mass transfer coefficients determinations

Permeability is defined as the ratio between the permeate flux and the corresponding pressure difference between feed and permeate sides, per unit membrane thickness [26]:

$$L = \frac{F^{P}/A}{\Delta P/l} \tag{2.3}$$

where L is the permeability, F^{P} is the permeate gas flow rate, ΔP is the pressure difference between feed and permeate sides, A is the membrane area and l is the membrane thickness.

In the present work, the permeability was expressed as mass transfer coefficient (k) because it was difficult to determine the thickness of the selective layer in the membrane. k is defined as the ratio between the

permeate flux (F^P/A) and the corresponding pressure difference between feed and permeate sides:

$$k = \frac{F^P/A}{\Delta P} \tag{2.4}$$

When k is invariant with ΔP, it can be obtained from the slope of the plot of F^P/A as a function of ΔP. Oxygen and nitrogen mass transfer coefficients in PDMS and PEI membranes were determined for each assembled membrane module. The permeate flow rate was measured for a feed pressure range of 0.15 to 0.50 MPa and at 10, 25 and 40ºC. Temperature restrictions of the glue and sealant used in the membrane modules set the experimental temperature upper limit. The permeate side was maintained at ambient pressure. The so-called ideal selectivity of oxygen/nitrogen is obtained from the ratio between the corresponding mass transfer coefficients. The ideal oxygen/nitrogen selectivities, $\alpha(O_2/N_2)$, and oxygen and nitrogen mass transfer coefficients of PDMS and PEI membranes, measured at three different temperatures, are summarized in Table 2.2.

PDMS and PEI membranes show higher permeability towards oxygen than towards nitrogen. The polymer with higher selectivity, PEI, shows relatively low permeability. The selectivities for the PDMS membrane modules are temperature dependent. As expected, the selectivity decreases with temperature increases.

The oxygen/nitrogen gas sensor was tested with PDMS (low selectivity) and PEI (medium selectivity) membranes.

The mixture mass transfer coefficient was obtained as a function of the feed composition. Permeation experiments were carried out at 25ºC, with PDMS membrane module #1 and PEI membrane module #1, using different oxygen feed compositions. For PDMS membrane, the feed pressure ranged between 0.14 and 0.50 MPa, while the permeate pressure was ambient (needle valve completely open). For PEI membrane, the permeate flow rate was measured for a pressure difference between feed and permeate sides

Table 2.2

Ideal O_2/N_2 selectivities, $\alpha(O_2/N_2)$, and mass transfer coefficients (k) for O_2 and N_2 in PDMS and PEI membranes determined at three different temperatures (T).

Membrane	Module #	T/ºC ± 1.1ºC**	$k/10^{-6}$ dm^3 (STP) s^{-1} m^{-2} Pa^{-1}*		$\alpha(O_2/N_2)$
			N_2	O_2	
PDMS	1	10.4	1.002 ± 0.0043	2.225 ± 0.0090	2.22 ± 0.013
		25.3	1.183 ± 0.0033	2.49 ± 0.010	2.11 ± 0.010
		39.4	1.514 ± 0.0048	3.02 ± 0.014	1.99 ± 0.011
	2	10.4	1.116 ± 0.0033	2.557 ± 0.0071	2.292 ± 0.0093
		24.7	1.395 ± 0.0031	3.01 ± 0.011	2.160 ± 0.0093
		39.9	1.732 ± 0.0062	3.52 ± 0.011	2.033 ± 0.0095
PEI	1	24.9	0.009859 ± 0.00011	0.04112 ± 0.00053	4.17 ± 0.071

*Precision. **Accuracy.

ranging from 0.21 to 0.27 MPa and at ambient permeate pressure. The mass transfer coefficient, k, was obtained from the slope of F^P/A as a function of ΔP, using Eq. (2.4). The feed flow rate was always much higher than the permeate flow rate. This guarantees that the retentate composition was essentially equal to the feed composition. The effect of the feed mixture composition on the mixture mass transfer coefficient is shown in Fig. 2.5. The results obtained indicate that when the oxygen feed concentration increases, the mixture mass transfer coefficient also increases. The permeate flow rate through the membrane module is therefore related to the gas mixture composition. The solid lines in the Fig. 2.5 represent the best second-degree polynomial curves fitted to the data points.

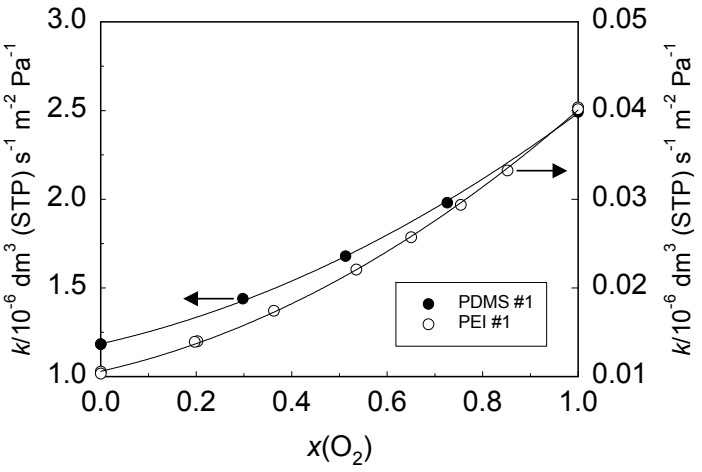

Fig. 2.5. Mixture mass transfer coefficient (k) as a function of the oxygen feed composition, $x(O_2)$, for PDMS membrane module #1 and PEI membrane module #1 at 25ºC. Lines are 2nd degree polynomial fittings.

2.4.2. Effect of temperature

Temperature variations could considerably affect the sensor response. It is therefore necessary to study this effect.

The effect of temperature for PDMS membrane module #1 was determined at 0.304 MPa feed pressure and for a temperature range from 5.5 to 49.8ºC. The oxygen feed molar fraction was $\overline{x}$ (mean) = 0.128, *s* (standard deviation) = 0.001, *N* (number of measurements) = 7. Fig. 2.6 shows the effect of temperature on the permeate pressure. It can be seen that the permeate pressure depends significantly on temperature. The slope of the plot obtained is 5.56 x 10^2 Pa ºC^{-1}.

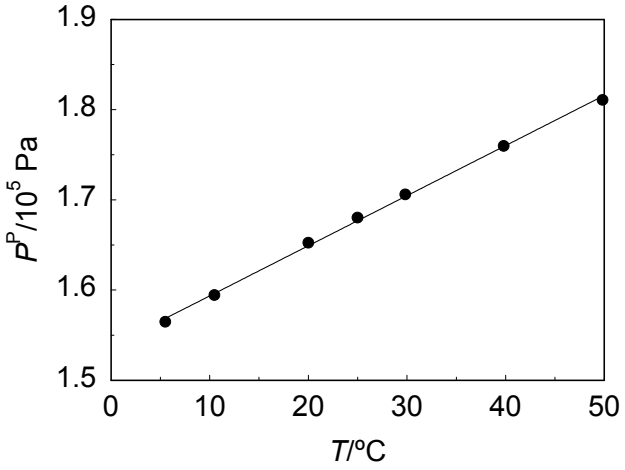

Fig. 2.6. Permeate pressure (P^P) as a function of temperature (T) for PDMS membrane module #1 at 0.304 MPa feed pressure. The oxygen feed molar fraction was 0.128. The line is a linear fitting.

2.4.3. Response curves

By measuring the pressure in the permeate side of the sensor, the oxygen feed concentration can be computed using the response curve. This curve can be obtained by measuring the permeate pressure at different oxygen feed compositions, keeping constant the feed pressure and temperature. Some response curves were obtained in our experimental set-up.

The permeate pressure and also the permeate flow rate were measured at different temperatures as a function of the oxygen feed molar fraction. The results are shown in Figs. 2.7 to 2.10 for PDMS and PEI membranes. Firstly, the permeate flow rate (F^P) was measured as a function of oxygen feed molar fraction, $x(O_2)$, for PDMS membrane module #1. The feed and permeate pressure were kept constant, at 0.304 MPa and ambient pressure, respectively, and the experiments were carried out at 24.9ºC. The results are shown in Fig. 2.7.

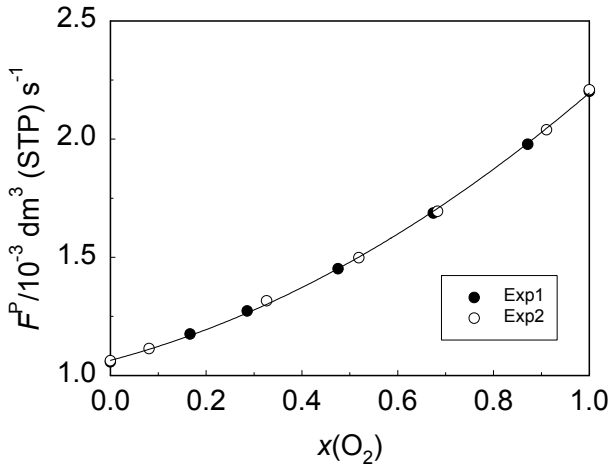

Fig. 2.7. Permeate flow rate (F^P) as a function of oxygen feed molar fraction, $x(O_2)$, for PDMS membrane module #1 at 24.9ºC. The line is a 2nd degree polynomial fitting. Open and solid symbols refer to experiments performed on different days.

At constant feed pressure, a second-degree polynomial fits the experimental data well. The results obtained from two sets of measurements, on different days, are reproducible.

The permeate pressure (P^P) was measured as a function of oxygen feed molar fraction, $x(O_2)$, for PDMS membrane modules #1 and #2, at different temperatures, keeping the feed pressure constant at 0.304 MPa. For module #1, the needle valve was set to 0.2 MPa permeate pressure when pure oxygen was being fed to the sensor, for each temperature considered. The pressure values read were 0.2025, 0.2027 and 0.2021 MPa at 10.4, 25.3 and 40.3ºC, respectively. In a second series of experiments, the needle valve was set to 0.2 MPa permeate pressure when pure oxygen was being fed at 25ºC to modules #1 and #2 and left unchanged for experiments performed at 10 and 40ºC. The pressure values read at 25ºC were 0.2025 and 0.2017 MPa, respectively, for the modules #1 and #2. The results are plotted in Figs. 2.8 and 2.9.

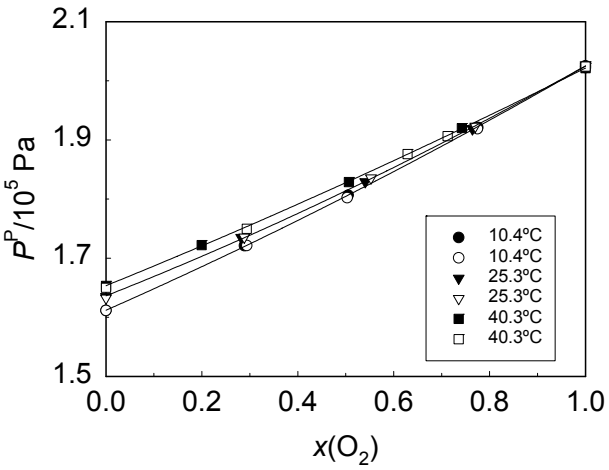

Fig. 2.8. Permeate pressure (P^P) as a function of oxygen feed molar fraction, $x(O_2)$, for PDMS membrane module #1. Lines are 2nd degree polynomial fittings. Open and solid symbols refer to experiments performed on different days.

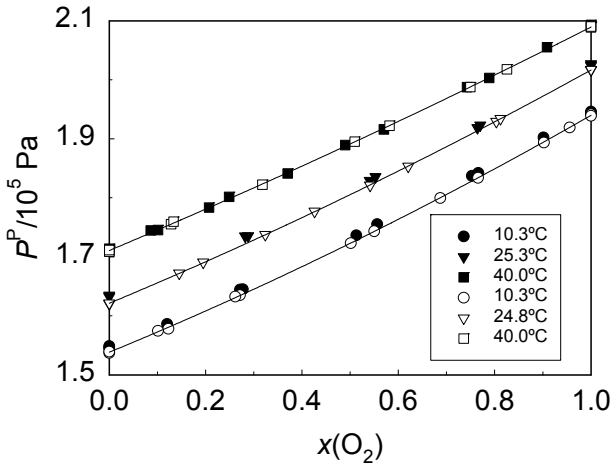

Fig. 2.9. Permeate pressure (P^P) as a function of oxygen feed molar fraction, $x(O_2)$, for PDMS membrane modules #1 (solid symbols) and #2 (open symbols). Lines are 2nd degree polynomial fittings.

It can be seen from these figures that when the needle valve of the permeate side of the membrane module is partially closed, the permeate pressure obtained is related to the permeate flow rate and, therefore, to the gas feed composition. The experimental points obtained on two different days fall on the same response curve. From figure 2.9 it is also possible to see that both PDMS membrane modules perform identically. Since the membrane volumetric permeability increases with temperature, the permeate pressure also increases.

Finally, similar experiments were conducted using the PEI membrane module #1. Similar responses were obtained. For this membrane, the needle valve was set to 0.1924 MPa permeate pressure when oxygen was fed to the device at 0.401 MPa feed pressure. Fig. 2.10 shows the experimental results obtained with PEI membrane module #1 at 24.7ºC. At constant feed pressure, a second-degree polynomial fits the experimental data quite well. The results showed reproducibility.

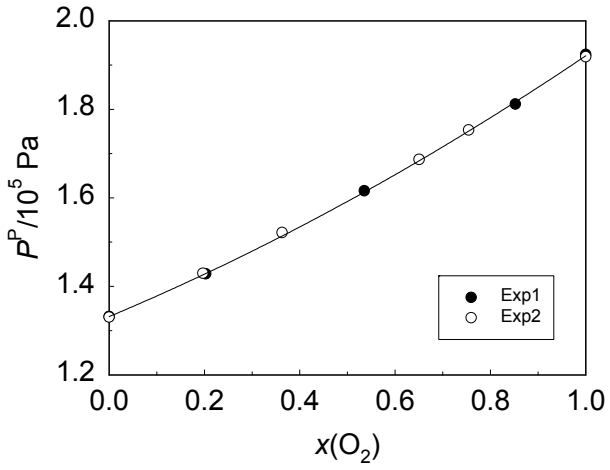

Fig. 2.10. Permeate pressure (P^P) as a function of oxygen feed molar fraction, $x(O_2)$, for PEI membrane module #1 at 24.7ºC. The line is a 2nd degree polynomial fitting. Open and solid symbols refer to experiments performed on different days.

The absolute or local sensitivity of the response (calibration) is defined as the slope of the response curve at the concentration of interest ($S = dP^P/dx(O_2)$) [27]. Comparing Figs. 2.8 and 2.9 with Fig. 2.10 it can be concluded that the sensitivity for PEI is higher than for PDMS, but the deviation from the linearity of the PDMS response curve is smaller. The absolute sensitivity depends on the membrane material and on the oxygen feed concentration. The sensitivity ranged from 0.0329 to 0.0450 MPa (0 and 100% oxygen, respectively) for PDMS module #1 and 0.0468 to 0.0708 MPa (0 and 100% oxygen, respectively) for PEI module #1, at 25ºC.

2.4.4. Experimental and modeled results

The model described above has two parameters, the minimum pressure at the permeate side, P^P_{min}, and the maximum pressure at the

permeate side, P^{P}_{max} , since the ambient pressure, P^{amb}, is postulated to be constant and known. These two parameters are obtained directly from the experimental data. Fig. 2.11 shows experimental and modeled results obtained for the permeate pressure (P^{P}) as a function of oxygen feed molar fraction, $x(O_2)$, at different temperatures, for both PDMS membrane modules and PEI membrane module #1. The modeled results were obtained using Eq. (2.1).

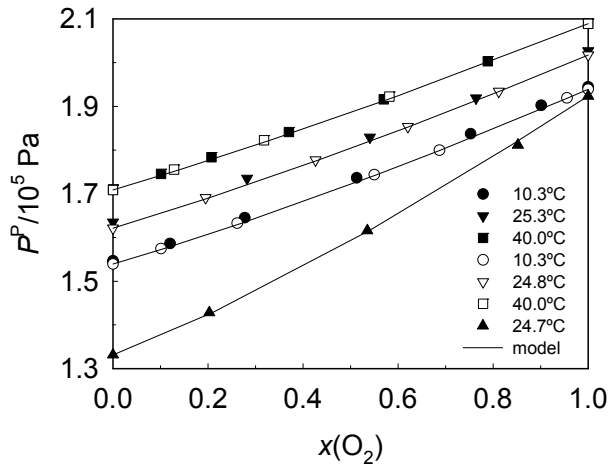

Fig. 2.11. Permeate pressure (P^{P}) as a function of oxygen feed molar fraction, $x(O_2)$, for experimental and modeled results, with PDMS membrane modules #1 (solid symbols) and #2 (open symbols) and PEI membrane module #1 (▲).

Data necessary for modeling are shown in Table 2.3. The model was in good agreement with experimental data, indicating that it adequately describes the behavior of the oxygen/nitrogen sensor, for these operating conditions. The model can further be used to optimize the sensor response for a given application.

Table 2.3

Experimental data for PDMS and PEI membranes measured at three different temperatures (T).

Membrane module		T/ºC	P^{F} /MPa	P^{P}_{min} /MPa	P^{P}_{max} /MPa	P^{amb} /MPa
PDMS	#1	10.3	0.304	0.1547	0.1944	0.1007
		25.3	0.304	0.1635	0.2027	0.1000
		40.0	0.304	0.1710	0.2090	0.1016
	#2	10.3	0.303	0.1539	0.1939	0.1005
		24.8	0.303	0.1621	0.2017	0.0994
		40.0	0.303	0.1709	0.2089	0.1001
PEI	#1	24.7	0.401	0.1332	0.1924	0.0998

Fig. 2.12 shows the oxygen feed molar fraction predicted by the model and obtained experimentally for both membranes and for different temperatures. It can also be seen from this figure that the model fits the experimental results quite well.

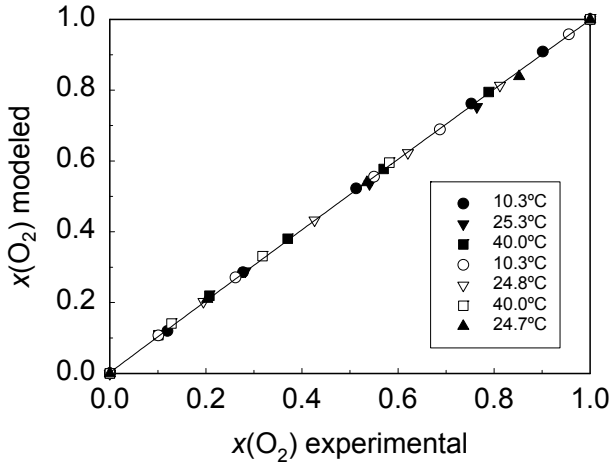

Fig. 2.12. Modeled oxygen feed molar fraction as a function of experimental oxygen feed molar fraction for PDMS membrane modules #1 (solid symbols) and #2 (open symbols) and PEI membrane module #1 (▲). The line is a linear fitting.

2.4.5. Response time and reversibility

The response time of a sensor to a change in the feed composition, $x(O_2)$, is an important parameter. In this study the response time is considered as the time taken to reach 95% of the full response ($t_{0-95\%}$). To determine experimentally the response time and reversibility of the sensor, it was fed alternately with oxygen and nitrogen, at 24.8-24.9ºC, keeping the feed pressure constant. The feed pressure was 0.300 and 0.399 MPa for PDMS membrane module #2 and PEI membrane module #1, respectively. Rapid switching between gas streams was achieved using a three-way valve.

Fig. 2.13 shows a plot of permeate pressure (P^P) as a function of time (t) for PDMS and PEI membranes. The PDMS membrane responds faster (a few seconds) than the PEI membrane (approximately 9 minutes). This relatively long response time for PEI is not satisfactory for practical applications.

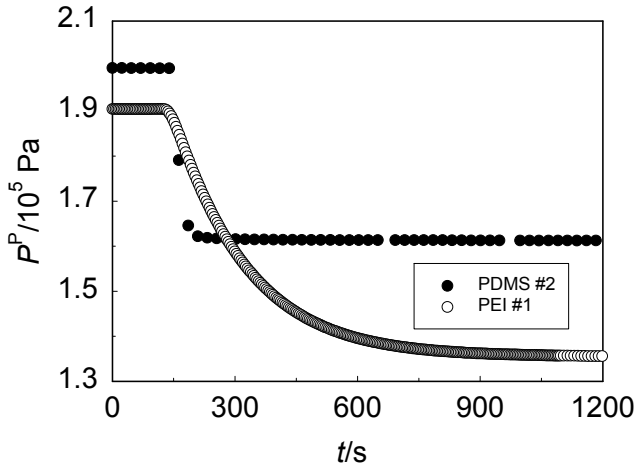

Fig. 2.13. Permeate pressure (P^P) as a function of time (t) for PDMS membrane module #2 and PEI membrane module #1 at 24.8-24.9ºC.

From Fig. 2.14 it can also be seen that the PDMS membrane module #2 response is fully reversible. The feed pressure was 0.300 MPa and the permeate pressure ranged from 0.1611 to 0.1997 MPa. In this figure, the solid and dashed arrows indicate, respectively, the time when the feed was changed from oxygen to nitrogen and from nitrogen to oxygen.

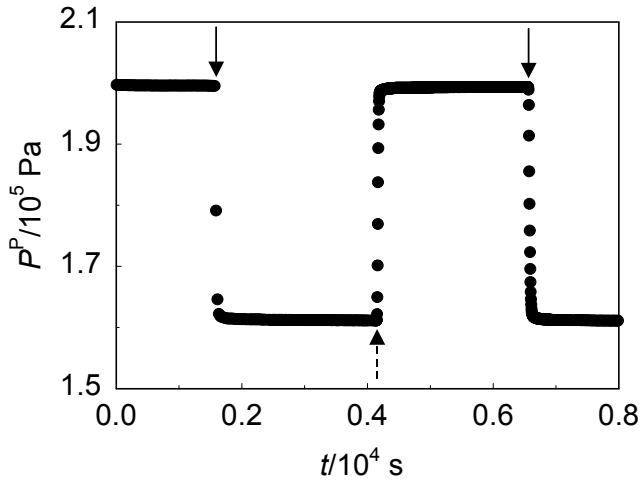

Fig. 2.14. Permeate pressure (P^P) as a function of time (t) for PDMS membrane module #2 at 24.7-24.8ºC.

2.4.6. Long-term stability

In the present study the long-term stability of the sensor was also checked. To determine experimentally the long-term stability of the sensor, it was fed alternately with oxygen, nitrogen and oxygen/nitrogen mixtures for two months at 10, 25 and 40ºC. The feed and permeate pressures ranged from, respectively, 0.14 to 0.50 and ambient to 0.25 MPa. During this period nitrogen and oxygen mass transfer coefficients in the PDMS membrane module #1 were obtained using Eq. (2.4) at 24.7-25.4ºC and at different times as shown in Fig. 2.15.

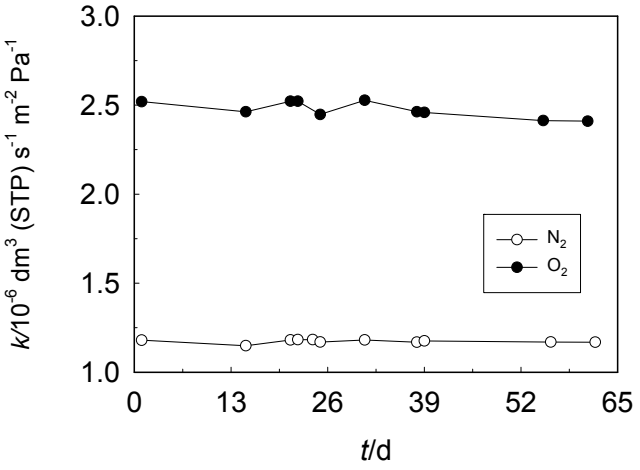

Fig. 2.15. Nitrogen and oxygen mass transfer coefficients (*k*) as a function of time (*t*) for PDMS membrane module #1 at 24.7-25.4ºC. The line is there for easy reading.

Since the measured nitrogen and oxygen mass transfer coefficients in the PDMS membrane stayed almost constant as a function of time ($\bar{k}$ (O_2) = 2.474 x 10^{-6} dm^3 (STP) s^{-1} m^{-2} Pa^{-1}, s = 0.045 x 10^{-6}, N = 10; $\bar{k}$ (N_2) = 1.173 x 10^{-6} dm^3 (STP) s^{-1} m^{-2} Pa^{-1}, s = 0.010 x 10^{-6}, N = 11), it may be concluded that no deterioration of the sensor response occurred during this period.

2.5. Conclusions and further research

A new oxygen/nitrogen gas sensor is described, tested and modeled. The most important application devised for this sensor is for monitoring the oxygen content in the outlet stream generated by medical oxygen concentration units. Other applications are possible. This sensor is characterized by simple instrumentation with no sample pre-treatment and a

short response time and can offer new possibilities for conventional oxygen/nitrogen concentration sensors.

The concentration sensor is suitable for the very low price and low/medium precision market to determine the composition of bi-component gas mixtures in the 0-100% range. Progress towards a commercial instrument is foreseen.

A PDMS membrane offers a number of useful features for application in the proposed sensor. It shows a fast response time, has very high oxygen permeability, optimized ideal oxygen/nitrogen selectivity and is low cost. The corresponding sensor has a high reproducibility and adequate sensitivity.

A more complicated mathematical model can be derived with predictable features, considering different operating conditions such as feed pressure, feed flow pattern, needle valve model and temperature effects. Further studies with other gas mixtures (carbon dioxide/methane, carbon dioxide/helium, hydrogen/nitrogen and hydrogen/methane) are presently underway.

Appendix

The steady state flux, F, through a membrane is given by [26]:

$$F_i = k_i\left(P^F x_i^F - P^P x_i^P\right) \quad (1)$$

where F_i (dm^3 (STP) s^{-1} m^{-2}) is the flux of component i, k (dm^3 (STP) s^{-1} m^{-2} Pa^{-1}) is the mass transfer coefficient, P^F (Pa) is the feed pressure, P^P (Pa) is the permeate pressure, x_i^F is the feed molar fraction and x_i^P is the permeate molar fraction.

Combining Eq. (1) with equation $x_A^P + x_B^P = 1$, where x_A^P and x_B^P are the permeate molar fractions for the components A and B of the binary gas mixture, respectively, gives:

$$F_A = k_A\left(P^F x_A^F - P^P x_A^P\right) \quad (2)$$

$$F_B = k_B\left[P^F\left(1 - x_A^F\right) - P^P\left(1 - x_A^P\right)\right] \quad (3)$$

The valve equation is given by [28]:

$$F_A + F_B = K\left(P^P - P^{amb}\right) \quad (4)$$

where P^{amb} (Pa) is the ambient pressure and K (dm^3 (STP) s^{-1} m^{-2} Pa^{-1}) is a model parameter.

Assuming that component A is the fastest (oxygen) and the feed stream contains only this gas, we get:

$$F_A = K\left(P_{max}^P - P^{amb}\right) \quad (5)$$

where P^{P}_{max} is the maximum pressure at the permeate side reached when the feed contains only the fastest gas.

For the slowest gas (nitrogen) it is possible to write a similar equation:

$$F_B = K\left(P^{P}_{min} - P^{amb}\right) \tag{6}$$

where P^{P}_{min} is the minimum pressure at the permeate side reached when the feed contains only the slowest gas.

The permeate molar fraction for the fastest component can be obtained from:

$$x^{P}_{A} = \frac{F_A}{F_A + F_B} \tag{7}$$

Introducing equations (2) and (3) in Eq. (4) and solving the resulting set of two equations as a function of x^{F}_{A}, we obtain:

$$x^{F}_{A} = \frac{K\left(P^{P} - P^{amb}\right) + x^{P}_{A}P^{P}\left(k_A - k_B\right) - k_B\left(P^{F} - P^{P}\right)}{P^{F}\left(k_A - k_B\right)} \tag{8}$$

The mass transfer coefficients, k_A and k_B, can be obtained from equations (2) and (3):

$$k_A = \frac{KP^{P}_{max}}{P^{F} - P^{P}_{max}} \tag{9}$$

$$k_B = \frac{KP^{P}_{min}}{P^{F} - P^{P}_{min}} \tag{10}$$

Finally, introducing these equations in Eq. (8) and after algebraic manipulation it is possible to obtain:

$$x_A^F = \frac{P^P - P_{min}^P}{P_{max}^P - P_{min}^P}\left[1 - \frac{P^{amb}\left(P^P - P_{max}^P\right)}{P^F\left(P^P - P^{amb}\right)}\right] \tag{11}$$

which is valid whenever $P^{amb} \neq 0$. For $P^{amb} = 0$, Eq. (11) becomes:

$$x_A^F = \frac{P^P - P_{min}^P}{P_{max}^P - P_{min}^P} \tag{12}$$

Acknowledgements

This work has been supported by Agência de Inovação, s.a., (project P0046/ICPME/S - Gassense). The authors thank Prof. Fernão Magalhães (FEUP) for the careful revision of this manuscript. Rosa Rego thanks Prof. Luís Carvalho (UTAD) for helpful discussions.

References

[1] C.G. Pinto, M.E.F. Laespada, J.L.P. Pavón, B.M. Cordero, Analytical applications of separations techniques through membranes, Laboratory Automation and Information Management 34 (1999) 115-130.

[2] T.L. Brook, R. Narayanaswamy, Polymeric films in optical gas sensors, Sens. Actuators B 51 (1998) 77-83.

[3] J.N. Demas, B.A. DeGraff, P.B. Coleman, Oxygen sensors based on luminescence quenching, Anal. Chem. 71 (1999) 793A-880A.

[4] Y. Amao, K. Asai, I. Okura, Fluorescence quenching oxygen sensor using an aluminum phthalocyanine-polystyrene film, Anal. Chim. Acta 407 (2000) 41-44.

[5] F. Navarro-Villoslada, G. Orellana, M.C. Moreno-Bondi, T. Vick, M. Driver, G. Hildebrand, K. Liefeith, Fiber-optic luminescent sensors with composite oxygen-sensitive layers and anti-biofouling coatings, Anal. Chem. 73 (2001) 5150-5156.

[6] Y. Amao, Y. Ishikawa, I. Okura, Green luminescent iridium (III) complex immobilized in fluoropolymer film as optical oxygen-sensing material, Anal. Chim. Acta 445 (2001) 177-182.

[7] K. Eaton, A novel colorimetric oxygen sensor: dye redox chemistry in a thin polymer film, Sens. Actuators B 85 (2002) 42-51.

[8] R.K. Kobos, S.J. Parks, M.E. Meyerhoff, Selectivity characteristics of potentiometric carbon dioxide sensors with various gas membrane materials, Anal. Chem. 54 (1982) 1976-1980.

[9] K. Katakura, A. Noma, Z. Ogumi, Z.-i. Takehara, An oxygen sensor composed of tightly stacked membrane/electrode/electrolyte, Chem. Lett. (1990) 1291-1294.

[10] T. Trapp, B. Ross, K. Cammann, E. Schirmer, C. Berthold, Development of a coulometric CO_2 gas sensor, Sens. Actuators B 50 (1998) 97-103.

[11] K. Wiegran, T. Trapp, K. Cammann, Development of a dissolved carbon dioxide sensor based on a coulometric titration, Sens. Actuators B 57 (1999) 120-124.

[12] M. Takahashi, T. Ishiji, N. Kawashima, Handmade oxygen and carbon dioxide sensors for monitoring the photosynthesis process as instruction material for science education, Sens. Actuators B 77 (2001) 237-243.

[13] R. Fasching, F. Keplinger, G. Hanreich, G. Jobst, G. Urban, F. Kohl, R. Chabicovsky, A novel miniaturized sensor for carbon dioxide dissolved in liquids, Sens. Actuators B 78 (2001) 291-297.

[14] X.-L. Su, X. Xingguo, T. Dallas, S. Gangopadhyay, H. Temkin, X. Wang, R. Walulu, J. Li, P.K. Dasgupta, A microfabricated amperometric moisture sensor, Talanta, 56 (2002) 309-321.

[15] K. Fukui, S. Nishida, CO gas sensor based on Au-La_2O_3 added SnO_2 ceramics with siliceous zeolite coat, Sens. Actuators B 45 (1997) 101-106.

[16] G. Li, S. Kawi, MCM-41 modified SnO_2 gas sensors: sensitivity and selectivity properties, Sens. Actuators B 59 (1999) 1-8.

[17] O. Hugon, M. Sauvan, P. Benech, C. Pijolat, F. Lefebvre, Gas separation with a zeolite filter, application to the enhancement of chemical sensors, Sens. Actuators B 67 (2000) 235-243.

[18] M. Vilaseca, J. Coronas, A. Cirera, A. Cornet, J.R. Morante, J. Santamaría, Use of zeolite films to improve the selectivity of reactive gas sensors, Catal. Today 82 (2003) 179-185.

[19] K. Kaneyasu, K. Otsuka, Y. Setoguchi, S. Sonoda, T. Nakahara, I. Aso, N. Nakagaichi, A carbon dioxide gas sensor based on solid electrolyte for air quality control, Sens. Actuators B 66 (2000) 56-58.

[20] A. Mendes, Gas mixtures concentration sensor and corresponding measuring process, Patent PT102 312 (2000).

[21] D. Lasik, H. Geistlinger, Method for measuring the concentration or the partial pressure of gases, especially oxygen, in fluids and a corresponding gas sensor, Patent WO 01/53796 A1, EP 1 157 265 A1, DE 199 25 842 A 1 (2001).

[22] http://www.anton-paar.com

[23] Ullmann's Encyclopedia of Industrial Chemistry, Electronic Release, 6th ed., Wiley-VCH, Weinheim, 2003, Chapter Plastics, Analysis.

[24] Personal communication: Eng. Ulrich Palm, Weinmann GmbH (2002).

[25] http://www.digiflo.org

[26] M. Mulder, Basic Principles of Membrane Technology, 2nd ed., Kluwer Academic Publishers, Dordrecht, 2000, Chapter 1.

[27] D.A. Skoog, J.J. Leary, Principles of Instrumental Analysis, 4th ed., Saunders College Publishing, Orlando, 1992, Chapter 1.

[28] R.B. Bird, W.E. Stewart, E.N. Lightfoot, Transport Phenomena, 2nd ed., John Wiley & Sons, Inc., United States of America, 2002, Chapter 2, pp 51.

3. Development of a new gas sensor for binary mixtures based on the permselectivity of polymeric membranes. Application to carbon dioxide/methane and carbon dioxide/helium mixtures

Abstract

Membrane-based gas sensors were developed and used for determining the composition on bi-component mixtures in the 0-100% range, such as oxygen/nitrogen and carbon dioxide/methane (biogas). These sensors are low cost and are aimed at a low/medium precision market.

The paper describes the use of this sensor for two gas mixtures: carbon dioxide/methane and carbon dioxide/helium. The membranes used are poly(dimethylsiloxane) (PDMS) and Teflon-AF hollow fibers. The response curves for both sensors were obtained at three different temperatures. The results clearly indicate that the permeate pressure of the sensors relates to the gas mixture composition at a given temperature. The data is represented by a third degree polynomial. The sensors enable quantitative carbon dioxide analysis in binary mixtures with methane or helium. The response of the sensors is fast (less than 50 s), continuous, reproducible and long-term stable over a period of 2.3×10^7 s (9 months). The absolute sensitivity of the sensors depends on the carbon dioxide feed concentration ranging from 0.03 to 0.13 MPa.

R. Rego, N. Caetano, A. Mendes, Anal. Chim. Acta 511 (2004) 215-221.

3.1. Introduction

The most widely used membrane-based process is dialysis, which aims to remove salts and low molecular weight solutes from solutions [1, 2] and also to pre-concentrating organic species [3].

In the field of analytical chemistry membranes have attracted increasing attention [4]. Polymeric and zeolite membranes have commonly been used in different types of chemical sensors in order to increase their selectivity [5-10]. Thus, membrane-based sensors are useful in the determination of reduced sugars such as glucose [11-13] and fructose [14, 15]. Proposals have been made to use membrane-based sensors for determinations in different matrices such as transaminases in blood serum [16], ethanol in alcoholic beverages [17], dissolved carbon dioxide in water and seawater [18], hydrogen sulphite in foods [19], and oxygen and carbon dioxide in photosynthesis processes [20]. Sensors have also been developed for environmental control, for instance, for the determination of biological oxygen demand [21], the hardness of water [22], ammonia [23, 24], nitrogen oxides [25, 26], sulphur dioxide [27], chlorinated hydrocarbons [28], hydrazines [29], and triazine herbicides [30] among others.

Recently, a new gas sensor based on the permselective effect of membranes has been proposed. The working principle of this sensor is based on the fact that different gases have different permeabilities on a selective membrane. Thus, when two gases flow along the membrane at constant pressure, the permeate flux depends directly on the feed composition. This flux can be determined by the pressure drop at a calibrated orifice or needle valve, so the pressure is indirectly correlated to the feed gas composition. The permeate pressure can be measured with a cheap pressure transducer [31, 32].

Based on a similar principle, a device to sense dissolved carbon dioxide in beverages has been developed [33]. A method for measuring the concentration or the partial pressure of gases in fluids, especially oxygen, using a plastic material has also been proposed. This material is only permeable to some specific gases and its exterior is in contact with the fluid

[34]. The molecular mass of a polymer can be determined from osmotic pressure across a membrane of a solution of this polymer (membrane osmometry) [35].

The carbon dioxide/methane gas sensor may have wide application in biogas controlling units such as wastewater treatment plants and landfills. Waste disposal is an important problem in developed countries. Sanitary landfills have been, and continue to be, one of the most common ways to dispose of urban and industrial wastes [36]. Landfill gas is formed when organic wastes decompose anaerobically in a landfill. Composed of almost equal parts of methane and carbon dioxide, the biogas is combustible and therefore potentially dangerous [37]. The US Environmental Protection Agency (EPA) has proposed regulations to control explosive gases emissions from municipal solid waste landfills [38]. The utilization of such a gas as fuel for electrical and thermal energy production could be an important way to reduce the landfill gas impact on the environment and could became a renewable energy source. For this purpose, on-site composition determination with real-time monitoring must be both cheaper and more effective. Infrared gas sensors are commonly used in landfill gas monitoring [39-41] but the installation of these sensors at every emitting site is not viable because the high costs involved. Therefore, there is an increasing need for very cheap sensors which can be placed at every emitting site.

Our proposed carbon dioxide/methane gas sensor could also play an important role in the safety market, in addition to infrared gas sensors for *in situ* biogas monitoring. The sensor can be used to measure and control methane emissions during methane recovery. As yet a well-defined market for the carbon dioxide/helium sensor has not yet been found.

The aim of this work is to develop and study sensors to determine the composition of carbon dioxide/methane and carbon dioxide/helium mixtures in the 0-100% range. Two different polymeric membranes are used: poly(dimethylsiloxane) (PDMS) and Teflon-AF hollow fibers. Results are given for carbon dioxide/methane and carbon dioxide/helium mixtures. For both sensors, calibration curves were obtained at three different temperatures. The reproducibility, sensitivity, response time and reversibility,

long-term stability and temperature dependence of these two sensors is studied.

3.2. Experimental

Fig. 3.1 is a sketch of the binary gas mixture sensor. The sensor is made of a permselective membrane, a pressure transducer for measuring the permeate pressure and a non-selective barrier (e.g. needle valve).

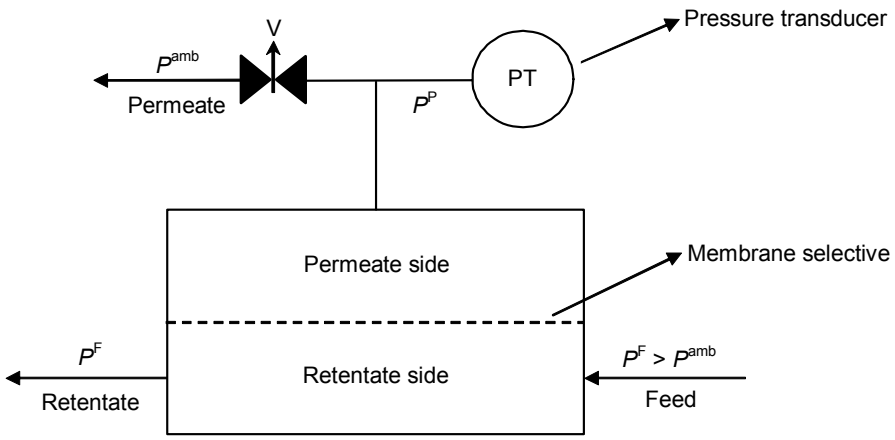

Fig. 3.1. Sketch of the binary gas mixture sensor.

The non-selective barrier controls the permeate outlet to the atmosphere. The gas mixture to be analyzed is supplied at a constant pressure which must be higher than the outlet permeate pressure (P^P). In our system, the feed pressure (P^F) was set to 0.3 MPa, while the permeate pressure after the needle valve (V) was the ambient pressure (P^{amb}) [32].

For both membranes used in this work, methane and helium are the slowest gases and carbon dioxide is the fastest when their permeation characteristics are compared. When, at different times the feed stream

contains only the slowest and the fastest gas, the permeate pressure attained at the permeate side is, respectively, the minimum (P^{P}_{min}) and the maximum (P^{P}_{max}) pressure.

The two sensors were tested in an experimental set-up similar to that described in [32]. The gases used were carbon dioxide, methane and helium, from Air Liquide, 99.995% purity.

Two different composite membranes were used: a poly(dimethylsiloxane) (PDMS) and a Teflon-AF hollow fibers (both supplied by GKSS, Germany). Teflon-AF is a perfluorinated co-polymer of tetra-fluoroethylene (PTFE) polymerized with perfluoro-2,2-dimethyl-1,3-dioxole [42]. Two membrane modules were assembled in our laboratory: a PDMS membrane module with 6 fibers and a work length of 113 mm and a Teflon membrane module with 3 fibers and a work length of 149 mm. The inside diameter of these fibers are, respectively, 0.71 and 0.63 mm. The modules were tested with hydrogen before being used in order to check for leakage. Fig. 3.2 is a sketch of a hollow fiber membrane module.

The feed gas mixture to be analyzed was fed to the bore side of the membrane module at the desired flow rate. The feed pressure was kept constant at 0.3 MPa with the help of two pressure regulators in series and was measured with a pressure transducer (Lucas Schaevitz, P941, range 0-1 MPa, $\leq$ ±0.1% FS). The temperature of the sensor was kept at the desired value by means of a thermostatic bath. Concentrations in feed were measured with an infrared carbon dioxide analyzer (Servomex, 1400 D, range 0-100% v/v, ±1% FS). The feed, permeate and retentate flow rates, carbon dioxide feed composition as well as feed and permeate pressures were continuously monitored by a computer-controlled data acquisition system. Additional details are given elsewhere [32]. Experiments were repeated three or four times for each operating condition on different days.

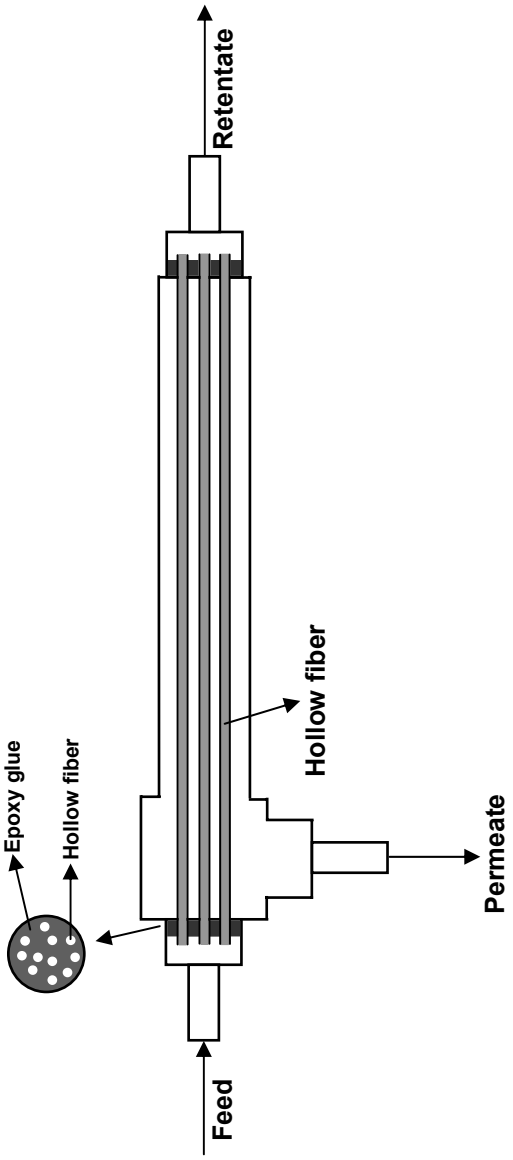

Fig. 3.2. Schematic view of hollow fiber membrane module.

3.3. Results and discussion

The study was organized as follows: firstly, characterization of the membranes to assess their performance inside the sensor; secondly, evaluation of the performance of the sensor itself. The membranes were characterized for mono and mixture permeation measurements and ideal selectivities at different temperatures. In order to evaluate the performance of the sensors several experiments were performed. These experiments aimed to determine the response curves (calibration curves), sensitivity, response time and reversibility, long-term stability and also the influence of operating conditions such as the temperature of the sensors.

3.3.1. Pure and mixture mass transfer coefficients

Permeability is defined as the ratio between the permeate flux and the corresponding pressure difference between feed and permeate sides, per unit membrane thickness [43]:

$$L = \frac{F^{P}/A}{\Delta P/l} \tag{3.1}$$

where L is the permeability, F^{P} is the permeate flow rate, ΔP is the pressure difference between feed and permeate sides, A is the membrane area and l is the membrane thickness.

In the present study, and because it is difficult to determine the thickness of the selective layer, it was decided to use a related parameter which is not normalized by the membrane thickness; i.e. the mass transfer coefficient (k). This is defined as the ratio between the permeate flux (F^{P}/A) and the corresponding pressure difference between feed and permeate sides:

$$k = \frac{F^{P}/A}{\Delta P} \tag{3.2}$$

When k is invariant with ΔP, it can be obtained from the slope of the plot of F^{P}/A as a function of ΔP. Carbon dioxide, methane and helium mass transfer coefficients in PDMS and Teflon-AF membranes were determined for each membrane module. The permeate flow rate was determined for a feed pressure range of 0.20 to 0.41 MPa and for 10, 25, 30 and 40ºC. The permeate pressure ranged from 0.11 to 0.24 MPa (needle valve partially closed). The so-called ideal selectivity of carbon dioxide/methane, $\alpha(CO_2/CH_4)$, and carbon dioxide/helium, $\alpha(CO_2/He)$, was obtained from the ratio between the corresponding mass transfer coefficients for both membrane materials. The ideal selectivities and mass transfer coefficients for PDMS and Teflon-AF membranes are summarized in Table 3.1. PDMS and Teflon-AF membranes show higher permeability towards carbon dioxide than towards methane or helium. The selectivities for PDMS and Teflon-AF membrane modules are temperature dependent. Methane and helium mass transfer coefficients in PDMS increase with temperature, while carbon dioxide mass transfer coefficients remain almost unchanged.

On the other hand, for the Teflon-AF membrane, the methane mass transfer coefficient increases slightly as the temperature increases, while the carbon dioxide coefficient decreases. As a result, for both membranes, carbon dioxide/methane and carbon dioxide/helium selectivities decrease as the temperature increases. For the Teflon-AF membrane, the carbon dioxide/methane selectivity is very high (Table 3.1).

The permeability of a membrane towards a solute can be obtained from the product between the sorption and diffusion coefficients [43]. The sorption coefficient decreases with the temperature while the diffusion coefficient increases. For PDMS and Teflon-AF the permeability towards carbon dioxide decreases with temperature (soption controlled transport) and the permeability towards methane and helium (which sorb very little) increases with temperature (diffusion controlled transport).

Table 3.1

Ideal CO_2/CH_4 and CO_2/He selectivities, $\alpha(CO_2/CH_4)$ and $\alpha(CO_2/He)$, and CO_2, CH_4 and He mass transfer coefficients (k) in PDMS and Teflon-AF membranes determined at different temperatures (T).

Membrane	T/ºC	$k/10^{-6}$ dm^3 (STP) s^{-1} m^{-2} Pa^{-1}			$\alpha(CO_2/CH_4)$	$\alpha(CO_2/He)$
	± 1.1 ºC*	CO_2	CH_4	He		
PDMS	10.3	14.67 ± 0.15	4.286 ± 0.018	2.664 ± 0.011	3.42 ± 0.038	5.51 ± 0.061
	24.8	14.27 ± 0.16	5.044 ± 0.025	3.691 ± 0.017	2.83 ± 0.035	3.87 ± 0.047
	30.4	14.25 ± 0.086	5.260 ± 0.016	-	2.71 ± 0.018	-
	39.9	14.14 ± 0.12	5.609 ± 0.022	4.730 ± 0.0082	2.52 ± 0.024	2.99 ± 0.026
Teflon-AF	10.4	14.43 ± 0.059	1.797 ± 0.0036	-	8.03 ± 0.037	-
	24.8	12.00 ± 0.060	1.767 ± 0.0068	10.78 ± 0.59**	6.79 ± 0.043	1.11 ± 0.061
	40.3	10.70 ± 0.038	1.949 ± 0.0049	-	5.49 ± 0.024	-

* Accuracy.

** Obtained from one experimental point.

The Teflon-AF membrane is unsuitable for the carbon dioxide/helium sensor due to its low selectivity, $\alpha(CO_2/CH_4)$ = 1.11 ± 0.061 at 24.8ºC. Therefore, the carbon dioxide/helium sensor was tested only with PDMS membranes, while the carbon dioxide/methane sensor was tested with both PDMS and Teflon-AF membranes. The nomenclature used is as follows: PDMS\$CO_2/CH_4$, for the carbon dioxide/methane sensor with PDMS membranes; Teflon\$CO_2/CH_4$, for the carbon dioxide/methane sensor with Teflon-AF membranes; and PDMS\$CO_2$/He, for the carbon dioxide/helium sensor with PDMS membranes.

The mass transfer coefficient was also obtained as a function of the feed composition. Permeation experiments were carried out with the three sensors, PDMS\$CO_2/CH_4$, Teflon\$CO_2/CH_4$ and PDMS\$CO_2$/He, using different carbon dioxide feed compositions at 24.7-25.1ºC. The permeate flow rate was measured for a pressure difference between feed and permeate sides ranging from 0.12 to 0.18 MPa. Mixture mass transfer coefficients were obtained from Eq. (3.2). The feed flow rate was always much higher than the permeate flow rate. Under these conditions, the retentate composition was essentially equal to the feed composition. The effect of the feed composition on the mixture mass transfer coefficient is shown in Fig. 3.3.

The results obtained indicate that when the carbon dioxide feed concentration increases, the mass transfer coefficient also increases. The permeate flow rate through the membrane module is therefore related to the gas mixture composition.

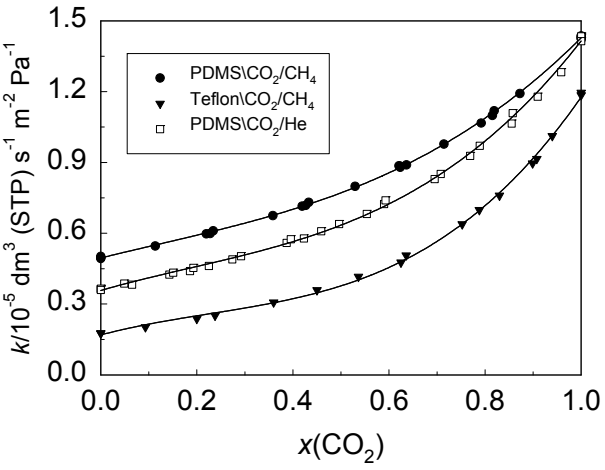

Fig. 3.3. Mixture mass transfer coefficient (k) as a function of carbon dioxide feed molar fraction, $x(CO_2)$, for the three sensors at 24.7-25.1ºC. The pressure difference between feed and permeate sides ranged from 0.12 to 0.18 MPa. Experimental points from four different runs are represented. The lines are 3rd degree polynomial fittings.

3.3.2. Response curves of the sensors

By measuring the pressure in the permeate side of the sensor, carbon dioxide feed concentration can be computed using the correct calibration curve. This curve can be obtained by measuring the permeate pressure at different carbon dioxide feed compositions, keeping the feed pressure and temperature constant. Some calibration curves were obtained in our experimental set-up.

The permeate pressure (P^P) was measured at different temperatures as a function of the carbon dioxide feed molar fraction, $x(CO_2)$. The results are shown in Figs. 3.4 and 3.5 for carbon dioxide/methane and carbon dioxide/helium sensors, respectively. The first sensor was tested with both PDMS and Teflon-AF membranes.

Fig. 3.4 shows the response of PDMS\$CO_2/CH_4$ and Teflon\$CO_2/CH_4$ sensors to different concentrations of carbon dioxide/methane mixtures at 0.301 MPa feed pressure. The needle valve was set to 0.18 MPa permeate pressure when pure carbon dioxide was fed to the devices at 24.8ºC and left unchanged for all experiments. The results shown are from four sets of measurements performed on different days and at three different temperatures. The best fit of the data was achieved with a third degree polynomial at constant feed pressure. The experimental points obtained from four different runs at a given temperature fall on the same calibration curve.

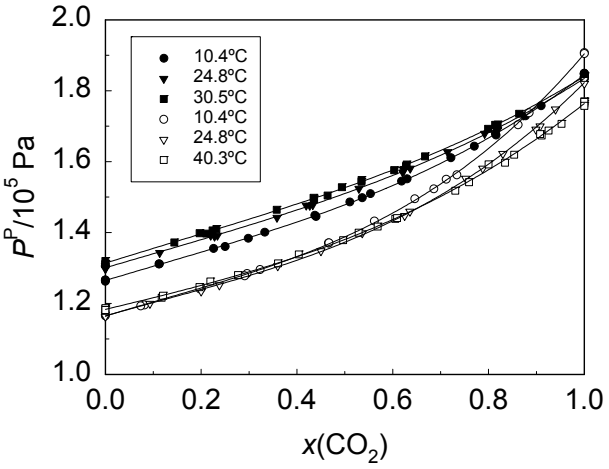

Fig. 3.4. Permeate pressure (P^P) as a function of carbon dioxide feed molar fraction, $x(CO_2)$, for PDMS\$CO_2/CH_4$ (close symbols) and Teflon\$CO_2/CH_4$ (open symbols) sensors at 0.301 MPa feed pressure and three different temperatures. The maximum permeate pressure was set to 0.1841 and 0.1831 MPa, for PDMS\$CO_2/CH_4$ and Teflon\$CO_2/CH_4$ sensors, respectively, at 24.8ºC. The lines are 3rd degree polynomial fittings.

Fig. 3.4 shows that the temperature effect on the response of the sensors is significantly different. For the PDMS\CO_2/CH_4 sensor, the temperature effect on the methane mass transfer coefficient is the dominant

factor, which accounts for the observed increase of the permeate pressure response of the sensor with the temperature. Also, PDMS membranes show a weak dependence of carbon dioxide permeability on the temperature. For the Teflon\$CO_2$/$CH_4$ sensor, the temperature effect on the sensor response remains essentially unchanged, in the 0-60% range of carbon dioxide feed concentration. The results found for the Teflon\$CO_2$/$CH_4$ sensor are very encouraging, as they suggest that the response of the sensor is not significantly affected by temperature variations of the gas mixtures when $x(CO_2) \leq 0.6$, compatible with biogas analysis.

Fig. 3.5 shows the response of PDMS\CO_2/He to different concentrations of carbon dioxide/helium mixtures at 0.300 MPa feed pressure.

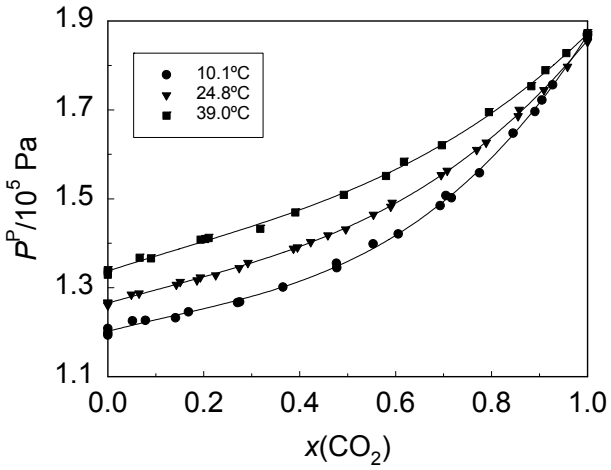

Fig. 3.5. Permeate pressure (P^P) as a function of carbon dioxide feed molar fraction, $x(CO_2)$, for PDMS\CO_2/He sensor at 0.300 MPa feed pressure and for three different temperatures. The maximum permeate pressure was set to 0.1853 MPa at 24.8ºC. The lines are 3rd degree polynomial fittings.

It produced qualitatively similar responses to the ones from PDMS\CO_2/CH_4. The maximum permeate pressure was also set to 0.18 MPa for 24.8ºC and left unchanged for all experiments. The results shown

are also from four sets of measurements performed on different days and for 10.1, 24.8 and 39.0ºC. At constant feed pressure, a third degree polynomial fits the experimental data quite well. The results seem to be reproducible. For the PDMS\CO_2/He sensor the response also depends on temperature except when $x(CO_2) \rightarrow 1$.

The precision of the sensors was evaluated from the response curves, which average several experimental points.

The absolute sensitivity of the sensors is defined as $S_{\text{absolute}} = \frac{\mathrm{d}P^{\mathrm{P}}}{\mathrm{d}x(\mathrm{CO}_2)}$.

Fig. 3.6 compares the sensitivity of the three sensors as a function of carbon dioxide feed molar fraction, $x(CO_2)$, for 0.301 MPa feed pressure and 24.7-25.1ºC. The highest sensitivity was achieved with the Teflon\CO_2/CH_4 sensor. The sensitivity depends on the carbon dioxide feed concentration and ranges from 0.03 to 0.13 MPa. Fig. 3.6 shows that the sensitivity stays approximately constant when $x(CO_2) \leq 0.3$.

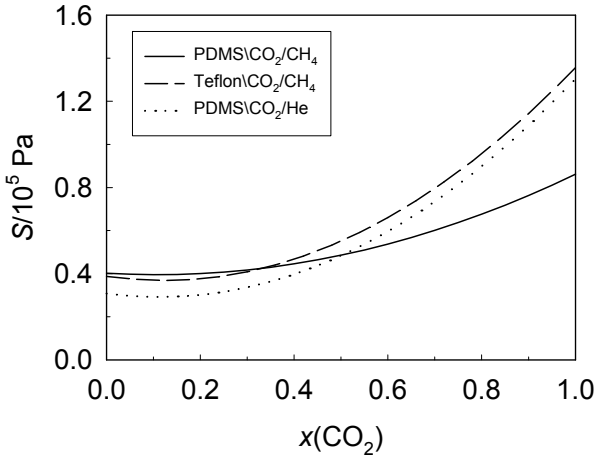

Fig. 3.6. Sensor sensitivity (S) as a function of carbon dioxide feed molar fraction, $x(CO_2)$, for the three sensors at 0.301 MPa feed pressure and 24.7-25.1ºC.

3.3.3. Response time and reversibility

The response time of a sensor to a change in the feed composition is an important characteristic of a sensor. In this study the response time is defined as the time taken to reach 95% of full response ($t_{0-95\%}$). The determination of the response time of a sensor is generally difficult because it depends on the measuring conditions. To determine experimentally the response time and the reversibility of the response of the three sensors (PDMS\$CO_2$/$CH_4$, Teflon\$CO_2$/$CH_4$ and PDMS\$CO_2$/He) they were fed alternately with carbon dioxide and methane or helium, at 24.7-24.8ºC, keeping the feed pressure constant. Rapid switching between gas streams was achieved using a three-way valve.

The comparison of the response times for the three sensors obtained under fixed experimental conditions is shown in Fig. 3.7. The same trend can be observed for all of them. The response time is less than 50 s for all the sensors, excluding the residence time of gases in the connecting tubes. These fast responses are suitable for practical measurements. In Fig. 3.7, the dashed and solid arrows indicate, respectively, time $t_{0\%}$ when switching occurs and time $t_{95\%}$ when a new steady signal has almost been reached.

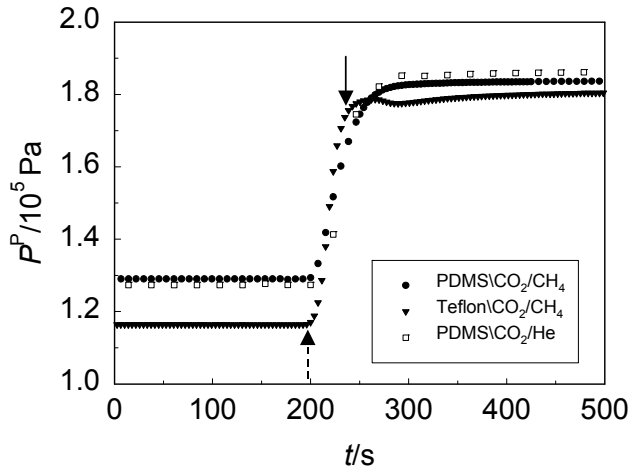

Fig. 3.7. Permeate pressure (P^P) as a function of time (t) for the three sensors at 24.7-24.8ºC. The feed pressure was 0.301, 0.300 and 0.303 MPa for PDMS\$CO_2/CH_4$, Teflon\$CO_2/CH_4$ and PDMS\$CO_2$/He sensors, respectively. The data was recorded every 4 s and 23 s for carbon dioxide/methane and carbon dioxide/helium sensors, respectively.

From Fig. 3.8 it is also possible to conclude that the response of the sensors is fully reversible. A square wave feed concentration change with a 1.1×10^4 s (3 hours) period was taken into account. In this figure, the dashed and solid arrows indicate the time when the feed was changed from methane or helium to carbon dioxide and from carbon dioxide to methane or helium, respectively.

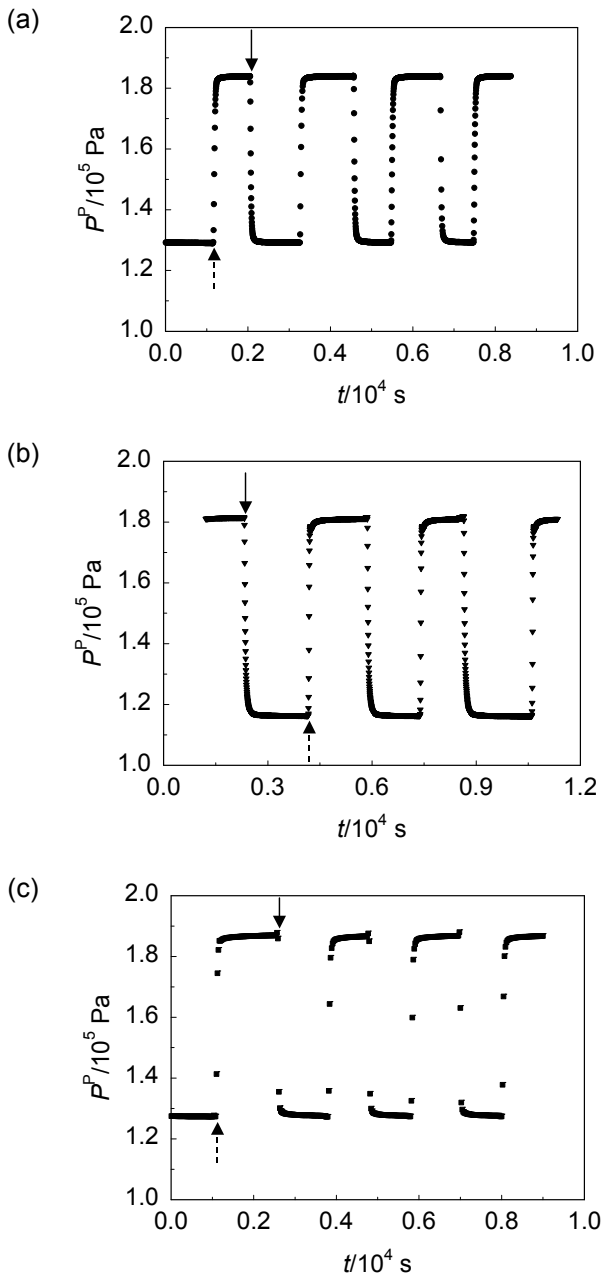

Fig. 3.8. Permeate pressure (P^P) as a function of time (t) for PDMS\$CO_2$/$CH_4$ (a), Teflon\$CO_2$/$CH_4$ (b) and PDMS\$CO_2$/He (c) sensors at 24.7-24.8ºC. The feed pressure was 0.301, 0.300 and 0.303 MPa for PDMS\$CO_2$/$CH_4$, Teflon\$CO_2$/$CH_4$ and PDMS\$CO_2$/He sensors, respectively. The data was recorded every 4 s and 23 s for carbon dioxide/methane and carbon dioxide/helium sensors, respectively.

3.3.4. Long-term stability

The long-term stability of the PDMS membrane module was tested in the present study. The PDMS membrane module was fed alternately with carbon dioxide, methane and helium, as well as with carbon dioxide/methane and carbon dioxide/helium mixtures for three months at 10, 25, 30 and 40ºC to determine, experimentally, its long-term stability. When not in use, the membrane module was stored at room temperature. The permeate flow rate was measured for a pressure difference between feed and permeate sides ranging from 0.112 to 0.122 MPa at 24.6-25.1ºC. During this period the carbon dioxide mass transfer coefficient in the PDMS membrane was obtained from Eq. (3.2) at different times. Since the measured carbon dioxide mass transfer coefficient in the PDMS membrane stayed almost constant as a function of time ($\bar{k}$ = 1.433 x 10^{-5} dm^3 (STP) s^{-1} m^{-2} Pa^{-1}, s = 0.012 x 10^{-5}, N = 23) it may be concluded that no degradation of the sensor response was observed over this time period. Also, the results suggest that the membrane module can be stored for many months without any effect on its response.

3.4. Conclusions and further research

Carbon dioxide/methane and carbon dioxide/helium gas sensors were designed, built and tested. These sensors are low cost and suitable for the low/medium precision market. Carbon dioxide/methane is particularly suited for *in situ* biogas monitoring. Possible applications for the carbon dioxide/helium sensor still have to be explored.

The results obtained suggest that the two membrane-based sensors can be used to determine the carbon dioxide concentration in binary mixtures with methane or helium. Reproducibility, sufficient/medium precision, long-term stability and fast response time were obtained for both applications. Other useful features of the sensors are their low cost, small

dimensions, simple design, solvent-free use, ease of automation and on-line and *in situ* monitoring.

The Teflon membrane seems to be more suitable for the carbon dioxide/methane sensor because it is barely affected by the gas mixture temperature when $x(CO_2) \leq 0.6$ evaluated for 10.4ºC<T<40.3ºC. Thus, there is no need for temperature compensation, which enables the manufacture of a very cheap instrument.

Interference of other gases in the response of the sensors, other than carbon dioxide and methane or helium, was not evaluated. More experimental work is needed in order to evaluate the carbon dioxide/methane sensor for biogas monitoring *in situ*.

While this work reports an interesting configuration and application of membrane-based sensors, the practical use of such a sensor for real world applications needs further research for robustness, longevity, manufacturability, and other performance requirements that will allow further commercialization of this device.

The study of other permselective sensors (hydrogen/nitrogen and hydrogen/methane) is currently underway and will be described in a following paper (Paper 4). A mathematical model can be derived with predictable features, considering different operating conditions such as feed pressure, feed flow pattern, needle valve model and temperature effects.

Acknowledgements

This work was financially supported by Agência de Inovação, s.a., (project P0046/ICPME/S - Gassense).

References

[1] K.K. Stewart, L.C. Craig, Anal. Chem. 42 (1970) 1257.
[2] B. Strandberg, P.-A. Bergqvist, C. Rappe, Anal. Chem. 70 (1998) 526.
[3] T.M. Pekol, J.A. Cox, Environ. Sci. Technol. 29 (1995) 1.
[4] C.G. Pinto, M.E.F. Laespada, J.L.P. Pavón, B.M. Cordero, Laboratory Automation and Information Management 34 (1999) 115.
[5] K. Fukui, S. Nishida, Sens. Actuators B 45 (1997) 101.
[6] T.E. Brook, R. Narayanaswamy, Sens. Actuators B 51 (1998) 77.
[7] G. Li, S. Kawi, Sens. Actuators B 59 (1999) 1.
[8] K. Kaneyasu, K. Otsuka, Y. Setoguchi, S. Sonoda, T. Nakahara, I. Aso, N. Nakagaichi, Sens. Actuators B 66 (2000) 56.
[9] O. Hugon, M. Sauvan, P. Benech, C. Pijolat, F. Lefebvre, Sens. Actuators B 67 (2000) 235.
[10] M. Vilaseca, J. Coronas, A. Cirera, A. Cornet, J.R. Morante, J. Santamaría, Catal. Today 82 (2003) 179.
[11] M. Koyama, Y. Sato, M. Aizawa, S. Suzuki, Anal. Chim. Acta 116 (1980) 307.
[12] M.J. Muehlbauer, E.J. Guilbeau, B.C. Towe, Anal. Chem. 61 (1989) 77.
[13] M. Mascini, D. Moscone, L. Bernardi, Sens. Actuators B 6 (1992) 143.
[14] G.F. Khan, E. Kobatake, H. Shinohara, Y. Ikariyama, M. Aizawa, Anal. Chem. 64 (1992) 1254.
[15] K.T. Kinnear, H.G. Monbouquette, Anal. Chem. 69 (1997) 1771.
[16] K. Kihara, E. Yasukawa, S. Hirose, Anal. Chem. 56 (1984) 1876.
[17] Y. Kitagawa, K. Kitabatake, M. Suda, H. Muramatsu, T. Ataka, Anal. Chem. 63 (1991) 2391.
[18] K. Wiegran, T. Trapp, K. Cammann, Sens. Actuators B 57 (1999) 120.

[19] M. Kuratli, M. Badertscher, B. Rusterholz, W. Simon, Anal. Chem. 65 (1993) 3473.
[20] M. Takahashi, T. Ishiji, N. Kawashima, Sens. Actuators B 77 (2001) 237.
[21] A. Ohki, K. Shinohara, O. Ito, K. Naka, S. Maeda, T. Sato, H. Akano, N. Kato, Y. Kawamura, Intern. J. Environ. Anal. Chem. 56 (1994) 261.
[22] Z. Hu, D. Qi, Anal. Chim. Acta 248 (1991) 177.
[23] F.L. Dickert, S.K. Schreiner, G.R. Mages, H. Kimmel, Anal. Chem. 61 (1989) 2306.
[24] S. Ozawa, P.C. Hauser, K. Seiler, S.S.S. Tan, W.E. Morf, W. Simon, Anal Chem. 63 (1991) 640.
[25] S.A. Glazier, E.R. Campbell, W.H. Campbell, Anal. Chem. 70 (1998) 1511.
[26] L.M. Moretto, P. Ugo, M. Zanata, P. Guerriero, C.R. Martin, Anal Chem. 70 (1998) 2163.
[27] J.S. Symanski, S. Bruckenstein, Anal. Chem. 58 (1986) 1771.
[28] J.R. Stetter, Z. Cao, Anal. Chem. 62 (1990) 182.
[29] D.L. Ellis, M.R. Zakin, L.S. Bernstein, M.F. Rubner, Anal Chem. 68 (1996) 817.
[30] C.G. Siontorou, D.P. Nikolelis, U.J. Krull, K.-L. Chiang, Anal. Chem. 69 (1997) 3109.
[31] A. Mendes, Patent PT102 312 (2000).
[32] R. Rego, N. Caetano, R. Vale, A. Mendes, Anal. Chim. Acta submitted for publication (2003).
[33] http://www.anton-paar.com
[34] D. Lasik, H. Geistlinger, Patent WO 01/53796 A1, EP 1 157 265 A1, DE 199 25 842 A 1 (2001).
[35] Ullmann's Encyclopedia of Industrial Chemistry, Electronic Release, 6th ed.; Wiley-VCH: Weinheim, 2003; Chapter Plastics, Analysis.
[36] U. Desideri, F.D. Maria, D. Leonardi, S. Proietti, Energ. Convers. Manage 44 (2003) 1969.
[37] M. A. Goossens, Renew. Energ. 9 (1996) 1015.
[38] The Federal Regulations for Municipal Solid Waste Landfills: 40 CFR 258 - Criteria For Municipal Solid Waste Landfill (2001).

[39] http://www.enviroequip.com

[40] http://www.enviroequipment.com

[41] http://www.geotechenv.com

[42] M.-B. Hagg, J. Membr. Sci. 177 (2000) 109.

[43] M. Mulder, Basic Principles of Membrane Technology, 2nd ed., Kluwer Academic Publishers, Dordrecht, 2000, Chapter 1.

4. Carbon dioxide/methane gas sensor based on the permselectivity of polymeric membranes for biogas monitoring

Abstract

Membrane based-sensors have been used for determining the composition of bi-component mixtures in the 0-100% range, such as oxygen/nitrogen, carbon dioxide/helium, carbon dioxide/methane, hydrogen/nitrogen and hydrogen/methane. These sensors are suited for the low cost and low/medium precision market.

The present study describes a carbon dioxide/methane sensor suitable for biogas composition monitoring. The membrane used is poly(dimethylsiloxane) (PDMS) hollow fiber. The calibration curves were obtained at three different temperatures. The results clearly show that the permeate pressure of the sensor is related to the gas mixture composition at a given temperature. The sensor enables quantitative carbon dioxide analysis in binary mixtures of carbon dioxide/methane with fast, continuous, reproducible and long-term stable response.

R. Rego, A. Mendes, Sens. Actuators B 103 (2004) 2-6.

4.1. Introduction

Low cost concentration sensors for monitoring processes would have a great impact on environmental preservation, for safety and in energy saving [1]. There is a growing market for such sensors and in particular for a cheap and reliable carbon dioxide/methane sensor of medium precision for biogas monitoring. Biogas is composed of almost equal parts methane and carbon dioxide. It therefore is combustible and potentially dangerous [2]. The utilization of this gas as fuel for electrical and thermal energy production could avert this danger, reduce the impact on the environment and could provide a renewable energy source [2, 3].

The biogas composition has been measured with biogas analyzers such as those produced by www.ados.de, www.kelma.com, www.enviroequip.com and www.omniinstruments.co.uk [4-7]. However, the cost of these apparatus is high (about € 2,500) and it is difficult to install them at each biogas-emitting site. The currently proposed carbon dioxide/methane sensor could be used to control the biogas emissions and to optimize the operating conditions of methane recovery units.

Recently, the use of a membrane-based sensor was proposed for determining the composition of binary mixtures, such as oxygen/nitrogen, for medical applications [8]. The sensor is based on the permselective effect of membranes. A small stream of the binary gas mixture, whose concentration is to be read, is supplied to the feed side of the sensor. Assuming that the membrane is selectively more permeable to one of the components in the feed gas then, if the feed pressure is kept constant, the permeate flow is related to the gas mixture concentration. A non-selective barrier such as a needle valve causes a pressure drop on the permeate outlet which is related to the permeate flow rate and, therefore, to the feed concentration. The pressure in the permeate side can be measured by means of a cheap pressure transducer [8-10].

This paper describes a permselective gas sensor for determining the composition of carbon dioxide/methane mixtures in the 0-100% range. A polymeric membrane is used: polydimethylsiloxane (PDMS) hollow fibers

(supplied by GKSS, Germany). For a PDMS membrane, response curves were obtained at three different temperatures. Reproducibility, sensitivity, response time and reversibility, long-term stability and temperature dependence of this sensor are discussed.

4.2. Experimental

The sketch of the binary gas mixture sensor is shown in Fig. 4.1. The sensor consists of a permselective membrane, a pressure transducer for measuring the permeate pressure and a needle valve (a non-selective barrier).

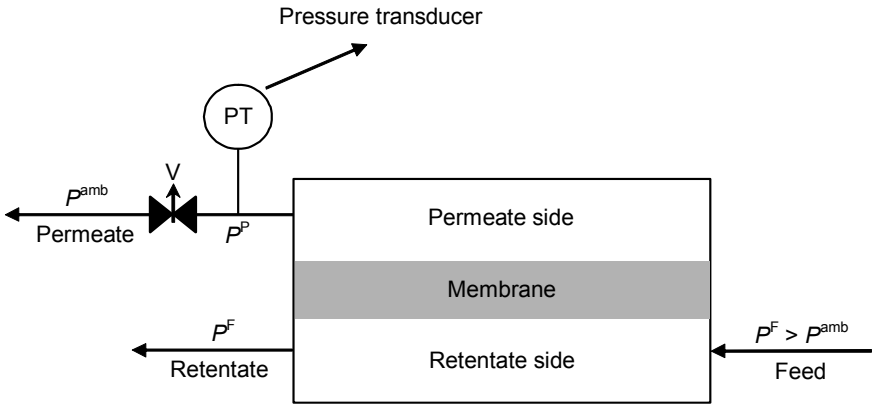

Fig. 4.1. Sketch of the binary gas mixture sensor.

The needle valve is used to control the permeate outlet to the atmosphere. The needle valve permeability changes slightly as a function of the permeate composition because the viscosity of the two components is different (0.150×10^{-4} and 0.112×10^{-4} Pa s, at 300 K, for carbon dioxide and methane, respectively [11]). The gas mixture to be analyzed should be supplied at a constant pressure, which must be higher than the outlet

permeate pressure (P^P). In our system, the feed pressure (P^F) was set to 3 bara (bar absolute), while the permeate pressure after the needle valve (V) was the ambient pressure (P^{amb}). A poly(dimethylsiloxane) (PDMS) composite membrane module with 6 hollow fibers and a work length of 113 mm was assembled. The inside diameter of these fibers is 0.71 mm. The module was tested with hydrogen for any leakage before the experiment began. For this membrane, carbon dioxide is the fastest gas and methane the slowest. When the feed contains only the slowest and the fastest permeable gases (one each time), the permeate pressure attained at the permeate side is the minimum and the maximum pressure respectively.

The sensor was tested in an experimental set-up similar to the one described in [5]. The gases tested were carbon dioxide and methane, from Air Liquid, 99.995% purity. The feed gas mixture to be analyzed was fed to the bore side in the membrane module at the desired flow rate. The feed pressure and the temperature were kept constant by means of two pressure regulators in series and a thermostatic bath, respectively. The temperature and the feed pressure were measured with a K type thermocouple connected to a digital thermometer and a pressure transducer (Lucas Schaevitz, P941, range 0-10 bara, $\leq$ ±0.1% FS), respectively. The permeate pressure was also measured with a pressure transducer (Lucas Schaevitz, PS10061, range 0-2.5 bara, $\leq$ ±0.1% FS). Feed composition measurements were made with an infrared carbon dioxide analyzer (Servomex, 1400D, range 0-100% v/v, $\pm$1% FS). The reproducibility of the carbon dioxide/methane sensor was also verified by repeating each experiment at least twice on different days. Additional details are given elsewhere [5].

4.3. Results and discussion

In order to evaluate the performance of the carbon dioxide/methane gas sensor, some experiments were made in the experimental set-up. The following issues were studied: sensor response, sensitivity, reproducibility,

response time and reversibility and long-term stability. The effect of the temperature was always considered. In order to characterize the membrane used mono and mixture mass transfer coefficients for both gases and ideal selectivities at each considered temperature were determined.

4.3.1. Mono and mixture mass transfer coefficients determinations

The mass transfer coefficient (k) is defined as the ratio between the permeate flux (F^P/A) and the corresponding pressure difference between feed and permeate sides (ΔP):

$$k = \frac{F^P/A}{\Delta P} \tag{4.1}$$

where, F^P is the permeate flow rate and A is the cross-flow area. When k is invariant with ΔP, it can be obtained from the slope of the plot of the permeate flux as a function of ΔP. The permeate flow rate was measured for a feed pressure range of 1.9 to 4.2 bara and for 284, 298, 304 and 313 K. The permeate pressure ranged from 1.1 to 2.1 bara (needle valve partially closed). Table 4.1 shows the ideal carbon dioxide/methane selectivity, $\alpha(CO_2/CH_4)$, and carbon dioxide and methane mass transfer coefficients in the PDMS membrane, measured at four temperatures. The PDMS membrane shows higher permeability towards carbon dioxide than towards methane. The CO_2/CH_4 selectivity is temperature dependent. The methane mass transfer coefficient for the PDMS membrane increases with temperature while the carbon dioxide mass transfer coefficient remains nearly constant. As a result, carbon dioxide/methane selectivity decreases when the temperature increases.

Table 4.1

Ideal CO_2/CH_4 selectivity, $\alpha(CO_2/CH_4)$, and CO_2 and CH_4 mass transfer coefficients (k) in PDMS measured at four different temperatures.

Temperature/K	kx10^{-4}/ml (STP) min^{-1} m^{-2} bar^{-1}		$\alpha(CO_2/CH_4)$
	CO_2	CH_4	
284	8.82	2.57	3.43
298	8.55	3.03	2.82
304	8.55	3.16	2.71
313	8.46	3.37	2.51

The effect of the feed composition on the mass transfer coefficients of the carbon dioxide/methane mixture was also studied. Permeation experiments were carried out with the PDMS membrane module using different carbon dioxide feed compositions. The permeate flow rate was measured for a pressure difference between feed and permeate sides ranging from 1.2 to 1.8 bara. The mixture mass transfer coefficient was obtained from Eq. (4.1). The feed flow rate was always high enough to guarantee no composition variation in the retentate side. Fig. 4.2 shows the results obtained at four different temperatures. It can be seen that when the carbon dioxide feed concentration increases, the mixture mass transfer coefficient also increases. A 3rd degree polynomial seems to fit the data quite well.

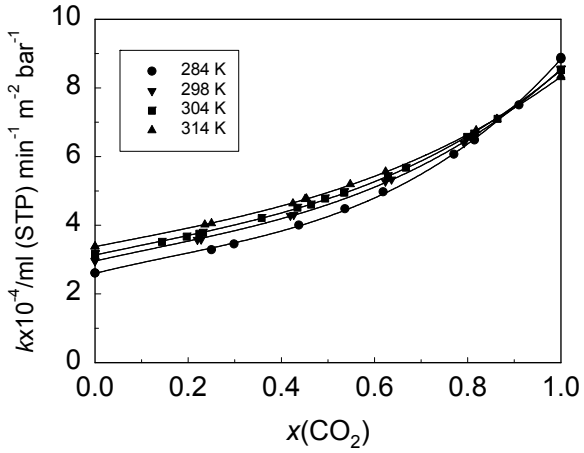

Fig. 4.2. Mixture mass transfer coefficient (k) as a function of carbon dioxide feed molar fraction, $x(CO_2)$, for the sensor at four different temperatures. The pressure difference between feed and permeate sides ranged from 1.2 to 1.8 bara. Experimental points from two different experiments are represented. The lines are 3rd degree polynomial fittings.

4.3.2. Response of the sensor

Fig. 4.3 shows the response of the sensor to different concentrations of carbon dioxide/methane at 3.01 bara feed pressure. The needle valve was set to 1.841 bara permeate pressure when pure carbon dioxide was being fed to the device at 298 K and left unchanged for all experiments. The results shown are from two sets of measurements performed on different days and at 284, 298 and 304 K. At constant feed pressure, a third degree polynomial fits the experimental data quite well. The experimental points obtained on different days fall on the same calibration curve.

Temperature variations could affect the sensor response. It can be seen from Fig. 4.3 that the PDMS permeability towards carbon dioxide shows a weak dependence on the temperature. It may also be concluded from Fig. 4.3 that the highest absolute sensitivity (which measure variations

in permeate pressure as a function of variations in binary mixture composition) was achieved at 284 K.

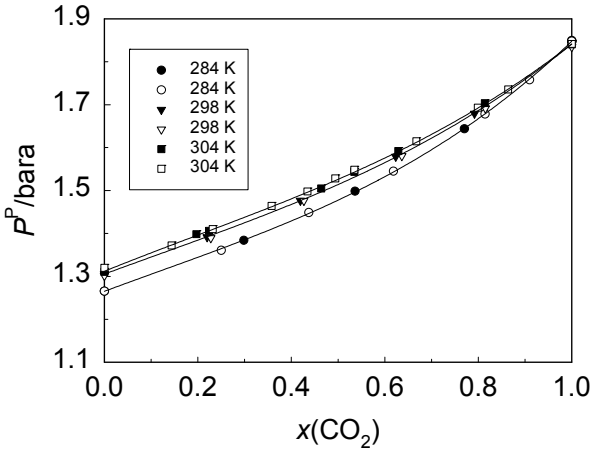

Fig. 4.3. Permeate pressure (P^P) as a function of carbon dioxide feed molar fraction, $x(CO_2)$, for PDMS sensor at 3.01 bara feed pressure and three different temperatures. The maximum permeate pressure was set to 1.841 bara at 298 K. The lines are 3rd degree polynomial fittings. Solid symbols - day 1; Open symbols - day 2.

4.3.3. Response time and reversibility

The response time of a sensor is defined as the time taken to attain 95% of the full response. To determine experimentally the response time and reversibility of the sensor, it was fed, alternately, with carbon dioxide and methane at 284, 298 and 304 K at 3.01 bara feed pressure.

Fig. 4.4 shows the plot obtained of permeate pressure (P^P) as a function of time (t). The response times were approximately 80 seconds, including the connecting tubes (residence time). From Fig. 4.4 it can also be seen that the sensor response is fully reversible for the three temperatures. In this figure, the solid and dashed arrows indicate the time when the feed was changed from carbon dioxide to methane and from methane to carbon dioxide, respectively.

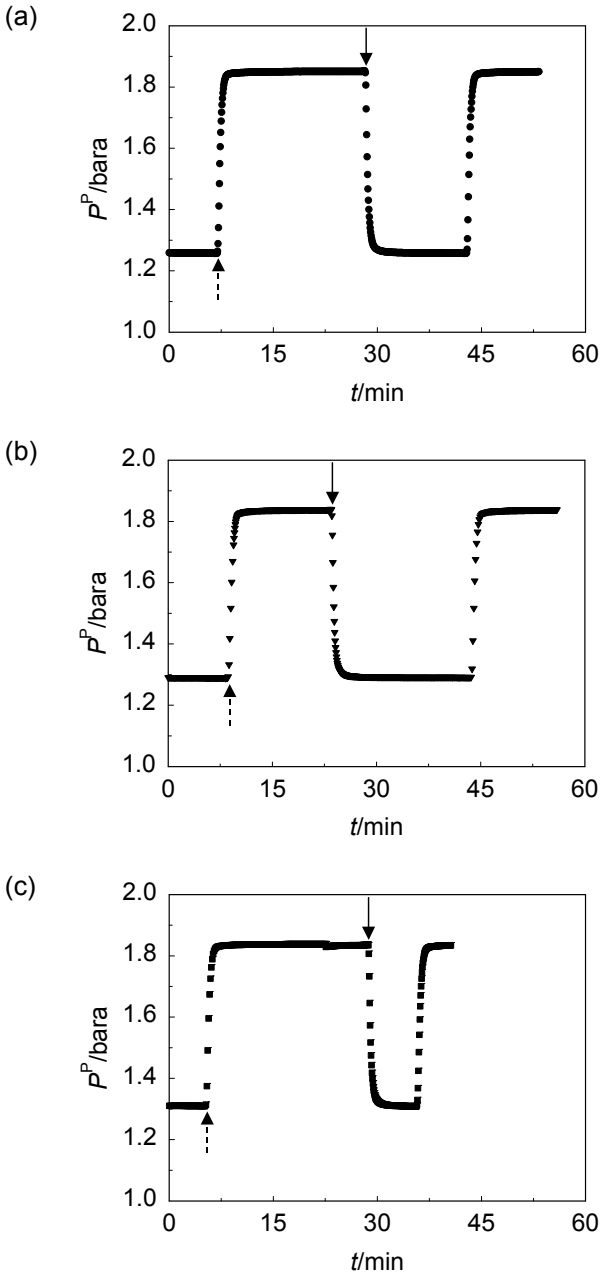

Fig. 4.4. Permeate pressure (P^P) as a function of time (t) for the PDMS sensor at 284 K (a), 298 K (b) and 304 K (c). The feed pressure was 3.01 bara for the three different temperatures.

4.3.4. Long-term stability

To determine experimentally the long-term stability of the PDMS membrane module, it was fed alternately with carbon dioxide, methane and carbon dioxide/methane mixture for three months at 283, 298, 303 and 313 K. The permeate flow rate was measured for a pressure difference between feed and permeate sides ranging from 1.03 to 1.22 and from 1.64 to 1.72 bara, respectively, for carbon dioxide and methane at 298 K. During this period the methane and carbon dioxide mass transfer coefficients were obtained for different times, as shown in Fig. 4.5.

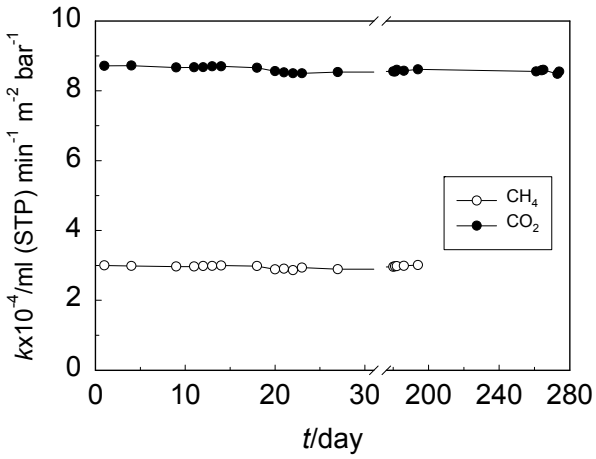

Fig. 4.5. Methane and carbon dioxide mass transfer coefficients (*k*) as a function of time (*t*) for the PDMS membrane at 298 K. The pressure difference between feed and permeate sides ranged from 1.03 to 1.22 and 1.64 to 1.72 bara, respectively, for carbon dioxide and methane. Lines were put for reading facility.

Since the measured methane and carbon dioxide mass transfer coefficients in the PDMS membrane stayed almost constant as a function of time, it may be concluded that no deterioration of the response of the sensor membrane module occurred during this period.

4.4. Conclusions

A new carbon dioxide/methane gas sensor is described and tested. An important application devised for this sensor is the monitoring of the carbon dioxide/methane content in a biogas stream. Other applications are possible.

Experimental results indicate that the studied sensor has medium precision, high reproducibility, long-term stability, reversibility and a response time shorter than 1.5 minutes. More importantly, its low cost and small dimensions offer the possibility of installing this sensor at every biogas-emitting site. As a result, it will be possible to control biogas emissions and to optimize the operating conditions of methane recovery units.

The PDMS membrane seems to be only slightly affected by temperature variations. However, when the biogas stream temperature is approximately constant, the temperature compensation system can be removed from the carbon dioxide/methane sensor without seriously compromising precision and reducing the price of the sensor.

Further experiments will be concerned with testing the carbon dioxide/methane sensor in a wastewater treatment plant and/or a landfill in order to make a final evaluation of the unit.

Acknowledgements

The present work was supported by Agência de Inovação, s.a., (Project P0046/ICPME/S - Gassense).

References

[1] J.P. Silveira, J. Anguita, F. Briones, F. Grasdepot, A. Bazin, Micromachined methane sensor based on low resolution spectral modulation of IR absorption radiation, Sens. Actuator B-Chem. 48 (1998) 305-307.

[2] M.A. Goossens, Landfill gas power plants, Renew. Energy 9 (1996) 1015-1018.

[3] U. Desideri, F. Di Maria, D. Leonardi, S. Proietti, Sanitary landfill energetic potential analysis: a real case study, Energy Conv. Manag. 44 (2003) 1969-1981.

[4] http://www.ados.de

[5] http://www.kelma.com

[6] http://www.enviroequip.com

[7] http://www.omniinstruments.co.uk

[8] R. Rego, N. Caetano, R. Vale, A. Mendes, Development of a new gas sensor for binary mixtures based on the permselectivity of polymeric membranes. 1 - Application to oxygen/nitrogen mixture, Anal. Chim. Acta Submitted (2003).

[9] A. Mendes, Gas mixtures concentration sensor and corresponding measuring processes, Patent PT 00/102312 (2000).

[10] R. Rego, N. Caetano, A. Mendes, Development of a new gas sensor for binary mixtures based on the permselectivity of polymeric membranes. 2 - Application to carbon dioxide/methane and carbon dioxide/helium mixtures, to be published in Anal. Chim. Acta (2004).

[11] R.H. Perry, D.W. Green, J.O. Maloney, Perry's Chemical Engineers' Handbook, Sixth Edition, McGraw-Hill International Editions, 1984, pp. 3-247.

5. Hydrogen/methane and hydrogen/nitrogen sensor based on the permselectivity of polymeric membranes

Abstract

A new gas sensor for measuring the concentration of binary gas mixtures in the 0-100% range based on the permselectivity of polymeric membranes has recently been developed by the authors. This sensor is not expensive and aimed at the low/medium precision market.

This paper describes the use of this sensor for a hydrogen/methane binary gas mixture. Preliminary results are also provided for a hydrogen/nitrogen gas mixture. The membranes used are poly(etherimide) (PEI), Teflon-AF and poly(dimethylsiloxane) (PDMS) hollow fibers. The sensor has been subjected to a series of experiments to evaluate its response in terms of stability, repeatability and accuracy as well as to the effects of temperature. The permeate flow rate of the sensor relates to the gas mixture composition at a given temperature; a needle valve at the permeate side leads to a pressure build up, which can be related to the permeate flow rate and then to the feed composition. The sensor allows quantitative hydrogen analysis in binary mixtures with methane, showing a second order polynomial response. The response of the sensor is fast, continuous, reversible, reproducible and long-term stable over a period of 1.5×10^7 s. The relative sensitivity of the sensor depends on the hydrogen feed concentration, ranging from 0.20 to 0.70. The sensitivity, temperature dependency and response time of the sensor is related to the membrane permeability and selectivity.

A mathematical model has recently been described whose results are in agreement with our experimental results for PEI and Teflon-AF membranes.

R. Rego, N. Caetano, A. Mendes, Sens. Actuators B 111-112 (2005) 150-159.

5.1. Introduction

Membranes can be used in a number of applications, such as micro-, ultra-, nano- and hyper filtration, pervaporation, dialysis, electrodialysis, gas separation and chemical reactors [1, 2].

In the field of sensor technology, membranes have attracted increasing attention [3-5]. Since the first analytical application of a membrane described by Hoch and Kok [6], carbon, zeolite and polymeric membranes have been used in different types of chemical- and bio- sensors in order to increase their selectivity [7-30]. The use of membrane-based sensors in different fields has been widely reported, for example, for the determination of fructose in fruit juices [31], ethanol in beer [32], transaminases in blood serum [33], ascorbic acid in pharmaceutical tablets [34], nitrate in fertilizers as well as in drinking and natural water [35, 36], and to determine the hardness of water [37], chemical oxygen demand (COD) in water [38], biochemical oxygen demand (BOD) [39], dissolved carbon dioxide in water and seawater [40], oxygen and carbon dioxide in the photosynthesis process [41] and carbon dioxide in air [42], among others. Multi-sensor systems, electronic tongues and noses, consisting of an array of chemical sensors with polymeric membranes have been developed and used for the detection of component parts of taste and aroma in coffee, tea, red wine and olive oil [43-45]. In the field of gas analysis, there is a generalized commercial need for low cost and low/medium precision sensors to improve the safety and performance of small to medium size gas separation units [46].

A new gas sensor was proposed in previous reports by our group to determine the composition of oxygen/nitrogen, carbon dioxide/methane and carbon dioxide/helium binary mixtures [47-49]. The sensor is based on the permselectivity of a membrane. At constant feed pressure there is a relationship between the gas input concentration and the permeate flow rate. On the other hand, the permeate flow rate can be related to the built up permeate pressure before a needle valve, which can be measured with a simple pressure transducer [50].

A few reports of sensors based on a similar principle can be found in the literature. Miller [51] describes an apparatus and method for measuring the oxygen concentration in a gas mixture of oxygen, nitrogen and argon. The oxygen concentration is determined from the shell side permeate flow rate through a hollow fiber permeable membrane module. Lazik and Geistlinger proposed a method using a plastic membrane for determining the concentration of gases, particularly oxygen, in liquids [52]. This plastic membrane should only be permeable to some specific gases. Recently, a device for determining dissolved carbon dioxide in beverages has been developed [53].

Hydrogen has been used in various fields, such as hydrogenation processes, petroleum transformation, fuel cells, soldering, cryogenic freezing, or chemical substances production [54]. The availability of sensors for detecting and monitoring hydrogen is, therefore, a necessary concern for these industries. Hydrogen concentration has been measured with thermal conductivity analyzers such as those produced by Panametrics, Teledyne and Thermco [55-57]. However, the cost of these apparati is high and they are difficult to install at each industrial process stream. Currently proposed hydrogen/methane and hydrogen/nitrogen sensors could be used to monitor quality control in manufacturing plants that use or produce hydrogen, such as ammonia plants and the metal industry. Other applications are possible. The low cost of such sensors is a significant contribution to the development of more generalized gas monitoring.

This work aims to study new applications for the permselective sensor. Three different polymeric membranes were used: poly(etherimide) (PEI), poly(dimethylsiloxane) (PDMS) and Teflon-AF hollow fibers.

Results are given for hydrogen/methane and hydrogen/nitrogen mixtures. For both sensors, response curves were obtained. The reproducibility, sensitivity, response time and reversibility, long-term stability and temperature dependence of a hydrogen/methane sensor were studied. Also, the influence of the membrane characteristics in the response of the sensors was evaluated.

5.2. Experimental

The developed binary gas mixture sensor is made of a permselective membrane, a pressure transducer for measuring the permeate pressure and a needle valve (Fig. 5.1).

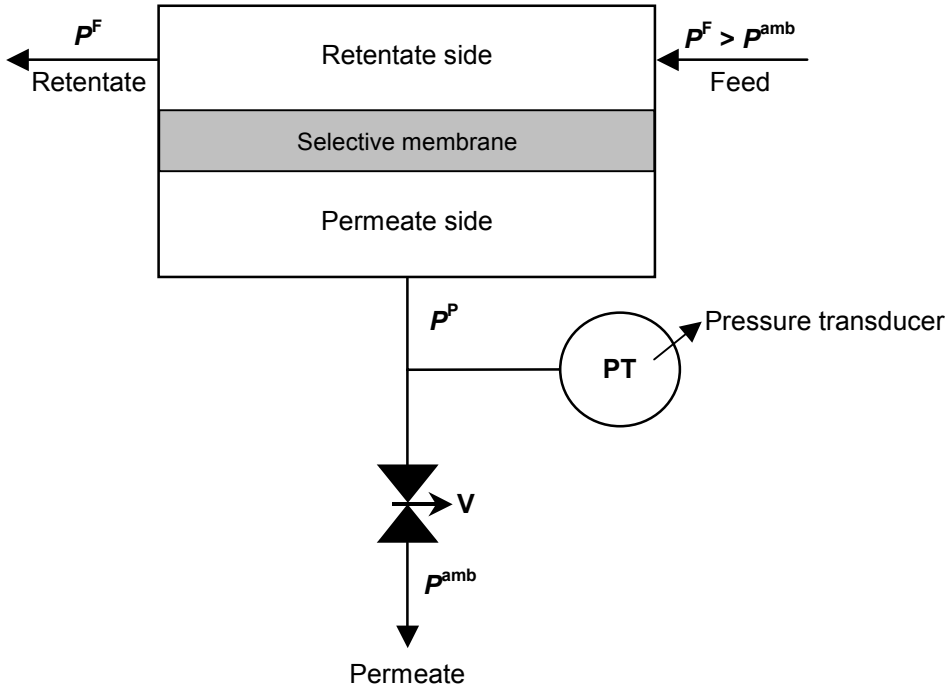

Fig. 5.1. Sketch of the binary gas mixture sensor.

The needle valve is only used to induce a pressure drop. A second membrane can be used in place of the needle valve. The second membrane will increase the sensor sensitivity if it has an inverted selectivity.

The needle valve controls the permeate outlet to the atmosphere. The needle valve permeability changes slightly as a function of the permeate composition because the viscosity of the components is different: 9.0×10^{-6},

11.2 x 10^{-6} and 18.0 x 10^{-6} Pa s, at 25ºC, for hydrogen, methane and nitrogen, respectively [58].

The gas mixture to be analyzed is supplied at a constant pressure, which must be higher than the outlet permeate pressure (P^P). In our system, the feed pressure (P^F) was set to 0.30 or 0.35 MPa, while the permeate pressure, after the needle valve (V), was the ambient pressure (P^{amb}).

For all membranes used in this work, methane and nitrogen are the slowest gases and hydrogen is the fastest when their permeation characteristics are compared. When, at different times the feed stream contains only the slowest and the fastest gas, the pressure attained at the permeate side is, respectively, the minimum (P^P_{min}) and the maximum (P^P_{max}) permeate pressure.

The experimental set-up was essentially as described in a previous work [47]. Fig. 5.2 shows the experimental set-up developed for testing the hydrogen/methane and hydrogen/nitrogen sensors. The gases used were hydrogen, methane and nitrogen obtained from Air Liquide and at 99.995% purity.

The hollow fibers used in this study were: poly(dimethylsiloxane) (PDMS) and Teflon-AF composite membranes and a poly(etherimide) (PEI) integral asymmetric membrane, supplied by GKSS, Germany. Their main differences are related to their permeation characteristics. Fig. 5.3 shows a scanning electron microscopy (SEM) of a PEI integral asymmetric membrane where the selective dense layer (bore side) and the porous support (shell side) are visible. SEM images were recorded using a Philips FEI Quanta 400 electron scanning microscope equipped with a tungsten (W) filament emission source running at 20/25 kV. The samples were gold coated using sputtering prior to investigation.

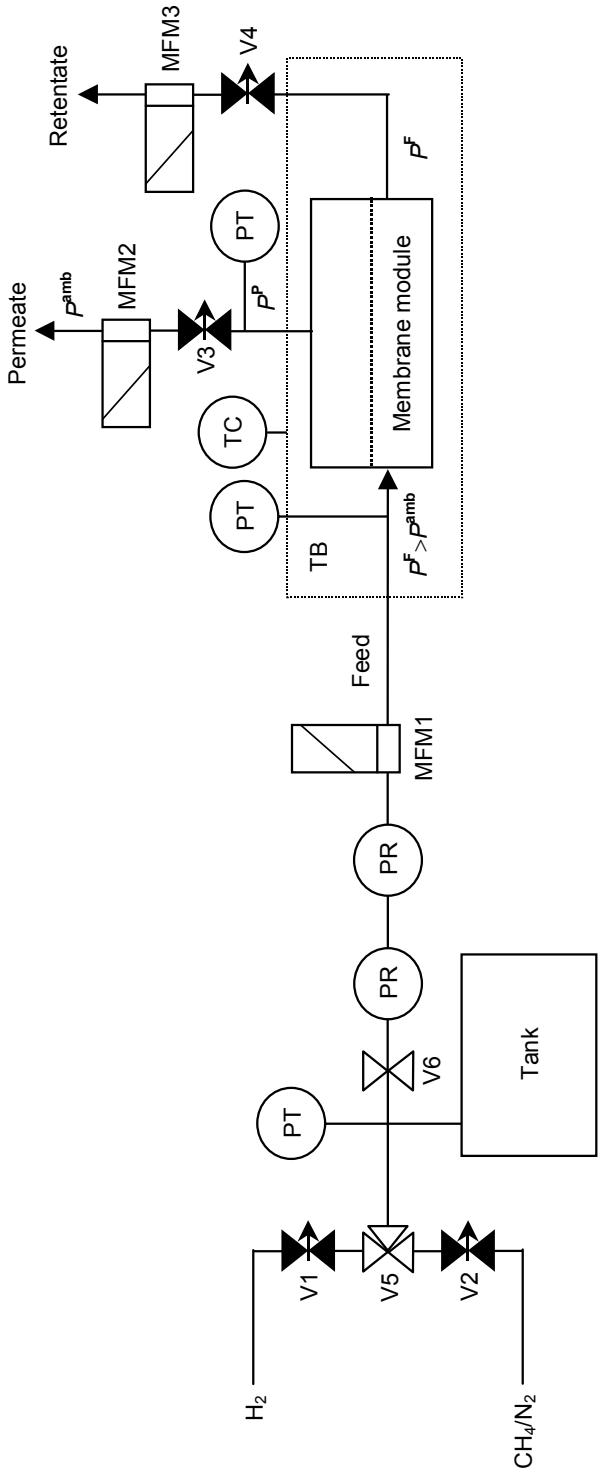

Fig. 5.2. Schematic experimental set-up. V1, V2, V3 and V4 are needle valves; V5 is a three-way valve; V6 is an on/off valve; PR is a pressure regulator; MFM1, MFM2 and MFM3 are mass flow meters; PT is a pressure transducer; TC is a thermocouple and TB is a thermostatic bath.

(a)

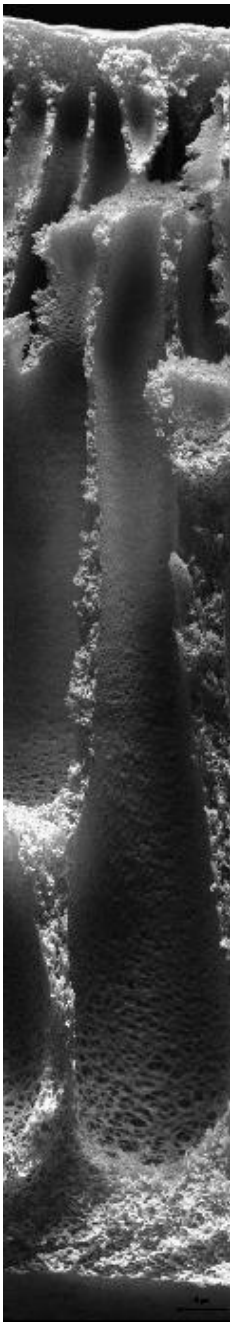

(b)

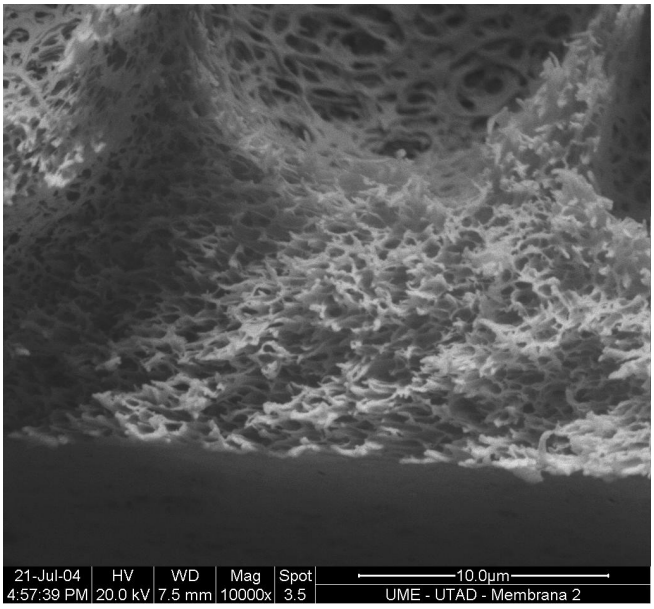

Fig. 5.3. Scanning electron microscopy image of the PEI membrane: (a) overall view of the cross section of the fiber (magnification x10,000); (b) view of the shell side (magnification x10,000).

Five membrane modules were prepared in our laboratory by inserting the hollow fibers into a polyurethane tube of 5.9 x 10^{-3} m (ID) (Festo, PU-6). Both ends of the modules were sealed with epoxy glue (Degussa AG, Agomet P 76). The characteristics of the hollow fiber membranes and the membrane modules are shown in Table 5.1. Before use, the membrane modules were tested with hydrogen in order to check for leakage.

Table 5.1

Characteristics of the hollow fiber membranes and membrane modules.

	Module reference				
	Poly(dimethylsiloxane) (PDMS)		Poly(etherimide) (PEI)	Teflon-AF	
#	#1	#2	#1	#1	#2
Number of fibers	6	10	14	3	6
Fiber OD/10^{-3} m	1.04	1.04	1.04	1.04	1.04
Fiber ID/10^{-3} m	0.71	0.71	0.72	0.63	0.63
Work fiber length/10^{-3} m	113	133	98	149	149
Area/10^{-3} m^2	1.512	2.967	3.103	0.8847	1.769

Different hydrogen mixtures (in the range 0-100%) were prepared using a 5 dm^3 tank equipped with a pressure transducer. Hydrogen was admitted up to a certain pressure to the evacuated tank. The second gas was then added to make the desired gas mixture and to fulfill the operating pressure of 0.8 MPa. The gas mixture in the tank was stirred with a magnetic stir bar to guarantee homogeneity. The pressure was measured with a pressure transducer connected to the tank (Lucas Schaevitz, P941, range 0-1 MPa, $\leq \pm 0.1\%$ FS).

The feed stream to be analyzed was then fed into the bore side of the membrane module at the desired flow rate and pressure. The proposed sensor does not need a stable input flow rate. The feed flow rate needs only to be large enough to guarantee that there is no concentration variation on

the retentate side. However, it is important to keep the feed pressure as constant as possible.

The feed pressure was kept constant with two pressure regulators in series and was measured with a pressure transducer (Lucas Schaevitz, P941, range 0-1 MPa, ≤ ±0.1% FS). The permeate pressure was also measured with the help of a pressure transducer (Lucas Schaevitz, PS10061, range 0-0.25 MPa, ≤ ±0.1% FS). The sensor was kept at a constant temperature by means of a thermostatic bath. A K type thermocouple (Omega, KMQSS-M150, accuracy ±1.1ºC), connected to a digital thermometer (TES, TES-1300, ± (0.3% of the read + 1.0ºC)), was kept as close as possible to the membrane module, allowing direct monitoring and control of the sensor's temperature. The feed, permeate and retentate flow rates, as well as feed and permeate pressures were continuously monitored and recorded using a computer acquisition system. Additional details are given elsewhere [47]. The experiments were repeated at least twice for each operating condition and on different days for reproducibility.

5.3. Results and discussion

Data on membranes permeabilities and ideal selectivities are necessary for estimating the sensor's performance. Thus, the selected membranes were characterized for permeabilities at different temperatures using mono and bi-component gas mixtures with different compositions. Then, in order to evaluate the overall performance of the sensors, response curves (calibration curves) were obtained and the sensitivity, response time and reversibility, long-term stability and also the influence of operating conditions such as temperature, were evaluated.

5.3.1. Pure and mixture mass transfer coefficients

The permeate steady flux, F^P/A, through a membrane is given by [59]:

$$F^P/A = k \times \Delta P \tag{5.1}$$

where F^P is the permeate flow rate, ΔP is the pressure difference between the feed and permeate sides, A is the membrane cross flow area and k is the permeance or mass transfer coefficient. In this study and because the membrane thickness was not known accurately, mass transfer coefficients were used instead of permeabilities to characterize the membrane mass transport.

When k is invariant with ΔP, it can be obtained from the slope of the F^P/A plot as a function of ΔP. Hydrogen, methane and nitrogen mass transfer coefficients in PDMS, PEI and Teflon-AF membranes were determined using this approach. It was verified that the mass transfer coefficients of the studied gases and the membranes considered were constant and independent of the feed and permeate pressures. The permeate flow rate was determined for a feed pressure range between 0.20 and 0.47 MPa and at 10, 25 and 40ºC. The permeate pressure ranged from ambient to 0.23 MPa (needle valve open or partially closed).

The so-called ideal selectivity of hydrogen/methane, $\alpha(H_2/CH_4)$, and hydrogen/nitrogen, $\alpha(H_2/N_2)$, was obtained from the ratio between the corresponding mass transfer coefficients for each membrane. The ideal selectivities and mass transfer coefficients for PDMS, PEI and Teflon-AF membranes are summarized in Table 5.2. The experimental error of the mass transfer coefficient was obtained from the standard deviation of the slope of the regression plot. PDMS, PEI and Teflon-AF membranes show higher mass transfer coefficients towards hydrogen than towards methane or nitrogen. The polymer with the highest selectivity, PEI, shows relatively low permeability. The two PDMS membrane modules show reproducible nitrogen mass transfer coefficients. Also, the reproducibility between the two

Teflon-AF membrane modules is satisfactory as shown by the results reported in Table 5.2. The selectivities for PEI and Teflon-AF membrane modules are temperature dependent. Hydrogen and methane mass transfer coefficients in PEI increase with the temperature. On the other hand, for the Teflon-AF membrane, the hydrogen and nitrogen mass transfer coefficients increase only slightly with temperature. As a result, hydrogen/nitrogen selectivity increases with temperature, although not as much as the corresponding hydrogen/methane selectivity. For the PEI membrane, the hydrogen/methane selectivity is very high (Table 5.2).

The permeability of a membrane towards a solute can be obtained from the product of the sorption and diffusion coefficients [59]. The sorption coefficient decreases with the temperature while the diffusion coefficient increases. For PEI and Teflon-AF, the permeability towards hydrogen, methane and nitrogen (which sorbs very little) increases with temperature, indicating a diffusion-controlled transport.

The PDMS membrane is unsuitable for the hydrogen/methane sensor due to its very low selectivity, $\alpha(H_2/CH_4) = 1.197 \pm 0.022$ at 25.0ºC.

The experimental results presented below were obtained by testing only three membrane modules, PEI, Teflon-AF #1 and PDMS #1. The hydrogen/methane sensor was tested with both PEI and Teflon-AF membranes and the hydrogen/nitrogen sensor was tested only with PDMS membranes. The nomenclature used is as follows: PEI\$H_2/CH_4$, for the hydrogen/methane sensor with PEI membranes; Teflon\$H_2/CH_4$, for the hydrogen/methane sensor with Teflon-AF membranes; and PDMS\$H_2/N_2$, for the hydrogen/nitrogen sensor with PDMS membranes.

The mass transfer coefficients of the binary mixtures were studied as a function of the feed composition. Fig. 5.4 shows the effect of the feed concentration on the mixture mass transfer coefficient.

Permeation experiments were carried out with all sensors, PEI\$H_2/CH_4$, Teflon\$H_2/CH_4$ and PDMS\$H_2/N_2$, using different hydrogen feed compositions. The PEI\$H_2/CH_4$ sensor was tested at three different temperatures, 10.3, 24.8 and 41.3ºC, while Teflon\$H_2/CH_4$ and PDMS\$H_2/N_2$ sensors were only tested at 25.0ºC.

Table 5.2

Ideal H_2/CH_4 and H_2/N_2 selectivities, $\alpha(H_2/CH_4)$ and $\alpha(H_2/N_2)$, and H_2, CH_4 and N_2 mass transfer coefficients (k) in PDMS, PEI and Teflon-AF membranes at different temperatures (T).

Membrane module	T/ºC ± 1.1 ºC*	$k/10^{-8}$ dm^3 (STP) s^{-1} m^{-2} Pa^{-1}			$\alpha(H_2/CH_4)$	$\alpha(H_2/N_2)$
		H_2	CH_4	N_2		
PDMS #1	25.0	484.73 ± 0.51	404.9 ± 7.5**	138.98 ± 0.42	1.20 ± 0.022	3.49 ± 0.011
PDMS #2	24.7	-	-	139.45 ± 0.31	-	-
PEI	10.3	33.70 ± 0.18	1.860 ± 0.022	-	18.12 ± 0.23	-
	24.8	52.00 ± 0.26	2.294 ± 0.014	0.986 ± 0.011	22.67 ± 0.18	52.7 ± 0.64
	41.3	67.73 ± 0.42	2.862 ± 0.026	-	23.66 ± 0.26	-
Teflon-AF #1	10.6	966.0 ± 3.7	-	-	-	-
	24.8	1013.8 ± 3.4	181.95 ± 0.47	-	5.57 ± 0.024	-
	40.1	1088.5 ± 3.7	-	-	-	-
Teflon-AF #2	24.8	953.44 ± 0.96	178.92 ± 0.88	-	5.33 ± 0.027	-

* Accuracy.
** Obtained from only one experiment.

The permeate flow rate was measured for a pressure difference between the feed and permeate sides ranging from 0.12 to 0.24 MPa. Mixture mass transfer coefficients were obtained using Eq. (5.1). Experimental points from three or four different runs are plotted. The feed flow rate was always much higher than the permeate flow rate. Under these conditions, the retentate composition was essentially equal to the feed composition. The results indicate that increasing the hydrogen feed concentration in the mixture increases the mass transfer coefficient for all sensors. This effect is more pronounced for the PEI\H_2/CH_4 sensor. As a result, the permeate flow rate through the membrane module can be related to the gas mixture composition. It can also be seen from Fig. 5.4 that the PEI mass transfer coefficients towards the binary mixtures are dependent on the temperature.

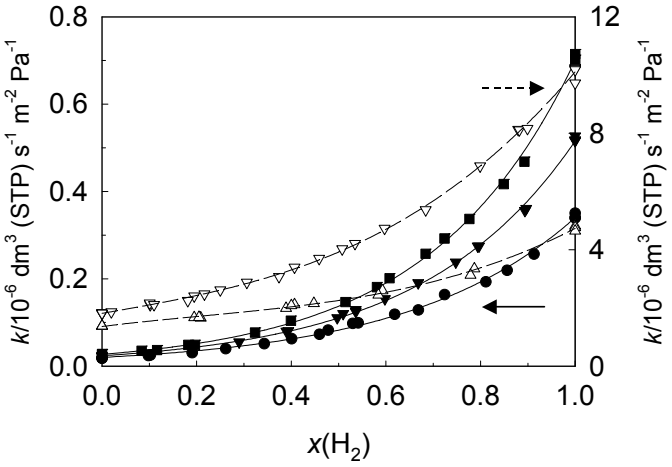

Fig. 5.4. Mixture mass transfer coefficient (*k*) as a function of hydrogen molar fraction in the feed, $x(H_2)$, for PDMS\$H_2/N_2$ at 25.0ºC (△), Teflon\$H_2/CH_4$ at 24.8ºC (▽) and PEI\$H_2/CH_4$ (solid symbols) at 10.3 (●), 24.8 (▼) and 41.3ºC (■). The pressure difference between feed and permeate sides ranged from 0.12 to 0.24 MPa. The dashed and solid lines are third order polynomial and exponential fittings, respectively.

5.3.2. Sensor's response curves

The permeate pressure of the sensor (P^P) was measured at different temperatures as a function of the hydrogen feed molar fraction, $x(H_2)$, at constant feed pressure. The results are shown in Figs. 5.5 and 5.6. The hydrogen/methane sensor was tested with PEI and Teflon-AF membranes, while the hydrogen/nitrogen sensor was tested only with PDMS membranes.

Fig. 5.5 compares the responses of PEI and Teflon-AF membranes to different concentrations of the hydrogen/methane mixtures at 0.353 and 0.301 MPa feed pressure, respectively. The needle valve was set to 0.1871 and 0.1505 MPa, respectively, for PEI\$H_2$/$CH_4$ and Teflon\$H_2$/$CH_4$ sensors at 25ºC when pure hydrogen was being fed, and left unchanged for experiments performed at 10, 25 and 40ºC. The PEI sensor was tested at three different temperatures: 10.3, 24.8 and 41.3ºC, while Teflon\$H_2$/$CH_4$ was tested only at 24.8ºC. The results were obtained from three or four sets of measurements performed on different days and appear to be reproducible. A second order polynomial fitted the data. The response of the sensors with PEI and Teflon-AF membranes is significantly different. The use of PEI membranes allows the preparation of sensors with improved sensitivity.

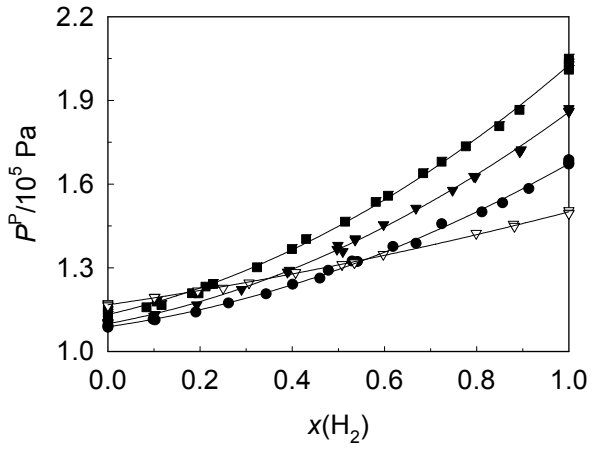

Fig. 5.5. Permeate pressure (P^P) as a function of hydrogen feed molar fraction, $x(H_2)$, for Teflon\$H_2$/$CH_4$ (open symbols) at 24.8ºC and PEI\$H_2$/$CH_4$ (solid symbols) at 10.3 (●), 24.8 (▼) and 41.3ºC (■). The lines are second order polynomial fittings.

Fig. 5.6 shows the response of PDMS membranes to different concentrations of the hydrogen/nitrogen mixtures at 0.303 MPa feed pressure. The needle valve was set to 0.1847 MPa permeate pressure when pure hydrogen was fed to the PDMS\H_2/N_2 device at 25.0ºC. The results obtained from three sets of measurements, on different days, seem to be reproducible. For this sensor, the plot exhibits linearity at hydrogen concentrations lower than about 70%. At higher hydrogen concentrations, the sensor's output (permeate pressure) levels off. Hydrogen is far less viscous than nitrogen (9.0 x 10^{-6} Pa s) and the needle valve permeability should increase as the hydrogen concentration increases on the permeate side. Eventually, this effect balances the membrane permeability increase with the hydrogen feed concentration, leading to the response plotted in Fig. 5.6.

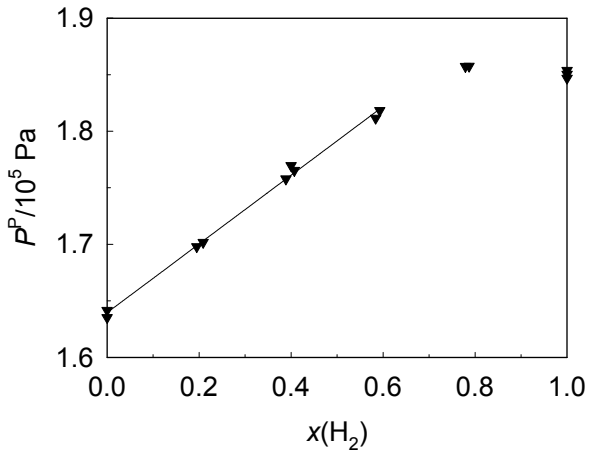

Fig. 5.6. Permeate pressure (P^P) as a function of hydrogen feed molar fraction, $x(H_2)$, for PDMS\H_2/N_2 sensor at 0.303 MPa feed pressure and 25.0ºC. The line is a linear fitting.

The precision of the sensors was evaluated from the response curves, which average several experiments. Sensitivity is a key requirement in

sensor applications. The absolute or local sensitivity of the sensor is defined as $S_{\text{absolute}} = \frac{\mathrm{d}P^{\mathrm{P}}}{\mathrm{d}x(\mathrm{H}_2)}$.

In this study, the sensitivity is normalized by the permeate pressure for PEI\$H_2$/$CH_4$ and Teflon\$H_2$/$CH_4$. Fig. 5.7 shows the relative sensitivity for these sensors as a function of hydrogen feed molar fraction, $x(H_2)$, at different temperatures. The feed pressure was 0.354 and 0.300 MPa, respectively, for PEI\$H_2$/$CH_4$ and Teflon\$H_2$/$CH_4$. The sensitivity depends on the membrane material and on the hydrogen feed concentration. The sensitivity of the Teflon\$H_2$/$CH_4$ sensor is low but it was clearly enhanced when PEI membranes were used. The sensitivity ranged from 0.20 to 0.28 (0 and 100% hydrogen, respectively) for Teflon\$H_2$/$CH_4$ sensor and from to 0.28 to 0.65 (0 and 100% hydrogen, respectively) for PEI\$H_2$/$CH_4$ sensor at 25ºC. It can also be seen from this figure that the sensitivity for PEI\$H_2$/$CH_4$ is temperature dependent. For this sensor, the sensitivity increases with the temperature.

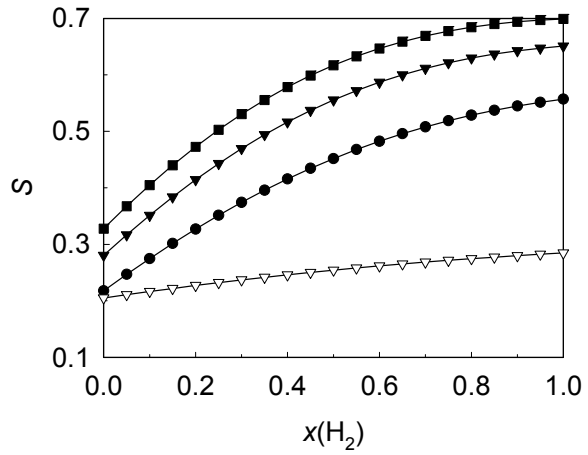

Fig. 5.7. Relative sensitivity of the sensor (S) as a function of hydrogen feed molar fraction, $x(H_2)$, for Teflon\$H_2$/$CH_4$ at 24.8ºC (open symbols) and PEI\$H_2$/$CH_4$ (solid symbols) at 10.3 (●), 24.8 (▼) and 41.3ºC (■).

5.3.3. Response time and reversibility

Sensors require time to stabilize and reach a steady state output signal. In sensor applications, membranes should provide response times, which are as short as possible. In this work the response time is defined as the time taken to reach 95% of the maximum signal $t_{0-95\%}$. This time was obtained for the PEI module, which shows the best sensitivity. Fig. 5.8 shows a plot of permeate pressure (P^P) as a function of time (t) for PEI\H_2/CH_4 sensor at three temperatures. The response time for the PEI membrane was estimated to be between 70 and 180 s. Teflon-AF and PDMS membranes respond must faster (a few seconds) because their permeability towards hydrogen is high. These response times are suitable for different applications.

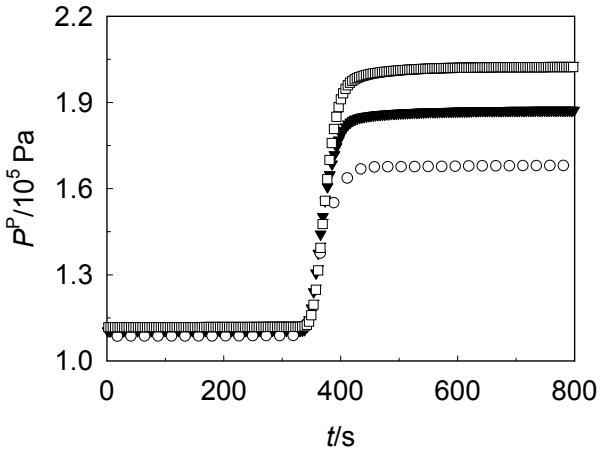

Fig. 5.8. Permeate pressure (P^P) as a function of time (t) for PEI\H_2/CH_4 at 10.3 (○), 24.8 (▼) and 41.3ºC (□). The feed pressure was 0.354 MPa. The data was recorded every 23 s at 10.3ºC and every 4 s at 24.8 and 41.3ºC.

The reversibility of the sensor was studied by alternately feeding the sensor with hydrogen and methane, keeping the feed pressure constant. Fig. 5.9 shows the response of PEI\H_2/CH_4 sensor at 24.8ºC and with a feed pressure of 0.354 MPa. A square wave feed concentration with a 8.5 x 10^3 s period was applied. This figure indicates that the signal of the sensor is fully reversible during the procedure. In this figure, the dashed and solid arrows indicate, respectively, the time when the feed was changed from methane to hydrogen and from hydrogen to methane.

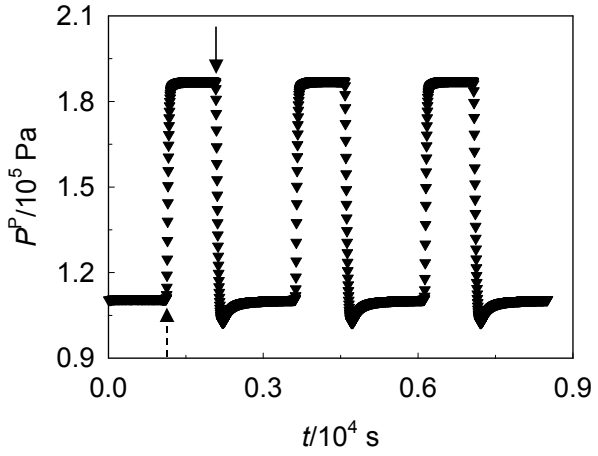

Fig. 5.9. Permeate pressure (P^P) as a function of time (t) for PEI\H_2/CH_4 at 24.8ºC. The feed pressure was 0.354 MPa. The data was recorded every 4 s.

5.3.4. Long-term stability

Long-term response stability of the sensors is required for most applications. Long-term stability measurements were performed using the sensor with the best sensitivity. In these experiments, PEI\H_2/CH_4 sensor was randomly fed with pure hydrogen or methane, as well as with hydrogen/methane mixtures at 10, 25 and 40ºC. The membrane module was stored at room temperature when not in use. During this time the hydrogen

and methane mass transfer coefficients for the PEI membrane module were obtained at different times, as shown in Fig. 5.10. Mixture mass transfer coefficients were obtained using Eq. (5.1). The permeate flow rate was determined for a feed pressure range of 0.22 to 0.47 MPa and at 25.0ºC. The permeate pressure ranged from ambient to 0.23 MPa (needle valve open or partially closed). The lines in this figure are given only as a visual aid. The data show that membrane modules can be stored for many months without ageing. More importantly, the mass transfer coefficients remain essentially constant as a function of time, indicating that no degradation of the sensor response was observed over this time period.

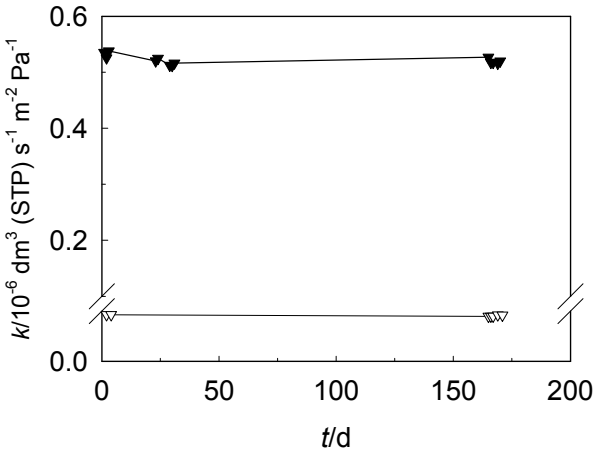

Fig. 5.10. Hydrogen (solid symbols) and methane (open symbols) mass transfer coefficients (k) as a function of time (t) for PEI membranes at 24.8ºC. Feed and permeate pressures ranged from 0.22 to 0.47 MPa and from ambient pressure to 0.23 MPa, respectively. The lines are there for easy reading.

5.3.5. Experimental and simulated results

A mathematical model has recently described the response of the sensor [47]. The model proposed is based on the following main

assumptions: ideal gas behavior, isothermal operation, perfectly mixed flow pattern on both the permeate and retentate sides, constant permeabilities with the retentate and permeate pressures used, constant feed pressure, and molar flow rate at the needle valve outlet proportional to the difference between permeate and ambient pressures. Data necessary for simulation are shown in Table 5.3.

The simulated results can be obtained using equation [47]:

$$\left(P^{\text{amb}} - P^{\text{F}}\right)\left(P^{\text{P}}\right)^2 + \left[P^{\text{F}} x_{\text{H}_2}\left(P^{\text{P}}_{\text{max}} - P^{\text{P}}_{\text{min}}\right) + P^{\text{F}}\left(P^{\text{amb}} + P^{\text{P}}_{\text{min}}\right) - P^{\text{amb}}\left(P^{\text{P}}_{\text{max}} + P^{\text{P}}_{\text{min}}\right)\right]P^{\text{P}} + \left[P^{\text{F}} x_{\text{H}_2} P^{\text{amb}}\left(P^{\text{P}}_{\text{min}} - P^{\text{P}}_{\text{max}}\right) + P^{\text{P}}_{\text{min}} P^{\text{amb}}\left(P^{\text{P}}_{\text{max}} - P^{\text{F}}\right)\right] = 0 \quad (5.2)$$

Table 5.3

Experimental data for PEI and Teflon-AF membranes measured at 24.8ºC.

Membrane	T/ºC	P^{F} /MPa	$P^{\text{P}}_{\text{min}}$ /MPa	$P^{\text{P}}_{\text{max}}$ /MPa	P^{amb} /MPa
PEI	24.8	0.352	0.1102	0.1864	0.1004
Teflon-AF	24.8	0.301	0.1168	0.1498	0.1008

Fig. 5.11 shows experimental and simulated results obtained for the permeate pressure (P^{P}) as a function of hydrogen feed molar fraction, $x(H_2)$, at 25ºC, for PEI and Teflon-AF membrane modules. Solid (PEI membranes) and open (Teflon-AF membranes) symbols represent experimental data while the solid line represents the proposed model. As shown in this figure, for both membranes, the theoretical prediction is a good fit with experimental data, indicating that it accurately describes the behavior of the hydrogen/methane sensor for the operating conditions considered.

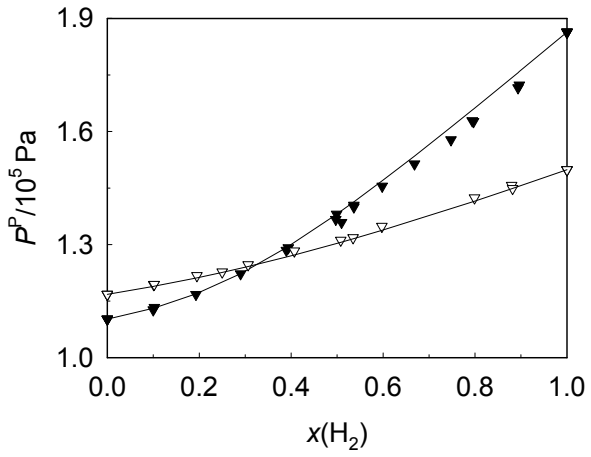

Fig. 5.11. Permeate pressure (P^P) as a function of hydrogen feed molar fraction, $x(H_2)$, for experimental and simulated results (solid line), with PEI (solid symbols) and Teflon-AF (open symbols) membranes at 24.8ºC.

5.4. Conclusions and further research

Permselective membranes were used in the development of low priced sensors for the analysis of binary gas samples. The use of inexpensive gas sensors offers an opportunity to design relatively cheap, small and rugged equipment with the potential for continuous on-line analysis of gas streams.

All of the three membrane materials (PEI, Teflon-AF and PDMS) discussed in the current study have long-term stability, but their permeation properties differ greatly and hence their suitability for membrane-based sensors. The results obtained indicate that PEI and PDMS membranes seem to be more suitable for hydrogen/methane and hydrogen/nitrogen sensors, respectively. The use of PEI membranes allows the preparation of sensors with high sensitivity and with a response time between 70 and 180 s. However, the response time of the Teflon\$H_2/CH_4$ sensor is expected to be only a few seconds. The effect of temperature on PEI\$H_2/CH_4$ sensor

response is significant. The sensitivity ranged from 0.20 to 0.28 (0 and 100% hydrogen, respectively) for Teflon\$H_2/CH_4$ sensor and from 0.28 to 0.65 (0 and 100% hydrogen, respectively) for PEI\$H_2/CH_4$ sensor at 25ºC. The PDMS membrane is suitable for the hydrogen/nitrogen sensor in the 0-70% range. However, further studies are required with this system. The response of PEI\$H_2/CH_4$ sensor is fast, continuous, reversible, reproducible and long-term stable over a period of 1.5×10^7 s. The choice of the membrane is generally a compromise between sensitivity, temperature dependence, response time and long-term stability of the sensor system.

PEI\H_2/CH_4 could be suitable for the direct assay of a binary gas mixture without prior sample preparation or purification. The sensor does not require reagents or complex associated instrumentation and could be adapted to field analysis. The advantages of this system over current well-established analytical methods are the easy-to-handle measurement set-up and fast response time. Also, the responses generated by these devices are independent of size, thus allowing for miniaturization.

Not covered here, but of great interest and therefore an important topic for future work, is the study/evaluation of the interference of other gases, such as water vapor and contaminants, in the response of the sensors.

Acknowledgements

The authors thank Agência de Inovação, S.A. (Project P0046/ICPME/S - Gassense) for its support of this research. Rosa Rego thanks a grant from Fundação Calouste Gulbenkian to attend to the Eurosensors XVIII Conference, Rome, Italy, September 12-15, 2004.

References

[1] D.C. Warren, New frontiers in membrane technology and chromatography: applications for biotechnology, Anal. Chem. 56 (1984) 1529A-1544A.

[2] R. Singh, Industrial membrane separation processes, Chemtech (*now* Chem. Innov.) 28 (1998) 33-44.

[3] P. Vadgama, Membrane based sensors: a review, J. Membr. Sci. 50 (1990) 141-152.

[4] P. Ball, Use of membranes in sensor technology, Membr. Technol. 101 (1998) 9-11.

[5] C.G. Pinto, M.E.F. Laespada, J.L.P. Pavón, B.M. Cordero, Analytical applications of separations techniques through membranes, Lab. Autom. Inform. Manage. 34 (1999) 115-130.

[6] G. Hoch, B. Kok, A mass spectrometer inlet system for sampling gases dissolved in liquid phases, Arch. Biochem. Biophys. 101 (1963) 160-170.

[7] B.K. Miremadi, K. Colbow, A hydrogen selective gas sensor from highly oriented films of carbon, obtained by fracturing charcoal, Sens. Actuators B 46 (1998) 30-34.

[8] K. Fukui, S. Nishida, CO gas sensor based on Au-La_2O_3 added SnO_2 ceramics with siliceous zeolite coat, Sens. Actuators B 45 (1997) 101-106.

[9] G. Li, S. Kawi, MCM-41 modified SnO_2 gas sensors: sensitivity and selectivity properties, Sens. Actuators B 59 (1999) 1-8.

[10] O. Hugon, M. Sauvan, P. Benech, C. Pijolat, F. Lefebvre, Gas separation with a zeolite filter, application to the enhancement of chemical sensors, Sens. Actuators B 67 (2000) 235-243.

[11] M. Vilaseca, J. Coronas, A. Cirera, A. Cornet, J.R. Morante, J. Santamaría, Use of zeolite films to improve the selectivity of reactive gas sensors, Catal. Today 82 (2003) 179-185.

[12] M. Koyama, Y. Sato, M. Aizawa, S. Suzuki, Improved enzyme sensor for glucose with an ultrafiltration membrane and immobilized glucose oxidase, Anal. Chim. Acta 116 (1980) 307-314.

[13] R.K. Kobos, S.J. Parks, M.E. Meyerhoff, Selectivity characteristics of potentiometric carbon dioxide sensors with various gas membrane materials, Anal. Chem. 54 (1982) 1976-1980.

[14] N. Oyama, T. Hirokawa, S. Yamaguchi, N. Ushizawa, T. Shimomura, Hydrogen ion selective microelectrode prepared by modifying an electrode with polymers, Anal. Chem. 59 (1987) 258-262.

[15] F.L. Dickert, S.K. Schreiner, G.R. Mages, H. Kimmel, Fiber-optic dipping sensor for organic solvents in wastewater, Anal. Chem. 61 (1989) 2306-2309.

[16] M.J. Muehlbauer, E.J. Guilbeau, B.C. Towe, Model for a thermoelectric enzyme glucose sensor, Anal. Chem. 61 (1989) 77-83.

[17] J.R Stetter, Z. Cao, Gas sensor and permeation apparatus for the determination of chlorinated hydrocarbons in water, Anal. Chem. 62 (1990) 182-185.

[18] K. Katakura, A. Noma, Z. Ogumi, Z.-i. Takehara, An oxygen sensor composed of tightly stacked membrane/electrode/electrolyte, Chem. Lett. 19 (1990) 1291-1294.

[19] S. Ozawa, P.C. Hauser, K. Seiler, S.S.S. Tan, W.E. Morf, W. Simon, Ammonia-gas-selective optical sensors based on neutral ionophores, Anal Chem. 63 (1991) 640-644.

[20] G.F. Khan, E. Kobatake, H. Shinohara, Y. Ikariyama, M. Aizawa, Molecular interface for an activity controlled enzyme electrode and its application for the determination of fructose, Anal. Chem. 64 (1992) 1254-1258.

[21] M. Kuratli, M. Badertscher, B. Rusterholz, W. Simon, Bisulfite addition reaction as the basis for a hydrogensulfite bulk optode, Anal. Chem. 65 (1993) 3473-3479.

[22] D.L. Ellis, M.R. Zakin, L.S. Bernstein, M.F. Rubner, Conductive polymer films as ultrasensitive chemical sensors for hydrazine and monomethylhydrazine vapor, Anal Chem. 68 (1996) 817-822.

[23] T.E. Brook, R. Narayanaswamy, Polymeric films in optical gas sensors, Sens. Actuators B 51 (1998) 77-83.

[24] J.N. Demas, B.A. DeGraff, P.B. Coleman, Oxygen sensors based on luminescence quenching, Anal. Chem. 71 (1999) 793A-880A.

[25] K. Kaneyasu, K. Otsuka, Y. Setoguchi, S. Sonoda, T. Nakahara, I. Aso, N. Nakagaichi, A carbon dioxide gas sensor based on solid electrolyte for air quality control, Sens. Actuators B 66 (2000) 56-58.

[26] Y. Amao, K. Asai, I. Okura, Fluorescence quenching oxygen sensor using an aluminum phthalocyanine-polystyrene film, Anal. Chim. Acta 407 (2000) 41-44.

[27] R. Fasching, F. Keplinger, G. Hanreich, G. Jobst, G. Urban, F. Kohl, R. Chabicovsky, A novel miniaturized sensor for carbon dioxide dissolved in liquids, Sens. Actuators B 78 (2001) 291-297.

[28] Y. Amao, Y. Ishikawa, I. Okura, Green luminescent iridium(III) complex immobilized in fluoropolymer film as optical oxygen-sensing material, Anal. Chim. Acta 445 (2001) 177-182.

[29] K. Eaton, A novel colorimetric oxygen sensor: dye redox chemistry in a thin polymer film, Sens. Actuators B 85 (2002) 42-51.

[30] X.-L. Su, X. Xingguo, T. Dallas, S. Gangopadhyay, H. Temkin, X. Wang, R. Walulu, J. Li, P.K. Dasgupta, A microfabricated amperometric moisture sensor, Talanta, 56 (2002) 309-321.

[31] K.T. Kinnear, H.G. Monbouquette, An amperometric fructose biosensor based on fructose dehydrogenase immobilized in a membrane mimetic layer on gold, Anal. Chem. 69 (1997) 1771-1775.

[32] Y. Kitagawa, K. Kitabatake, M. Suda, H. Muramatsu, T. Ataka, A. Mori, K. Tamiya, I. Karube, Amperometric detection of alcohol in beer using a flow

cell and immobilized alcohol dehydrogenase. Anal. Chem. 63 (1991) 2391-2393.

[33] K. Kihara, E. Yasukawa, S. Hirose, Sequential determination of glutamate-oxalacetate transaminase and glutamate-pyruvate transaminase activities in serum using an immobilized bienzyme-poly(vinyl chloride) membrane electrode, Anal. Chem. 56 (1984) 1876-1880.

[34] P.G. Veltsistas, M.I. Prodromidis, C.E. Efstathiou, All-solid-state potentiometric sensors for ascorbic acid by using a screen-printed compatible solid contact, Anal. Chim. Acta 502 (2004) 15-22.

[35] L.M. Moretto, P. Ugo, M. Zanata, P. Guerriero, C.R. Martin, Nitrate biosensor based on the ultrathin-film composite membrane concept. Anal Chem. 70 (1998) 2163-2166.

[36] S.A. Glazier, E.R. Campbell, W.H. Campbell, Construction and characterization of nitrate reductase-based amperometric electrode and nitrate assay of fertilizers and drinking water, Anal. Chem. 70 (1998) 1511-1515.

[37] Z. Hu, D. Qi, Water hardness ion-selective electrode based on a neutral carrier, Anal. Chim. Acta 248 (1991) 177-181.

[38] Y.-C. Kim, K.-H. Lee, S. Sasaki, K. Hashimoto, K. Ikebukuro, I. Karube, Photocatalytic sensor for chemical oxygen demand determination based on oxygen electrode, Anal. Chem. 72 (2000) 3379-3382.

[39] C. Schan, M. Lehmann, K. Chan, P. Chan, C. Chan, B. Gruendig, G. Kunze, R. Renneberg, Designing an amperometric thick-film microbial BOD sensor, Biosens. Bioelectron. 15 (2000) 343-353.

[40] K. Wiegran, T. Trapp, K. Cammann, Development of a dissolved carbon dioxide sensor based on a coulometric titration, Sens. Actuators B 57 (1999) 120-124.

[41] M. Takahashi, T. Ishiji, N. Kawashima, Handmade oxygen and carbon dioxide sensors for monitoring the photosynthesis process as instruction material for science education, Sens. Actuators B 77 (2001) 237-243.

[42] T. Trapp, B. Ross, K. Cammann, E. Schirmer, C. Berthold, Development of a coulometric CO_2 gas sensor, Sens. Actuators B 50 (1998) 97-103.

[43] L. Lvova, A. Legin, Y. Vlasov, G.S. Cha, H. Nam, Multicomponent analysis of Korean green tea by means of disposable all-solid-state potentiometric electronic tongue microsystem, Sens. Actuators B 95 (2003) 391-399.

[44] A. Riul Jr., R.R. Malmegrim, F.J. Fonseca, L.H.C. Mattoso, An artificial taste sensor based on conducting polymers, Biosens. Bioelectron. 18 (2003) 1365-1369.

[45] R. Stella, J.N. Barisci, G. Serra, G.G. Wallace, D. De Rossi, Characterisation of olive oil by an electronic nose based on conducting polymer sensors, Sens. Actuators B 63 (2000) 1-9.

[46] A. Mendes, F. Magalhães, C. Costa, New Trends on Membrane Science in: J. Fraissard, C.W. Conner (Eds.), Fluid Transport in Nanoporous Materials, Kluwer Academic Publishers, in press.

[47] R. Rego, N. Caetano, R. Vale, A. Mendes, Development of a new gas sensor for binary mixtures based on the permselectivity of polymeric membranes. Application to oxygen/nitrogen mixture, J. Membr. Sci. 244 (2004) 35-44.

[48] R. Rego, N. Caetano, A. Mendes, Development of a new gas sensor for binary mixtures based on the permselectivity of polymeric membranes. Application to carbon dioxide/methane and carbon dioxide/helium mixtures, Anal. Chim. Acta 511 (2004) 215-221.

[49] R. Rego, A. Mendes, Carbon dioxide/methane gas sensor based on the permselectivity of polymeric membranes for biogas monitoring, Sens. Actuators B 103 (2004) 2-6.

[50] A. Mendes, Gas mixtures concentration sensor and corresponding measuring process, Patent PT102 312 (2000).

[51] G.W. Miller, Method and apparatus for oxygen concentration analysis, US Patent 5101656 (1992).

[52] D. Lazik, H. Geistlinger, Method for measuring the concentration or the partial pressure of gases, especially oxygen, in fluids and a corresponding gas sensor, Patent WO 01/53796 A1, EP 1 157 265 A1, DE 199 25 842 A 1 (2001).

[53] http://www.anton-paar.com

[54] X. Bévenot, A. Trouillet, C. Veillas, H. Gagnaire, M. Clément, Hydrogen leak detection using an optical fibre sensor for aerospace applications, Sens. Actuators B 67 (2000) 57-67.

[55] htpp://www.gepower.com/panametrics

[56] http://www.teledyne-ai

[57] http://www.thermco.com

[58] R.H. Perry, D.W. Green, J.O. Maloney, Perry's Chemical Engineers' Handbook, sixth ed., McGraw-Hill International Editions, 1984, pp. 3-247.

[59] M. Mulder, Basic Principles of Membrane Technology, second ed., Kluwer Academic Publishers, Dordrecht, 2000 (Chapter 1).

6. Temperature compensation of a gas sensor for binary mixtures based on the permselectivity of polymeric membranes

Abstract

A new concentration sensor for binary gas mixtures based on the permselectivity of polymeric membranes has been recently developed. The sensor responds to temperature changes. This work describes a simple way to compensate most of the temperature effect on the sensor's response. Different membrane materials and gas mixtures were tested. The present approach proved to be especially beneficial for a PDMS based sensor when analyzing oxygen/nitrogen gas mixtures.

R. Rego, N. Caetano, A. Mendes, submitted (2005).

6.1. Introduction

Polymeric membranes have been used in the development of low cost sensors for analyzing binary gas mixtures. By using inexpensive gas sensors it is possible to design relatively cheap, small and rugged analyzers capable of continuous on-line analysis of gas streams.

The concentration sensor is made of a membrane module, a pressure sensor and a needle valve. The needle valve is placed at the permeate outlet. The pressure sensor reads the pressure of the permeate chamber [1]. At a given temperature and when the sample is being fed at a constant pressure, the permeate chamber pressure relates to the sample composition [2-5].

The calibration curves obtained with this sensor, for some applications at different temperatures, differ from each other mostly by a translation, see Fig. 6.2a. In some cases the response of the sensor is directly proportional to the absolute temperature variation, as happens with the pressure of an ideal gas,

$$P_{\text{translate}} = \left(T_{\text{translate}} / T_{\text{input}}\right) P_{\text{input}} \tag{6.1}$$

The response of the sensor can then be easily corrected if a differential pressure sensor is used; one of the pressure sensor terminals can be connected to a small container filled with an ideal gas (e.g. nitrogen), while the other can be connected to the permeate chamber, Fig. 6.1. If the temperature increases, the permeate pressure increases approximately proportionally to the absolute temperature variation, exactly in the same way as the gas in the container. This way most of the temperature effect on the concentration sensor's response is cancelled.

To increase the precision of the response, the pressure sensor range should be only slightly larger than the permeate pressure range of the concentration sensor; the pressure in the container should be, e.g., equal to the lowest permeate pressure, see Fig. 6.3a. However, when at rest, the

permeate pressure should be the ambient pressure and a high pressure difference might occur. For this reason the pressure sensor should stand at a high over pressure, as is the case of the Honeywell-143PC05D (pressure range, ± 5 psi; maximum overpressure, 30 psi; repeatability, ± 0.15%).

This improvement was tested with three gas mixtures, oxygen/nitrogen, carbon dioxide/helium and hydrogen/methane and two membrane materials, poly(dimethylsiloxane) (PDMS) and poly(etherimide) (PEI) hollows fibers.

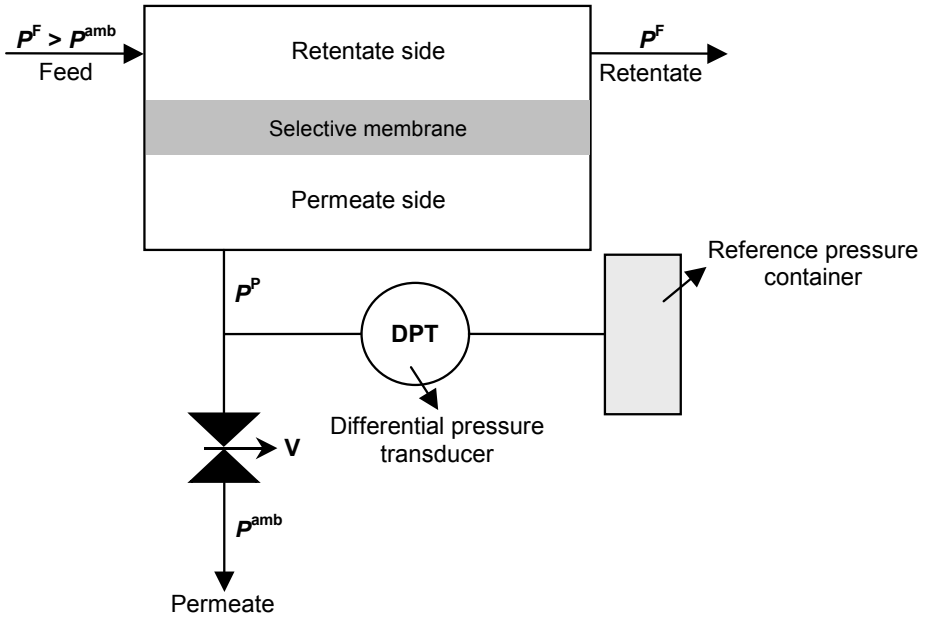

Fig. 6.1. Sketch of the concentration sensor.

6.2. Results and discussion

The experimental data presented below, figures 6.2-6.4, were obtained previously [2-4]. Three gas mixtures and two polymers were studied: oxygen/nitrogen with PDMS membranes, PDMS\$O_2/N_2$; carbon dioxide/helium with PDMS membranes, PDMS\$CO_2$/He, and hydrogen/methane with PEI membranes, PEI\$H_2/CH_4$.

The response of the sensor's permeate pressure depends both on the membrane and needle valve bi-component permeabilities. The temperature has different effects on these permeabilities. The combined result is hard to forecast but in some cases it follows a simple pattern.

Fig. 6.2 shows the concentration sensor response to three temperatures, 283, 298 and 313 K. The response of each sensor, permeate pressure, increases with the temperature. However, sensor PDMS\CO_2/He shows a behavior with the temperature that is different from the others.

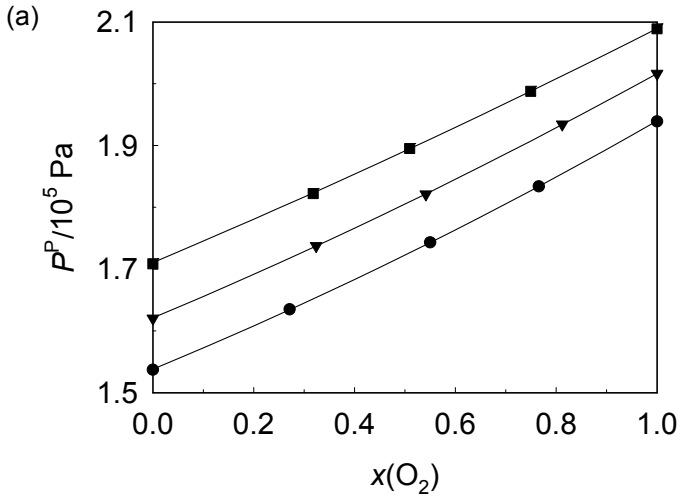

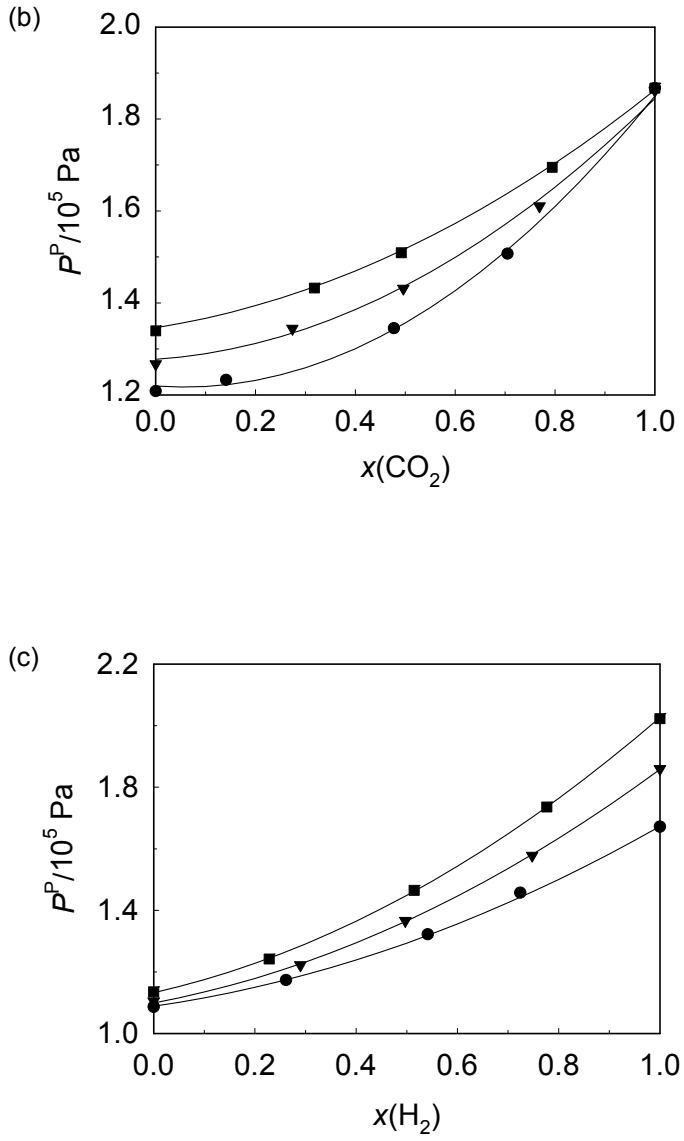

Fig. 6.2. Permeate pressure (P^P) as a function of the feed molar fraction (x): (a) PDMS\$O_2$/$N_2$ sensor at 283.45 (●), 297.95 (▼) and 313.15 K (■) [2]; (b) PDMS\$CO_2$/He sensor at 283.25 (●), 298.05 (▼) and 312.15 K (■) [3] and (c) PEI\$H_2$/$CH_4$ sensor at 283.45 (●), 297.95 (▼) and 314.45 K (■) [4]. Lines are 2nd degree polynomial fittings.

In Fig. 6.3, the previous response curves obtained at 283 and 313 K were translated to 298 K using Eq. (6.1). This correction corresponds to the use of a differential pressure sensor instead of an absolute one.

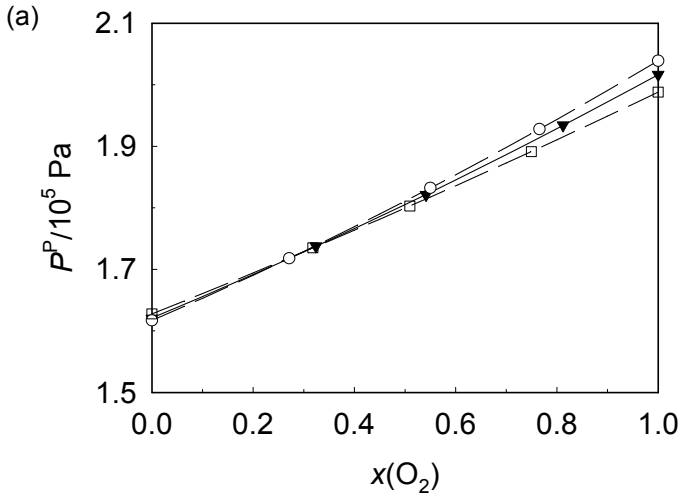

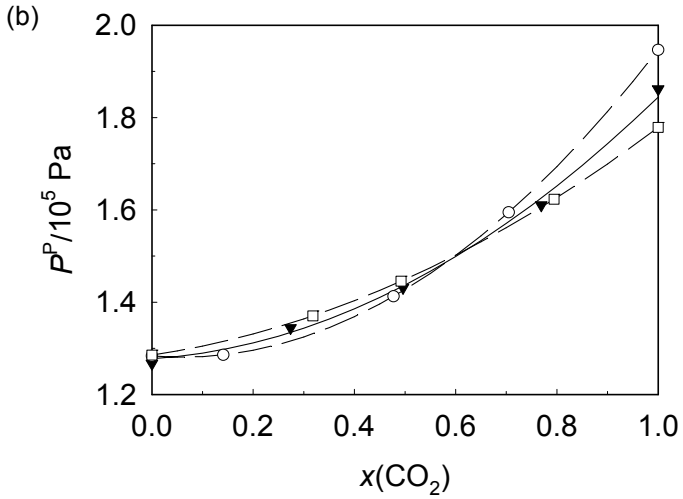

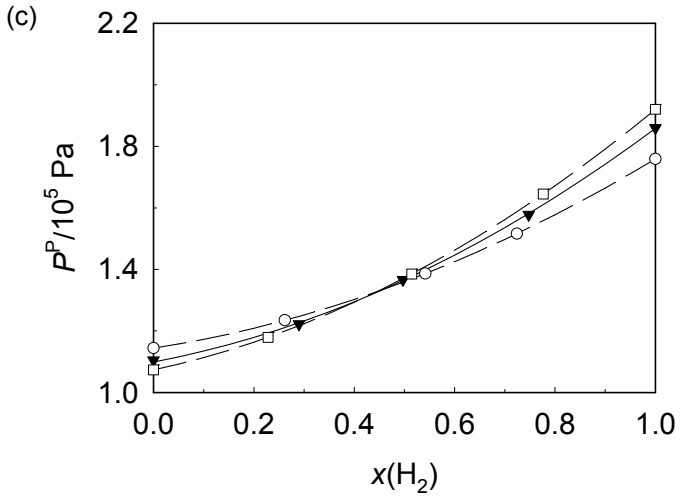

Fig. 6.3. Permeate pressure (P^P) as a function of feed molar fraction (x). Open symbols and dashed lines were translated using Eq. (6.1): (a) PDMS\$O_2$/$N_2$ sensor at 283.45 (○), 297.95 (▼) and 313.15 K (□); (b) PDMS\$CO_2$/He sensor at 283.25 (○), 298.05 (▼) and 312.15 K (□) and (c) PEI\$H_2$/$CH_4$ sensor at 283.45 (○), 297.95 (▼) and 314.45 K (□). Lines are 2nd degree polynomial fittings.

From this figure it is possible to see that for the PDMS\$O_2$/$N_2$ sensor the correction is quite good when $x(O_2) \leq 0.6$. The absolute error on the oxygen feed molar fraction ranges from 5.7 x 10^{-4} to 5.0 x 10^{-2}, oxygen molar fractions respectively 0.25 and 1.0 and 283.45 K, and from 8.0 x 10^{-4} to 6.4 x 10^{-2}, oxygen molar fractions respectively 0.30 and 1.0 and 313.15 K. Fig. 6.4 shows the permeate pressure (P^P) as a function of temperature (T) for the PDMS\$O_2$/$N_2$ sensor when the oxygen feed molar fraction was 0.128, temperature ranges from 278.65 to 322.98 K. The solid symbols are experimental data [2] and the solid line was obtained using Eq. (6.1). It can be seen that Eq. (6.1) fits quite well the experimental data for $x(O_2) = 0.128$.

Sensor PDMS\CO_2/He shows a qualitatively similar response to the previous sensor but here the deviations are slightly higher, especially for $x(CO_2) \geq 0.7$. The absolute error on the carbon dioxide feed molar fraction

ranges from 3.2 x 10^{-3} to 9.2 x 10^{-2}, carbon dioxide molar fractions respectively 0.60 and 1.0 and 283.25 K, and from 3.8 x 10^{-3} to 7.5 x 10^{-2}, carbon dioxide molar fractions respectively 0.65 and 0.05 and 312.15 K.

Sensor PEI/H_2/CH_4 functions differently and the errors are higher than for the previous systems. The absolute error on the hydrogen feed molar fraction ranges from 1.5 x 10^{-3} to 1.2 x 10^{-1}, hydrogen molar fractions respectively 0.45 and 0 and 283.45 K, and from 2.3 x 10^{-3} to 9.9 x 10^{-2}, hydrogen molar fractions respectively 0.40 and 0 and 314.45 K.

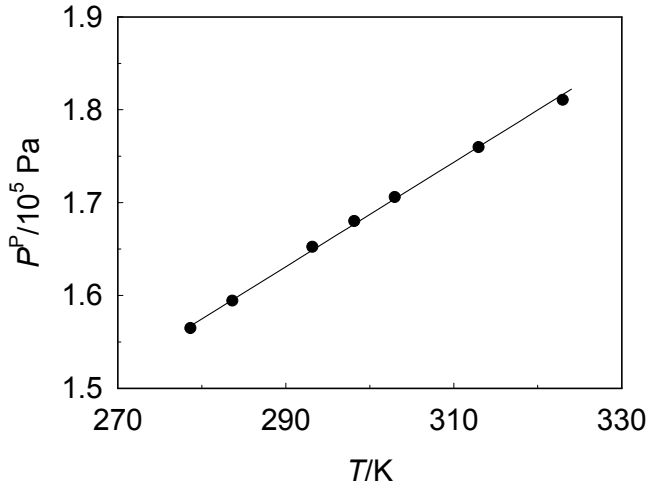

Fig. 6.4. Permeate pressure (P^P) as a function of temperature (T) for PDMS\O_2/N_2 sensor. The oxygen feed molar fraction was 0.128. Solid symbols are experimental data obtained previously [2] and the solid line was calculated using Eq. (6.1).

6.3. Conclusions

A simple method to compensate the temperature dependence of the concentration sensor is described and evaluated for different membrane materials and gas mixtures. This method corrects most of the temperature effects of sensor PDMS\O_2/N_2 for oxygen molar fractions below 0.60,

absolute error smaller than 5.7 x 10^{-4}, when temperature is changed to ± 15 K around 298 K. For molar fractions above 0.60, the maximum absolute error obtained was about 5.0 x 10^{-2}. For sensors PDMS\$O_2$/$N_2$ and PDMS\$CO_2$/He, the proposed method corrects most of the temperature effects and reduces the need for sophisticated algorithms to correct the response of the sensor to temperature variations.

References

[1] A. Mendes, Gas mixtures concentration sensor and corresponding measuring process, Patent PT102 312 (2000).

[2] R. Rego, N. Caetano, R. Vale, A. Mendes, Development of a new gas sensor for binary mixtures based on the permselectivity of polymeric membranes. Application to oxygen/nitrogen mixture, J. Membr. Sci. 244 (2004) 35-44.

[3] R. Rego, N. Caetano, A. Mendes, Development of a new gas sensor for binary mixtures based on the permselectivity of polymeric membranes. Application to carbon dioxide/methane and carbon dioxide/helium mixtures, Anal. Chim. Acta 511 (2004) 215-221.

[4] R. Rego, N. Caetano, A. Mendes, Hydrogen/methane and hydrogen/nitrogen sensor based on the permselectivity of polymeric membranes, Sens. Actuators B in press (2005).

[5] R. Rego, A. Mendes, Carbon dioxide/methane gas sensor based on the permselectivity of polymeric membranes for biogas monitoring, Sens. Actuators B 103 (2004) 2-6.

PART III

Membrane-based extraction techniques

7. Preliminary study of membrane extraction thermal desorption. Application to herbicides analysis by GC-FID

Abstract

This work presents a study of a membrane-based sample preparation technique. It describes a new technique that combines membrane extraction with a sorbent interface (MESI) and a thermal membrane desorption application (TMDA) called membrane extraction thermal desorption (METD). This technique uses a hollow fiber selective membrane to selectively pre-concentrate the solute previous to injection in a GC. The solute injection is done by heating up the membrane. The thermally desorbed solute is focused in the GC column which is kept at room temperature. After this step a temperature program is started and the solute is analyzed by GC-FID. Molinate and cycloate, two herbicides, were used as model compounds.

The hollow fiber membranes used were poly(dimethylsiloxane) (PDMS) and poly(etherimide) (PEI), which were characterized using thermal analysis (sorption/desorption and thermal stability), scanning electron microscopy (morphology) and electron-dispersive spectroscopy (herbicides profile concentration). The PEI membrane was found to be unsuitable for the membrane extraction because it has a very high permeability towards the carrier gas (He). PDMS hollow fibers proved to be very promising.

The METD allows the pre-concentration of the solutes orders of magnitude in a selective way. Method validation has not yet been thoroughly established.

R. Rego, A. Mendes, submitted (2005).

7.1. Introduction

Growing concern about the effects of organic solvents on both human health and the environment has created a demand for solvent-free sample preparation techniques in analytical chemistry laboratories. Given this concern membrane-based techniques have recently been added to the few analytical methods available [1]. A fundamental feature of membrane-based analytical techniques is the selective permeability of the membrane towards target compounds, making the membrane an essential part of the technique [2]. Examples of solvent-free membrane-based sample preparation techniques are membrane introduction mass spectrometry (MIMS) [3] and membrane extraction with sorbent a interface (MESI) [4].

Since the first analytical application of a membrane, described by Hoch and Kok in the 1960's [5], MIMS has been used for environmental and blood analysis, as well as for fermentation monitoring [6-11]. In this technique, analytes are introduced into a mass spectrometer through a membrane by pervaporation [11]. The MESI technique includes a membrane module that extracts the analytes from liquid or gas phase (headspace). A stripping gas flows through the permeate side collecting the permeated/extracted analyte molecules in a sorbent trap (cooled, if required), where the analyte is enriched and subsequently desorbed and transferred to a gas chromatograph (GC) for separation and quantification [12-14, 4]. In the environmental field, MESI has been applied to the determination of volatile organic compounds (VOCs), mainly BTEX (benzene, toluene, ethylbenzene, xylenes), and chlorinated compounds [15-25] in different matrices. For the extraction of semivolatile organics compounds (SVOCs), such as phenols from water, a high-pressure membrane module has been developed to allow the use of liquid carbon dioxide as the stripping phase [26, 27]. More recently, the method has been applied to monitoring terpenoids [25], thermal degradation products of poly(acrylonitrile) (PAN) [28], as well as polystyrene [29], biogenic emissions from *Eucalyptus dunnii* leaves [30, 31], and human breath [32, 33]. The

MESI system has also been improved by introducing catalytic reactions together with the membrane extraction by using a catalytic membrane [2].

A somewhat different technique of MESI, involving the type of heating, physical arrangement of the membrane and detector used (SnO_2 or CO_2 sensor) has been described [34-38, 33]. Of these techniques, the thermal membrane desorption application (TMDA) is one of the most interesting [39]. In TMDA, the analytes are set free by thermal desorption of the membrane module. This technique has been applied mainly to monitoring fermentation processes [39, 40]. In comparison to MESI, TMDA can sample less volatile organic and polar compounds more effectively [41].

To our knowledge, none of the published works has focused on pesticide analysis. Hence, the purpose of the present work is to describe a new analytical technique, membrane extraction thermal desorption (METD), coupled to a GC-flame ionization detector (FID) and to study its performance using herbicides, molinate (*S*-ethyl azepane-1-carbothioate or *S*-ethyl hexahydro-1*H*-azepine-1-carbothioate or *S*-ethyl perhydroazepine-1-thiocarboxylate) and cycloate (*S*-ethyl *N*-cyclohexyl-*N*-ethylthiocarbamate). Molinate is a thiocarbamate herbicide used worldwide for weed control in rice fields. Its carcinogenicity for humans (group C) has been suggested [42]. Contamination with molinate, as a result of its application, occurs on surface, ground and underground waters [43-46]. Molinate was chosen from the pesticides that are more commonly used in Portugal in rice fields [47, 48]. Cycloate was also used as the internal standard on the GC analysis.

In the METD technique the hollow fiber selectively pre-concentrates the analytes from the liquid phase or headspace. Then, the fiber is heated in an oven to desorb the analytes. The stripping gas (carrier gas) that flows inside the membrane transfers the desorbed analytes to GC-FID for quantitative analysis. METD is a robust and cost-effective technique using a single hollow fiber of adjustable dimensions that can improve the sampling of less volatile organic compounds.

The hollow fiber membranes used in this work were characterized using thermal analysis methods, scanning electron microscopy (SEM) and electron-dispersive spectroscopy (EDS) to assess their stability and to gain

insights into the best operating conditions for sorption/desorption of the analytes in the membranes.

7.2. Experimental

7.2.1. Experimental set-up

The sketch of the experimental set-up developed for testing the membrane extraction thermal desorption technique is shown in Fig. 7.1, and includes the polymeric membrane (hollow fiber), a laboratory-made programmable temperature oven and a GC-FID.

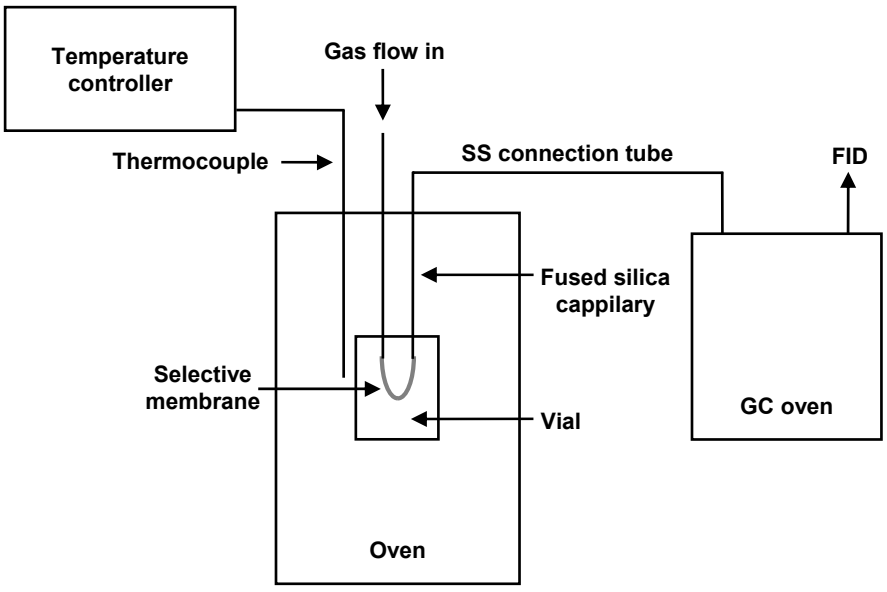

Fig. 7.1. Sketch of the experimental set-up developed for testing the membrane extraction thermal desorption technique coupled to GC-FID. When the oven is switched on, the vial is removed.

Two polymeric membranes were selected based on their thermal stability and low water affinity. The selected hollow fiber membranes were a poly(dimethylsiloxane) (PDMS) composite membrane (porous poly(etherimide) (PEI) support) and a PEI integral asymmetric membrane, both supplied by GKSS, Geesthacht, Germany. The inside diameter of these fibers is 0.71 and 0.72 mm, respectively. Their main differences are related to their permeation characteristics. PDMS and PEI membranes permeability towards helium is 3.69 ± 0.02 x 10^{-6} dm^3 (STP) s^{-1} m^{-2} Pa^{-1} at 24.8ºC [49] and 6.5 x 10^{-6} dm^3 (STP) s^{-1} m^{-2} Pa^{-1} [50], respectively. The thickness of the selective layer of the membranes is not accurately known. The hollow fiber membranes were cut to give an effective fiber length of 6 cm. The solutes investigated in this work were weighed and put into 40 ml amber glass vials sealed with a cap having black Viton® septa from Supelco (Bellefonte, PA, USA). Two 20 cm long pieces of a fused silica column (Tracsil with media polarity, 0.53 mm i.d., Teknokroma, Barcelona, Spain) were used to cross the septa, Fig. 7.1a.

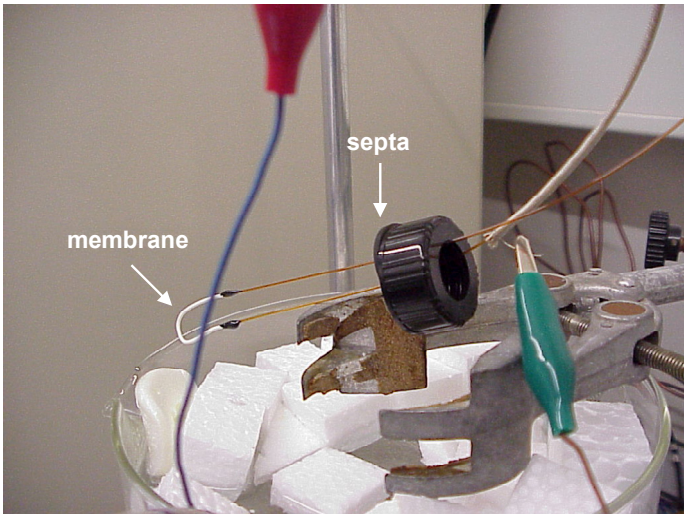

Fig. 7.1a. View of the fused silica column crossing the septa and glued to the hollow fiber membrane.

On one side of the septa the two silica column ends were glued (polyimide resin, Restek, Bellefonte, PA, USA) to the hollow fiber membrane while on the other side the silica columns were connected to the GC 1/16" stainless steel (SS) tubes using zero dead-volume fittings from Valco (Ref. ZU1, Houston, TX, USA). A Dani Instruments S.p.A. (Milan, Italy) GC equipped with a FID was used.

The oven temperature was controlled using a K type thermocouple connected to a PID temperature controller. The thermocouple was kept as close as possible to the membrane.

7.2.2. Instrumentation

GC: all GC analyses were performed on a Dani GC 1000 gas chromatograph equipped with a split-splitless injector (SL/IN 86/2) and flame ionization detector, FID (86/10). A DB-1701 (14%-cyanopropyl-phenyl-methylpolysiloxane, film thickness 1 μm) fused silica capillary column (30 m x 0.53 mm i.d.) from Agilent J&W (Palo Alto, CA, USA) was used. The carrier gas used was helium from Air Liquide, 99.9995% purity, at a flow rate of 4.9 ml min^{-1}. The injector and detector temperatures were set at 230ºC and 290ºC, respectively. A medium temperature septa, MTS-300 7/16'' disc (11 mm), from J&W Scientific and a glass pre-column from Dani were used. The oven temperature was programmed as follows: 50ºC (1 min) and then from 50ºC to 55ºC at 5ºC min^{-1}; 55ºC to 170ºC at 50ºC min^{-1}; 170ºC to 190ºC at 2ºC min^{-1}; 190ºC to 240ºC at 30ºC min^{-1}. The final temperature, 240ºC, was held for 1 min. The FID gases were hydrogen (38 ml min^{-1}) and air (320 ml min^{-1}) and the make-up gas was helium (38 ml min^{-1}) all from Air Liquide, 99.9995% purity. Data acquisition and analysis was done using CSW32 software from DataApex (Prague, Czech Republic).

The response linearity, limits of detection and quantification, precision evaluated by repeatability (coefficient of variation of six assays performed on 1 day) and by intermediate precision (coefficient of variation of six assays performed on 3 days) and accuracy, were previously studied for the direct

injection of molinate solutions in the GC. The molinate concentration for the quantitative herbicide analysis ranged from 0.574 to 49.7 mg l^{-1} (r^2 = 0.999). Cycloate was used as the internal standard at a concentration of 13.5 mg l^{-1}. Precision expressed by repeatability and intermediate precision was 3.14% and 3.37%, respectively (c = 9.56 mg l^{-1}, molinate). The limit of detection obtained was 1.57 mg l^{-1}. In direct injection the standards (1 μL) were injected in splitless mode (1 min).

Identification of analytes was based on the retention times obtained with the standards of dichloromethane solutions of molinate and cycloate.

Thermal gravimetric analysis (TGA): samples of the hollow fiber membranes for TGA studies were transferred to open platinum crucibles and analyzed using a Rheometric Scientific TG 1000 thermobalance, at a heating rate of 10ºC min^{-1} using dried argon (Ar) as a purging gas (20 ml min^{-1}). Each sample was heated from 25ºC to 700ºC.

Differential scanning calorimetry (DSC): samples for DSC studies with masses of approximately 10 mg were placed in 40 μl aluminum cans. The cans were hermetically sealed and the thermograms recorded using a DSC131 Setaram DSC. The purge gas used in all experiments was nitrogen (Air Liquide, 99.9995%) supplied at a constant 35 ml min^{-1} flow rate. Each sample was heated from 25ºC to 300ºC at 5ºC or 10ºC min^{-1}. In some cases, a second heating cycle was performed.

SEM/EDS: A Philips FEI Quanta 400 scanning electron microscope was used to observe the membrane morphology at high magnification. Membrane samples were cut to yield cross-sections using a blade and then sputtered with a thin layer of gold/palladium (Au/Pd(10%)) prior to investigation. After visual SEM examination, the chlorine (Cl) and sulfur (S) atoms concentration along the entire sample thickness were determined using the EDS attachment (EDAX/EDAM) with ZAF quantification without standard. EDS data are presented in percent atoms of detected elements greater than atomic number 8 (oxygen, O). For the Cl and S atoms, only K lines were used.

7.2.3. Chemicals

Herbicide analytical standards, molinate and cycloate, were purchased from Riedel-de Haën (Seelze, Germany) and were > 99% pure. Some properties of molinate and cycloate are given in Table 7.1. Dichloromethane with residue analysis grade was purchased from Fluka (Switzerland). Aqueous stock solutions of standards were prepared with concentrations ranging from 90 to 776 mg kg^{-1}, according to individual solubility and stored at 4ºC. The standard stock solutions were also prepared in dichloromethane for direct injection. Work solutions were prepared by adequate dilution of the stock solutions with water or dichloromethane. De-ionized water was used in all experiments. Sodium chloride with purity > 99.5% was purchased from Panreak Quimica SA (Barcelona, Spain).

Table 7.1
Molinate and cycloate properties [51, 52].

	Herbicide	
	molinate	cycloate
Formula	$C_9H_{17}NOS$	$C_{11}H_{21}NOS$
Molar mass/g mol^{-1}	187.3	215.4
Water solubility/mg l^{-1} (25ºC)	970	93
Density/g ml^{-1} (20ºC)	1.0643	1.0243
log P_v[a] (25ºC)	2.87	2.92
log P[b]	3.21 (25ºC)	4.11 (20ºC)

[a] logarithmic value of vapor pressure (mPa).

[b] logarithmic value of octanol-water partition coefficient.

7.2.4. Sampling

For sampling, 40 ml vials were filled with 25 g or 30 g of pesticides aqueous solutions. Concentrations are given in ppm and refer to the mass ratio in the aqueous phase. NaCl concentration in all aqueous samples was 250 g l^{-1} and the pH was not modified. For pH measurements, a WTW GmbH (Weilheim, Germany) pH90, combination glass electrode was used. Samples were heated at a stirring rate of ca. 500 rpm with a poly(tetrafluoroethylene) (PTFE) coated magnetic stir bar in a hot plate stirrer unit Labinco (L32) from Labnorma (Lisboa, Portugal).

For each analysis, the fibers were exposed to the aqueous sample or its headspace for an optimized time of 45 min at 55ºC [46]. The membrane sample was then removed from the solution and put in the oven for thermal desorption at 210ºC for 10 min under a helium flow rate of 10 ml min^{-1}, while the GC column was at 50ºC. Thermally released analytes were transferred to the column in splitless mode. After desorption, the membrane was placed in an empty vial at room temperature, the flow rate of the carrier gas was put at 4.9 ml min^{-1} and a temperature program of the GC was carried out.

7.3. Results and discussion

This study was organized as follows: firstly, the membranes were characterized to assess their performance as matrices for extraction; secondly, the performance of the analytical method of the pesticides was evaluated. PDMS and PEI membrane samples characterization included thermal gravimetric analysis (TGA), differential scanning calorimetry (DSC), scanning electron microscopy (SEM) and energy-dispersive spectroscopy (EDS). The experiments were conducted in order to evaluate the performance of the METD method, aiming to study the effect of different parameters, such as the time and temperature of the sorption and desorption steps and the matrix composition, ionic strength (NaCl concentration) and the organic solvent (dichloromethane) content.

7.3.1. Thermal characterization of the membranes and sorption/ desorption studies

The interaction between the membrane samples and the analytes was investigated by thermal analysis. Thermal analysis is a generic term for methods such as thermal gravimetric analysis (TGA) and differential scanning calorimetry (DSC), where a variable is measured when the sample temperature is increased as a function of the time [53]. Phenomena such as sorption and desorption can thus be monitored by recording changes in the heat flow (DSC) and sample mass loss (TGA) [54].

The aim of this part of the study was to gain insight into the sorption/desorption on the PDMS and PEI membrane samples before and after the sorption of molinate and/or cycloate, namely, to determine the most appropriate sorption and desorption temperatures to improve the characteristics of the analytical method. Two sets of experiments were performed; in the first one the membrane samples were allowed direct contact with herbicide aqueous solutions, while in a second set of experiments the membranes were put in contact with the gas phase of pure herbicide samples (headspace). After a certain contact time, the membrane samples were analyzed for the loss of mass as a function of the temperature increase (TGA).

In the first set of experiments, eight aqueous molinate and/or cycloate solutions with different concentrations were weighed (30 g) and introduced into 40 ml vials which were then sealed with caps carrying black Viton® septa, Table 7.2. The aqueous solutions also contained 250 g l^{-1} of NaCl, previously verified to improve the herbicides extraction, and the final pH was approximately 5.6. PDMS and PEI membrane samples with approximately 25 mg (6 cm long) were then immersed in these solutions and stirred at 55 ºC for 45 min. The introduction of the membranes did not modify the pH of the solutions. After the period of time indicated, the membranes were removed from the solutions and stored in closed vials at room temperature and relative humidity. There were no visible condensed particles on either of the membrane surfaces.

Table 7.2

Concentration of the aqueous solutions in contact with the membrane samples.

Membrane	Samples #	Solution concentration/mg kg^{-1}	
		molinate	cycloate
PDMS	1	0	0
	2	98.4	0
	3	98.5	0
	4	100	101
	5	48.8	43.4
	6	0	75.7
	7	0	34.3
PEI	8	48.5	43.4

A typical TGA curve for both membranes is given in Fig. 7.2. Both membranes are very stable even at temperatures close to 500°C.

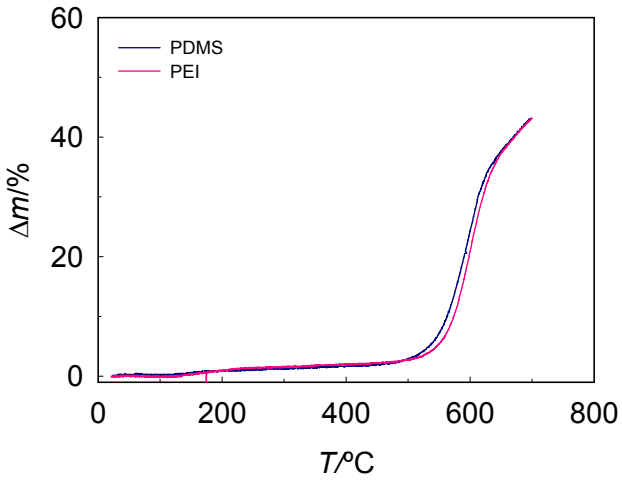

Fig. 7.2. Mass variation ($\Delta m = (m_i - m)/m_i$) as a function of temperature (T) of the PDMS and PEI membrane samples.

Fig. 7.3 shows the TGA curves of the different membrane samples given in Table 7.2. From this figure it can be concluded that up to 210°C most of the sorbed species are desorbed. It is also noticeable that the loss of mass is related to the membrane herbicide concentration.

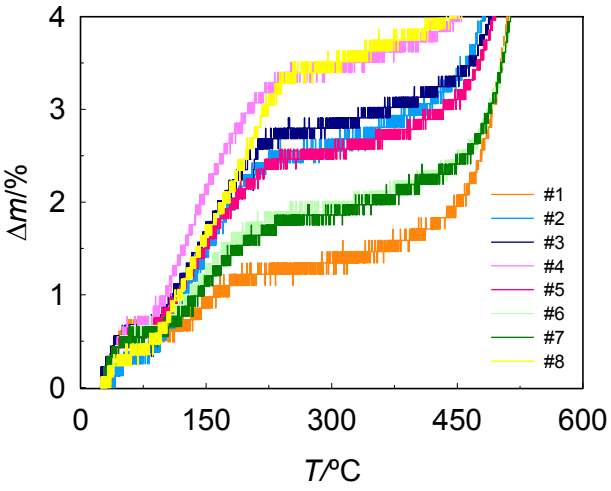

Fig. 7.3. Mass variation ($\Delta m = (m_i - m)/m_i$) as a function of temperature (T) of the PDMS and PEI membrane samples in contact with the herbicides aqueous solutions (Table 7.2).

In the second set of experiments, 10 μl of pure molinate and/or cycloate was placed in 1 ml vial and the PDMS and PEI membrane samples left in contact with the gas phase for 48 hours at room temperature (Table 7.3).

Table 7.3

Amount of pure herbicide introduced in the vial in contact with the membrane samples (headspace).

Membrane	Samples #	Herbicide amount/mg	
		molinate	cycloate
PDMS	9	10.6	0
	10	0	10.2
	11	5.3	5.1
	13	5.3	5.1
PEI	12	5.3	5.1

The TGA curves of these membranes are given in Fig. 7.4. It can be seen that the shape of these curves is similar to the previous ones (Fig. 7.3), while the temperature at which most of the species are desorbed increased to about 300°C.

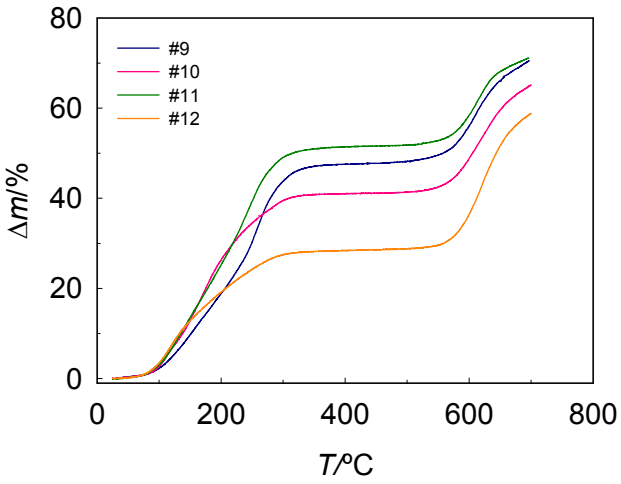

Fig. 7.4. Mass variation ($\Delta m = (m_i - m)/m_i$) as a function of temperature (T) of the PDMS and PEI membrane samples in contact with the herbicides headspace (Table 7.3).

Fig. 7.4 also shows a ten fold increase in the mass variation as a function of the temperature, which indicates that a far larger mass of sorbed species are being desorbed. The increase in the desorbed temperature from about 210ºC to 300ºC could be related to the tremendous increase of sorbed herbicides.

Fig. 7.5 shows the DSC curves of the PDMS (composite membrane with PEI porous support) and PEI (integral membrane) membrane samples with no herbicide sorbed. The glass transition of the PEI polymer is visible at about 212°C. Above this temperature it becomes very difficult to work with these fibers as they lose mechanical properties and collapse easily. It may thus be concluded that the best desorption temperature should be very close to 210°C and below the glass transition.

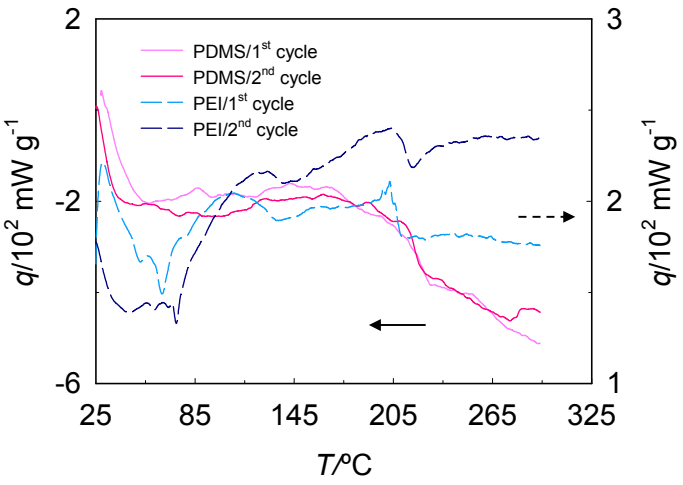

Fig. 7.5. Heat flow (*q*) as a function of temperature (*T*) of the PDMS (composite membrane with PEI porous support) and PEI (integral membrane) membrane samples.

7.3.2. Membrane morphology and chlorine and sulfur concentration profile on the membranes cross section

SEM and EDS analyses were performed on non-treated PDMS and PEI membrane samples, on samples after contact with molinate and/or cycloate (Tables 7.2 and 7.3) and on samples after being used in the METD technique (Table 7.4). SEM analyses show the morphological effects of the sorption of various herbicides and after applying the METD technique on the membrane samples, while the EDS characterizes the concentration profile on the membrane samples cross section.

Table 7.4

Concentration of the aqueous solutions and thermal desorption conditions used in the METD technique.

Membrane	Sample #	Solution concentration mg kg^{-1}		Thermal desorption conditions		
		molinate	cycloate	*T*/ºC	*t*/min	Flow rate (*F*) ml min^{-1}
PDMS	A14	0.631	0.326	210	15	10
	A15	0.663	0	210	10	10
	A17	1.33	0	-	-	-
	A18	25.0	22.5	-	-	-
PEI	A16	0.709	0.550	210	10	0.9

Fig. 7.6 shows SEM pictures of the membrane samples cross-section, where the selective dense layer (bore side) and the porous support (shell side) are visible: (a) original membranes; (b) membranes after contact with herbicide aqueous solution (samples #4 and #8); (c) membranes after contact with herbicide in gas phase (samples #11 and #12); (d) membranes after being used in the METD technique, which implies a temperature desorption cycle up to 210°C (run #A14 and run #A16). It can be seen that the membrane samples show no visible morphological changes after the thermal treatment (METD) and only a slight swelling of sample #12 after molinate and cycloate sorption.

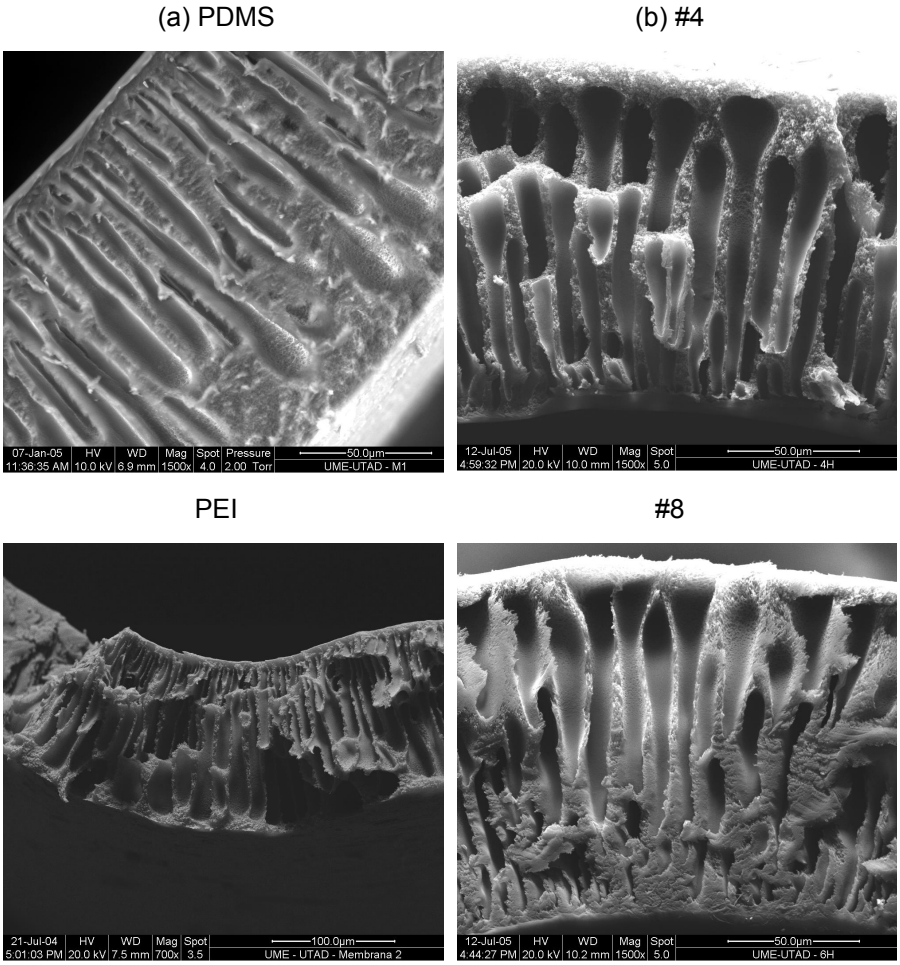

Fig. 7.6. SEM pictures of membrane samples cross-section: (a) non-treated (c) membranes after contact with herbicide in gas phase; (d) membranes after

(c) #11

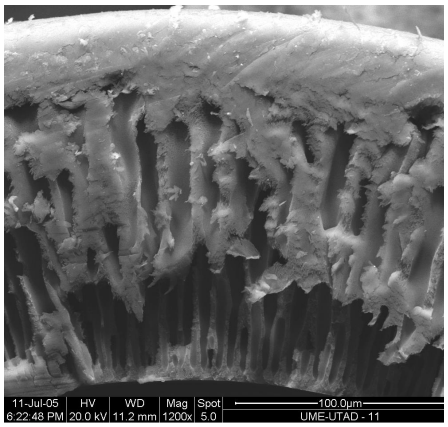

(d) #A14

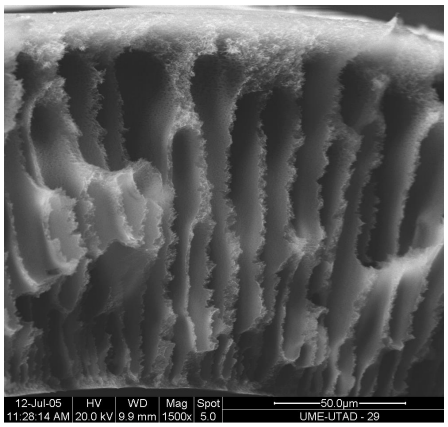

#12

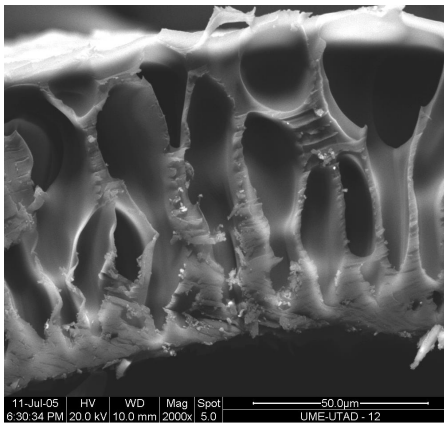

#A16

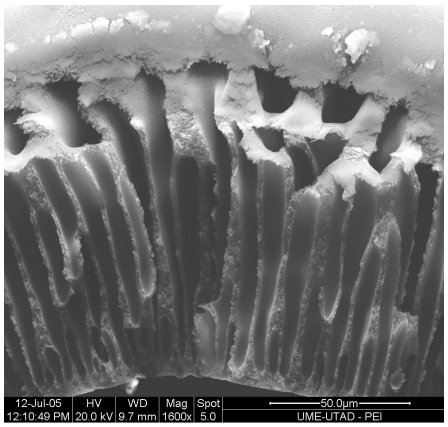

membranes; (b) membranes after contact with herbicide aqueous solution; being used in the METD technique.

EDS studies were conducted to determine the profiles of the Cl (NaCl penetration) and S (both molinate and cycloate penetration) atoms along the membrane thickness (from shell to bore side). Both PDMS and PEI membranes contain neither Cl nor S atoms. Semi-quantitative Cl and S elemental profiles of PDMS and PEI membrane samples are displayed in Fig. 7.7 (a) to (c).

The most significant conclusion that can be drawn from this figure is that Cl content decreases when approaching the selective layer (dense layer) (Fig. 7.7a). The Cl content on the selective layer is below the detection limit of the analyzer. The concentration of S atom is more or less uniform across the support layer of both membranes, after contact with the herbicides and before thermal desorption (Fig. 7.7b). After the thermal desorption there are still some S atoms in the membranes (Fig. 7.7c), indicating an incomplete desorption.

(a)

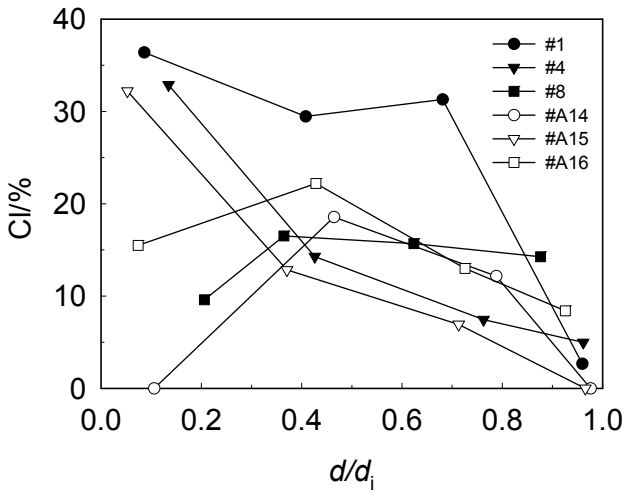

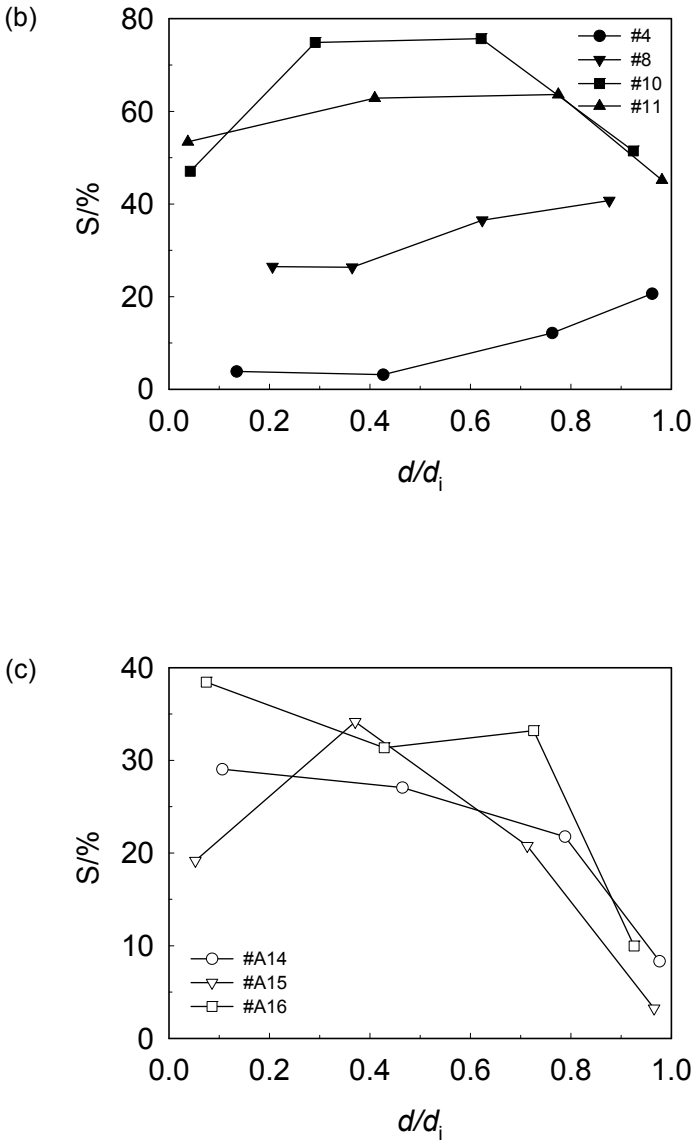

Fig. 7.7. Cl (a) and S ((b) and (c)) elemental profiles of PDMS and PEI membrane samples. Closed symbols refer to samples before thermal desorption and open symbols refer to samples after thermal desorption.

7.3.3. Applicability of METD technique to the herbicides analysis

This section assesses the applicability of the METD technique to determining herbicides concentration in aqueous solutions. The headspace extraction mode in which analytes are extracted from the gaseous phase over liquid was selected because it produces a clean signal (less background noise) and reduces the matrix effects, which is related to the pre-concentration ability of this technique. In this study extractions were carried out at 55ºC for 45 min, as suggested in the literature [46].

The salt concentration (NaCl) was optimized to help the headspace membrane extraction of the herbicides. A concentration of 250 g l^{-1} of NaCl was effective in helping the herbicides extraction. The salt increases the ionic strength of the solution and then decreases the solubility of the analyte and the affinity of the analyte to gaseous phase increases.

When dichloromethane was added to the herbicides aqueous solutions, the extraction ability of the membranes (both in liquid phase or headspace) was tremendously reduced. Herbicide samples containing dichloromethane were therefore not longer used with the METD technique.

Changes in humidity affect the overall composition of the headspace above a sample. The hydrophilic sites, possibly in the form of impurities, are responsible in part for the water sorption in PDMS [55]. However, the hydrophobic nature of both membranes under study prevents excessive water vapor from entering the analytical system (GC-FID). The water was analyzed using the METD technique prior to being spiked with the herbicides, to ensure that it was free of interfering compounds.

The PEI integral asymmetric membrane is unsuitable for the METD technique due to its very high permeability towards the carrier gas helium, k_{He}=6.5 x 10^{-6} dm^3 (STP) s^{-1} m^{-2} Pa^{-1} [50], leading to a loose flow-rate control of the inlet carrier gas in the GC.

Figures 7.8 and 7.9 show chromatograms of the molinate (run #A17) and molinate and cycloate (run #A18), respectively (Table 7.4). Figures 7.8 and 7.9 show a retention time (t_r), between 8.5 to 10.5 min. The data were obtained with progressively greater desorption temperatures and/or

desorption time durations. The most important conclusion derived from these GC analyses is that the response can be related with the desorption temperature. During membrane heating, however, the sorbed analyte cannot be completely desorbed into the stripping gas, as some analytes return to the air stream, so only a fraction can be detected at the GC-FID.

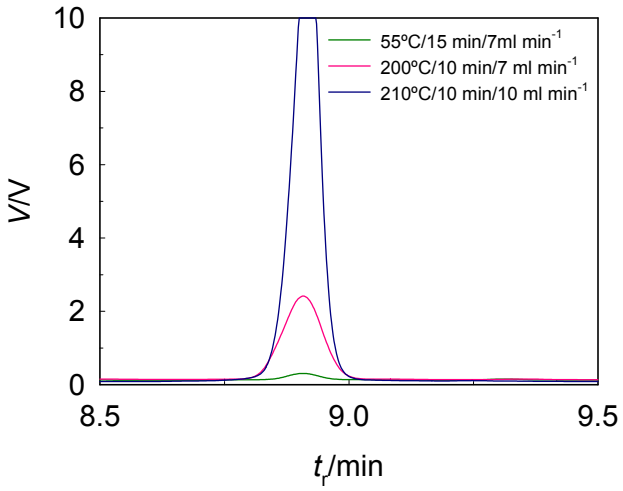

Fig. 7.8. Chromatograms (electric potential (*V*) as a function of retention time (t_r)) of the molinate for run #A17 (Table 7.4) under different experimental desorption conditions. The retention time of molinate is 8.9 min.

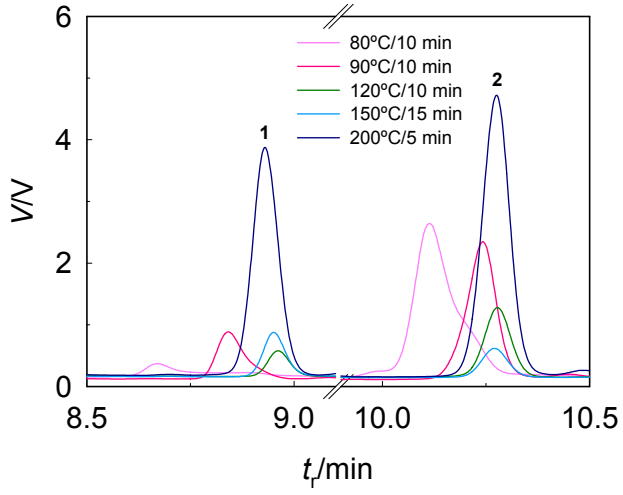

Fig. 7.9. Chromatograms (electric potential (*V*) as a function of retention time (t_r)) of the molinate and cycloate for run #A18 (Table 7.4) under the different experimental desorption conditions. The retention time for cycloate is 10.3 min. Helium flow rate was 4.9 ml min^{-1}. Peaks: 1 - molinate; 2 - cycloate.

To confirm that the METD technique can provide better sensitivity due to sample pre-concentration, a direct injection of herbicide dichloromethane solution (1 μl, 1.15 mg l^{-1}) was performed in the same GC-FID. Two molinate chromatograms are shown in Fig. 7.10. The first was obtained by applying the METD technique with a molinate aqueous solution of 0.663 mg kg^{-1} (run #A15; desorption temperature, 210°C; desorption time, 10 min and flow rate, 10 ml min^{-1}) while the second was obtained with the direct injection of 1.15 mg l^{-1} molinate in dichloromethane solution (1 μl). It can be seen that the METD technique produces a far cleaner chromatogram and shows a higher sensitivity; it also allows a direct analysis of molinate in an aqueous solution.

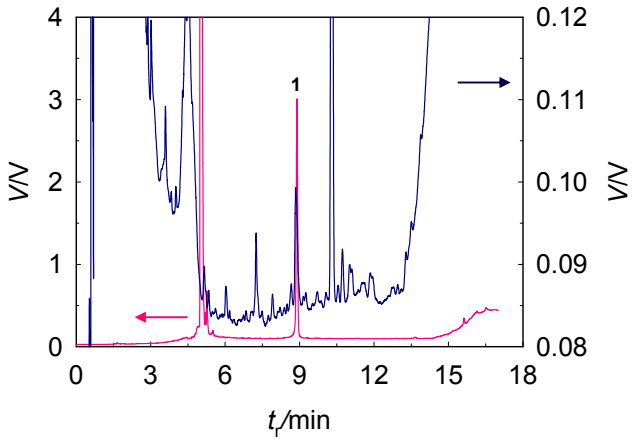

Fig. 7.10. Molinate chromatograms (electric potential (*V*) as a function of retention time (t_r)) for the METD technique (run #A15, pink line) and the direct injection of the 1.15 mg l^{-1} molinate in dichloromethane solution (blue line). Peak 1 - molinate.

Carryover may occur with the METD technique. The carryover arises if the membrane partially retains an analyte after the desorption step of the METD technique. It generally results in an overestimation of the analyte in subsequent analyses. To determine experimentally the carryover, three consecutive GC injections were made after applying the METD technique for runs #A14 and #A15 (see Table 7.4).

Fig. 7.11 displays the peak area of molinate as a function of the injection number (#injection), injection #1 being the METD technique. These data show that the PDMS membrane undergoes a memory effect, especially noticeable during the 2^{nd} injection (#2injection), vanishing afterwards. Condensation on the connecting fused silica columns and stainless steel tubes linked to the GC injection system (see Fig. 7.1) was investigated but no condensation was observed.

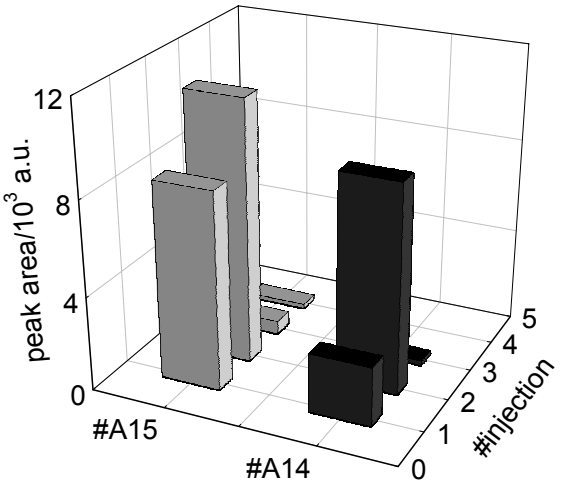

Fig. 7.11. Peak area (arbitrary units) of molinate as a function of the injection number (#injection) for runs #A14 and #A15, Table 7.4.

The herbicides can sorb on the walls of the glass vial or volumetric flask and on septa or other surfaces (e.g., the stir bars used in extraction). To confirm this effect, 5 μl of molinate and cycloate were placed in a 5 ml volumetric flask and the PDMS membrane sample was allowed contact with the headspace (sample #13) for 48 hours at room temperature (Table 7.3). The membrane was then removed from the volumetric flask and stored in a closed vial. The stir bar was also removed, dried and put in a clean 5 ml volumetric flask. The two 5 ml volumetric flasks were then filled with dichloromethane, stirred and analyzed by direct injection. The results obtained (data not shown) demonstrated that both herbicides were present at significant levels both on the stir bar and in the volumetric flask.

7.4. Conclusions and future work

A new membrane-based sample preparation technique is described and studied. The hollow fibers used prevent particles and large molecules in samples from being extracted. Thus, apart from analyte enrichment, the procedure also serves as a clean-up step. More commonly, pre-concentration and pre-separation steps are needed for samples with trace amounts of analytes, especially when the detector is not sufficiently sensitive.

The results obtained demonstrate that the METD technique coupled with GC-FID, is easy to use and suitable for the analysis of herbicides in aqueous samples. Therefore, the advantages of the METD technique are that it is simple and low cost, it excludes water and allows selective pre-concentration and sampling of the less volatile organic compounds, such as herbicides. However, the technique has some limitations, such as the sample carryover. The PDMS composite membrane used presents a number of valuable features for applications with the proposed technique. It is non-polar and thermally stable up to about 300ºC. However, the support layer of this membrane is PEI which has a glass transition temperature of 212°C. Above this temperature the membrane looses mechanical properties and easily collapses.

The proposed METD technique, while very promising, still needs to be more thoroughly investigated. Critical challenges need to be addressed: to increase the robustness of technique by improving the technique protocol (e.g. the sorption/desorption workflow); to better understand the membrane memory effects observed; to use the technique with other analytes and to investigate its performance with "real" samples.

Acknowledgements

Thanks are due to Agência de Inovação, S.A. (Project P0046/ICPME/S - Gassense) for partial support. The authors are grateful to GKSS for supplying the membranes (Mr. Kneifel, Dr. Fritsch and Dr. Peinemann). Rosa Rego wishes to thank Prof. V. Bermudez (UTAD) for her valuable comments and Prof. M. Silva (University of Minho) for the TGA measurements.

References

[1] J.-Å. Jönsson, L. Mathiasson, Membrane-based techniques for sample enrichment, J. Chromatogr. A 902 (2000) 205-225.

[2] Y. Shen, J. Pawliszyn, Catalytic reductions in membrane extraction as sample preparation for gas chromatographic analysis, J. Sep. Sci. 24 (2001) 623-626.

[3] S. Bauer, Membrane introduction mass spectrometry; an old method that is gaining new interest through recent technological advances, Trends Anal. Chem. 14 (1995) 202-213.

[4] M.J. Yang, J. Pawliszyn, Membrane extraction with a sorbent interface, LC·GC Int. 9 (1996) 283-296.

[5] G. Hoch, B. Kok, A mass spectrometer inlet system for sampling gases dissolved in liquid phases, Arch. Biochem. Biophys. 101 (1963) 160-170.

[6] L.B. Westover, J.C. Tou, J.H. Mark, Novel mass spectrometric sampling device-hollow fiber probe, Anal. Chem. 46 (1974) 568-571.

[7] J.S. Brodbelt, R.G. Cooks, J.C. Tou, G.J. Kallos, M.D. Dryzga, In vivo mass spectrometric determination of organic compounds in blood with a membrane probe, Anal. Chem. 59 (1987) 454-458.

[8] M.E. Bier, R.G. Cooks, Membrane interface for selective introduction of volatile compounds directly into the ionization chamber of a mass spectrometer, Anal. Chem. 59 (1987) 597-601.

[9] M.A. LaPack, J.C. Tou, C.G. Enke, Membrane mass spectrometry for the direct trace analysis of volatile organic compounds in air and water, Anal. Chem. 62 (1990) 1265-1271.

[10] T. Kotiaho, F.R. Lauritsen, T.K. Choudhury, R.G. Cooks, G.T. Tsao, Membrane introduction mass spectrometry, Anal. Chem. 63 (1991) 875A-883A.

[11] X. Yang, C. Shang, Quantification of aqueous cyanogen chloride and cyanogen bromide in environmental samples by MIMS, Water Res. 39 (2005) 1709-1718.

[12] A.A. Boyd-Boland, M. Chai, Y.Z. Luo, Z. Zhang, M.J. Yang, J.B. Pawliszyn, T. Górecki, New solvent-free sample preparation techniques based on fiber and polymer technologies, Environ. Sci. Technol. 28 (1994) 569A-574A.

[13] M.J. Yang, Y.Z. Luo, J. Pawliszyn, A two-step sample prep for GC, Chemtech 24 (1994) 31-37.

[14] J. Pawliszyn, Process and device for continuous extraction and analysis of fluid using membrane, US Patent 5,492,838 (1996).

[15] K.F. Pratt, J. Pawliszyn, Gas extraction kinetics of volatile organic species from water with a hollow fiber membrane, Anal. Chem. 64 (1992) 2101-2106.

[16] K.F. Pratt, J. Pawliszyn, Water monitoring system based on gas extraction with a single hollow fiber membrane and gas chromatographic cryotrapping, Anal. Chem. 64 (1992) 2107-2110.

[17] M. J. Yang, J. Pawliszyn, Multiplex gas chromatography with a hollow fiber membrane interface for determination of trace volatile organic compounds in aqueous samples, Anal. Chem. 65 (1993) 1758-1763.

[18] M.J. Yang, S. Harms, Y.Z. Luo, J. Pawliszyn, Membrane extraction with a sorbent interface for capillary gas chromatography, Anal. Chem. 66 (1994) 1339-1346.

[19] Y.Z. Luo, M.J. Yang, J. Pawliszyn, Membrane extraction combined with a sorbent coated fiber interface for capillary gas chromatography, J. High Resol. Chromatogr. 18 (1995) 727-732.

[20] M.J. Yang, J. Pawliszyn, Headspace membrane extraction combined with multiplex gas chromatography and mass selective detector for monitoring of volatile organic compounds, J. Microcolumn Separations, 8 (1996) 89-98.

[21] Y. Luo, Membrane extraction with a sorbent interface, Ph.D. Thesis, University of Waterloo, Ontario, Canada (1999) 1-173.

[22] T. Górecki, J. Pawliszyn, Modern sample-preparation technologies for fast GC analysis with field-portable instrumentation, LC·GC Int. 12 (1999) 123-127.

[23] A. Segal, T. Górecki, P. Mussche, J. Lips, J. Pawliszyn, Development of membrane extraction with a sorbent interface-micro gas chromatography system for field analysis, J. Chromatogr. A 873 (2000) 13-27.

[24] Y.Z. Luo, J. Pawliszyn, Membrane extraction with a sorbent interface for headspace monitoring of aqueous samples using a cap sampling device, Anal. Chem. 72 (2000) 1058-1063.

[25] I. Ciucanu, J. Pawliszyn, Design of continuous-monitoring device based on membrane extraction with sorbent interface and micro-gas chromatograph, Field Analyt. Chem. Technol. 5 (2001) 69-74.

[26] M.J. Yang, J. Pawliszyn, Extraction of semivolatile organic compounds from aqueous samples using high-density carbon dioxide and hollow fiber membrane module, Anal. Chem. 65 (1993) 2538-2541.

[27] M.J. Yang, Membrane extraction techniques for sample preparation, Ph.D. Thesis, University of Waterloo, Ontario, Canada (1995) 1-245.

[28] M. Kaykhaii, A. Sarafraz-Yazdi, M. Chamsaz, J. Pawliszyn, Membrane extraction with sorbent interface-gas chromatography as an effective and fast means for continuous monitoring of thermal degradation products of polyacrylonitrile, Analyst 127 (2002) 912-916.

[29] I. Ciucanu, M. Kaykhaii, L. Montero, J. Pawliszyn, J. Szubra, Continuous monitoring of thermooxidative degradation products of polystyrene by membrane extraction with sorbent interface-gas chromatography, J. Chromatogr. Sci. 40 (2002) 350-354.

[30] L. Wang, H. Lord, R. Morehead, F. Dorman, J. Pawliszyn, Sampling and monitoring of biogenic emissions by eucalyptus leaves using membrane

extraction with a sorbent interface (MESI), J. Agric. Food Chem. 50 (2002) 6281-6286.

[31] X. Liu, R. Pawliszyn, L. Wang, J. Pawliszyn, On-site monitoring of biogenic emissions from Eucalyptus dunnii leaves using membrane extraction with sorbent interface combined with a portable gas chromatograph system, Analyst 129 (2004) 55-62.

[32] H. Lord, Y. Yu, A. Segal, J. Pawliszyn, Breath analysis and monitoring by membrane extraction with sorbent interface, Anal. Chem. 74 (2002) 5650-5657.

[33] Y. Yu, J. Pawliszyn, On-line monitoring of breath by membrane extraction with sorbent interface coupled with CO_2 sensor, J. Chromatogr. A 1056 (2004) 35-41.

[34] B.V. Burger, W.J.G. Burger, I. Burger, Trace determination of volatile organic compounds in water using permeation through a hollow fiber membrane and carrier gas stripping, J. High Resol. Chromatogr. 19 (1996) 571-576.

[35] S. Mitra, N. Zhu, X. Zhang, B. Kebbekus, Continuous monitoring of volatile organic compounds in air emissions using an on-line membrane extraction-microtrap-gas chromatographic system, J. Chromatogr. A 736 (1996) 165-173.

[36] M. Straková, E. Matisová, P. Šimon, J. Annus, J.M. Lisý, Silicone membrane measuring system with SnO_2 gas sensor for on-line monitoring of volatile organic compounds in water, Sens. Actuators B 52 (1998) 274-282.

[37] X. Guo, S. Mitra, Theoretical analysis of non-steady-state, pulse introduction membrane extraction with a sorbent trap interface for gas chromatographic detection, Anal. Chem. 71 (1999) 4587-4593.

[38] M. Straková, E. Matisová, P. Šimon, On-line combination of a silicone-tubing-probe measuring system with HRGC for the analysis of VOCs from water samples, Intern. J. Environ. Anal. Chem. 73 (1999) 59-69.

[39] G. Matz, F. Lennemann, On-line monitoring of biotechnological processes by gas chromatographic-mass spectrometric analysis of fermentation suspensions, J. Chromatogr. A 750 (1996) 141-149.

[40] G. Matz, M. Loogk, F. Lennemann, On-line gas chromatography-mass spectrometry for process monitoring using solvent-free sample preparation, J. Chromatogr. A 819 (1998) 51-60.

[41] G. Matz, G. Kibelka, J. Dahl, F. Lennemann, Experimental study on solvent-less sample preparation methods. Membrane extraction with a sorbent interface, thermal membrane desorption application and purge-and-trap, J. Chromatogr. A 830 (1999) 365-376.

[42]http://www.healthgoods.com/Education/Healthy_Home_Information/Pesticides/pesticidal_carcinogens.htm

[43] C. Aguilar, S. Peñalver, E. Pocurull, F. Borrull, R.M. Marcé, Solid-phase microextraction and gas chromatography with mass spectrometric detection for the determination of pesticides in aqueous waters, J. Chromatogr. A 795 (1998) 105-115.

[44] F. Hernandez, J. Beltran, F.J. Lopez, J.V. Gaspar, Use of solid-phase microextraction for the quantitative determination of herbicides in soil and water samples, Anal. Chem. 72 (2000) 2313-2322.

[45] D.A. Lambropoulou, I.K. Konstantinou, T.A. Albanis, Factors affecting multiresidue determination of priority herbicides when using solid-phase microextraction, J. AOAC Int. 85 (2002) 486-493.

[46] M. Sakamoto, T. Tsutsumi, Applicability of headspace solid-phase microextraction to the determination of multi-class pesticides in waters, J. Chromatogr. A 1028 (2004) 63-74.

[47] M.J. Cerejeira, P. Viana, S. Batista, T. Pereira, E. Silva, M.J. Valério, A. Silva, M. Ferreira, A.M. Silva-Fernandes, Perticides in Portuguese surface and ground waters, Water Res. 37 (2003) 1055-1063.

[48] M. Castro, A.C. Silva-Ferreira, C.M. Manaia, O.C. Nunes, A case study of molinate application in a Portuguese rice field: herbicide dissipation and proposal of a clean-up methodology, Chemosphere, 59 (2005) 1059-1065.

[49] R. Rego, N. Caetano, A. Mendes, Development of a new gas sensor for binary mixtures based on the permselectivity of polymeric membranes. Application to carbon dioxide/methane and carbon dioxide/helium mixtures, Anal. Chim. Acta 511 (2004) 215-221.

[50] Personal communication: Mr. Kneifel, GKSS, Geesthacht, Germany (2000).

[51] http://risk.lsd.ornl.gov/cgi-bin/tox/TOX_select?select=csf

[52] http://www.epa.gov/oppsrrd1/REDs/cycloate_red.pdf

[53] J.W. Dodd, K.H. Tonge, Thermal Methods, Analytical Chemistry by Open Learning, John Wiley & Sons, London, Chapter 1 (1987).

[54] S. Strathmann, Sample conditioning for multi-sensor systems, Ph.D. Thesis, University of Tübingen, Germany (2001) 1-176.

[55] J.M. Watson, M.G. Baron, The behaviour of water in poly(dimethylsiloxane), J. Membr. Sci. 110 (1996) 47-57.

PART IV

General conclusions and future work

8. General conclusions and future work

This thesis deals with the study and development of very low cost concentration gas sensors with which to determine the concentration of binary or pseudo-binary gas mixtures in the 0-100% range, and a solvent-free extraction technique, both membrane-based.

The three membrane materials considered in this study, PDMS, PEI, and Teflon-AF, displayed thermal and long-term stability, but their sorption and permeation properties differed greatly and consequently affected their suitability for the applications considered.

Membrane extraction thermal desorption (METD) is a sample preparation technique suitable for semi-volatile organic compounds analysis. The hollow fiber membrane used allowed the model analytes (herbicides molinate and cycloate) to selectively permeate from the aqueous sample or its headspace into the stripping gas phase (GC carrier gas) thus preventing water from entering the GC system.

The main features of the METD technique coupled with GC-FID are its solvent-free nature, roughness and simple design, and single-step process, which allows minimal sample loss and human error in the analysis, as well as providing easy automation and on-site operation. The PEI hollow fiber proved to be unsuitable for the membrane extraction because it has a very high permeability towards the carrier gas (He). However, the PDMS membrane was more promising. The METD technique was less suitable for sequential testing applications due to incomplete analyte desorption from the membrane (sample carryover).

To establish METD as a technique for routine sample preparation, further research is required; namely, it is necessary to improve the technique protocol and find more suitable membranes for different analytes. Other possible applications of the METD technique have yet to be explored and its performance must be investigated with "real" samples.

The new concentration gas sensor described in this work is based on the permselectivity of polymeric membranes. When the feed pressure is kept constant, the permeate flow rate is related to the gas mixture concentration. However, gas flow meters are expensive and using this principle to determine the concentration is not a promising solution. Nevertheless, if a non-selective barrier (e.g. needle valve) is used on the permeate outlet, the permeate pressure relates to the permeate flow rate and, as a result, to the feed concentration. The selected binary gas mixtures studied were oxygen/nitrogen, carbon dioxide/methane, carbon dioxide/helium and hydrogen/methane. Preliminary results are also given for a hydrogen/nitrogen mixture. In order to evaluate the overall performance of the sensor, data on response curves, reproducibility/repeatability, sensitivity, response time, reversibility, long-term stability and also the influence of temperature were obtained.

This study identified three target, low/medium precision markets in particular, and several others in general, for the concentration gas sensor. In the medical field there is a strong demand for a rugged, low cost device, to monitor the output concentration of oxygen concentrators, with medium precision (precision $\pm$2.5% and average concentration around 90% of oxygen). This oxygen concentrator unit uses an adsorption cycle to concentrate oxygen from air. It equally concentrates argon present in the air with 0.9% concentration. A 90% oxygen stream should also contain 5% argon and 5% nitrogen. The new sensor can be used in this field despite this fact, because the membrane used, PDMS, shows a similar permeability towards oxygen and argon. In this way the ternary oxygen/nitrogen/argon mixture behaves like a binary one. The world market for this system, which serves people with insufficient breathing ability, is about 500,000 units per year.

Biogas controlling units (e.g. wastewater treatment plants and landfills) is the second identified market (carbon dioxide/methane sensor). The third target application includes industrial safety monitoring, primarily in semiconductor plants, metals processing and hydrogen generation plants

(hydrogen/methane and hydrogen/nitrogen sensor). Up to now no well-defined market for the carbon/helium sensor has been identified.

At a constant feed pressure, the permeate pressure relates to the more permeable gas feed molar fraction (response curves) for a given temperature. Reproducibility/repeatability, sufficient/medium precision, adequate sensitivity, reversibility, and long-term stability were obtained at different temperatures with the selected applications.

The oxygen/nitrogen sensor was tested with PDMS and PEI membranes. The response curves for both membranes at different temperatures display a quasi-linear behavior. However, PDMS membranes are more suitable for this application because of their faster response time (a few seconds) and an optimized oxygen/nitrogen selectivity.

Carbon dioxide/methane and carbon dioxide/helium gas sensors were tested with PDMS and Teflon-AF membranes. The results obtained suggest that the two membrane-based sensors can be used to determine the carbon dioxide concentration in binary mixtures with methane or helium and in fast response times (a few seconds). The PDMS and Teflon-AF membranes seem to be only slightly affected by temperature.

PDMS, PEI and Teflon-AF were used with hydrogen/methane and hydrogen/nitrogen sensors. The results obtained indicate that PEI and PDMS membranes seem to be more suitable for hydrogen/methane and hydrogen/nitrogen sensors, respectively. The use of PEI membranes allows the preparation of sensors with high sensitivity and with a response time between 70 and 180 s. For the hydrogen/nitrogen sensor the response curves exhibit linearity at hydrogen concentrations lower than 70%. At higher hydrogen concentrations, the output of the sensor (permeate pressure) levels off.

The temperature dependency, sensitivity and response time of the sensor relates to the membrane and the non-selective barrier permeabilities.

As the sensor responds to temperature changes, a method to compensate the temperature effect on the concentration gas sensor response is described and evaluated for different membrane materials and gas mixtures. The proposed method corrects most of the temperature effects

when using PDMS membranes with oxygen/nitrogen and carbon dioxide/helium mixtures, and reduces the need for sophisticated algorithms to correct the response of the sensor.

A very simple mathematical model has been developed to describe the response of the sensors and applied to the oxygen/nitrogen and hydrogen/methane mixtures. This mathematical model is in good agreement with the experimental results. A more sophisticated mathematical model can be developed to include predictable features.

The use of inexpensive gas sensors offers an opportunity to design relatively cheap, small and robust devices with the potential for continuous on-line analysis of gas streams. All the concentration sensors developed could be suitable for the direct assay of a binary gas mixture without prior sample preparation or purification. The sensor does not require reagents or complex associated instrumentation and could be adapted to field work. The advantages of this system over current well-established analytical methods are essentially related to the cost/precision balance, which is believed to be very favorable for the new sensors, despite their being limited to the analysis of only a binary gas mixture. Also, the responses generated by these devices are independent of size, thus allowing for miniaturization.

While this work reports an interesting configuration and application of membrane-based sensors, the practical use of such a sensor in "real applications" needs further assessment. A Portuguese company, HBS, of Lisbon, is now investigating the possible industrialization of an oxygen/nitrogen sensor for medical oxygen concentrators.